UC San Diego
UC San Diego Electronic Theses and Dissertations

Title

Bioengineering synovial fluid with theoretical and experimental models of the synovial joint

Permalink

https://escholarship.org/uc/item/3z11921w

Author

Blewis, Megan E.

Publication Date

2008

Peer reviewed|Thesis/dissertation

UNIVERSITY OF CALIFORNIA, SAN DIEGO

BIOENGINEERING SYNOVIAL FLUID WITH THEORETICAL AND EXPERIMENTAL MODELS OF THE SYNOVIAL JOINT

A dissertation submitted in partial satisfaction of the

requirements for the degree Doctor of Philosophy

in

Bioengineering

by

Megan E. Blewis

Committee in charge:

      Professor Robert L. Sah, Chair
      Adjunct Professor William D. Bugbee
      Professor Gary S. Firestein
      Professor Jeff M. Hasty
      Professor Marcos Intaglietta

2008

The dissertation of Megan E. Blewis is approved, and it is acceptable in quality and form for publication on microfilm and in digital formats:

_____

_____

_____

_____

_____
Chair

University of California, San Diego

2008

iii

TABLE OF CONTENTS

LIST OF FIGURES AND TABLES

ACKNOWLEDGMENTS

I would like to thank all of the individuals without whom this work would not have been possible.

Most importantly, I thank my thesis advisor, Dr. Robert Sah for welcoming me into the Cartilage Tissue Engineering (CTE) Laboratory and providing me with the wonderful opportunity to be part of this outstanding research group. During the past six years, he has given endless support, advice, and direction on this thesis project. He has set an inspiring example of hard work and dedication, not only in striving for high-quality publication of work and maintaining constant funding for his large laboratory, but also in making his students a priority by devoting so much of his time to them and making himself available to guide each one to success. I am extremely fortunate to have been mentored by Dr. Sah, as the training he has provided in areas of technical skills, scientific writing, grant proposals, and mentoring have no doubt helped shape me into the individual that I am today, and have excellently prepared me for future endeavors.

I would also like to thank the very generous and supportive collaborators of this thesis project. First and foremost, Dr. Gary Firestein expanded my scientific knowledge beyond the cartilage horizon and into the very exciting world of synoviocyte biology. Without his continued guidance, insightful feedback, and valuable contribution of human synoviocyte sources, this thesis would not have developed into what it is today. Dr. William Bugbee provided valuable clinical motivation and considerations in pursuing this work, in addition to numerous human synovium samples. Dr. Kyle Jadin spent much time preparing and characterizing the

In the CTE lab, I have had the wonderful opportunity to mentor several individuals who have helped me with this thesis, and it is a tribute to Dr. Sah's own mentoring of me that these interactions have been so productive and rewarding. I would especially like to thank Brian Lao who worked with me for the past two years as an undergraduate student. Brian has contributed immensely in many parts of the

Finally, I thank my family: my mom Linda for teaching me that I can achieve anything in life and for demonstrating the hard work and determination to do so; my dad Robert for reminding me to hold fast to my dreams; my sisters Kati and Robin for infusing laughter into my life; and my boyfriend Hideru for providing endless patience (especially in these last few months!), unwavering support, and a sincere interest in my accomplishments.

VITA

2002	B.S., Biomedical Engineering University of Miami, Coral Gables, Florida
2002-2008	Graduate Student Researcher Cartilage Tissue Engineering Laboratory University of California, San Diego, La Jolla, California
2004	M.S., Bioengineering University of California, San Diego, La Jolla, California
2008	Ph.D., Bioengineering University of California, San Diego, La Jolla, California

Journal Articles

Blewis ME, Lao BJ, Schumacher BL, Bugbee WD, Firestein GS, Sah RL: Interactive Cytokine Regulation of Synoviocyte Secretion of Synovial Fluid Lubricants, Hyaluronan and Proteoglycan 4. *Arthritis Research & Therapy* (submitted), 2008.

Bae WC, Wong VW, Hwang J, Antonacci JM, Nugent-Derfus GE, Blewis ME, Temple-Wong MM, Sah RL: Wear-lines and split-lines of human patellar cartilage: relation to tensile biomechanical properties. *Osteoarthritis Cartilage* 16:841-5, 2008.

Blewis ME, Nugent-Derfus GE, Schmidt TA, Schumacher BL, Sah RL: A model of synovial fluid lubricant composition in normal and injured joints. *Eur Cell Mater* 13:26-39, 2007.

Blewis ME, Schumacher BL, Klein TJ, Schmidt TA, Voegtline MS, Sah RL: Microenvironment regulation of PRG4 phenotype of chondrocytes. *J Orthop Res* 25:685-95, 2007.

Klein TJ, Schumacher BL, Blewis ME, Schmidt TA, Voegtline MS, Thonar EJ-MA, Masuda K, Sah RL: Tailoring secretion of proteoglycan 4 (PRG4) in tissue-engineered cartilage. *Tissue Eng* 12:1429-39, 2006.

Selected Abstracts

Blewis ME, Jadin KD, Lao BJ, McCarty WJ, Antonacci JM, Bugbee WD, Firestein GS, Sah RL: Bioengineering of lubricious synovial fluid in a biomimetic bioreactor. *TERMIS* :, 2008.

Blewis ME, Lao BJ, Orwoll BE, Schumacher BL, Bugbee WD, Firestein GS, Sah RL: Lubricant secretion by human synoviocytes on small intestinal submucosa. *Bio Scaff Reg Med* 5: 1499, 2008.

Blewis ME, Lao BJ, Schmidt TA, Derfus GE, Antonacci JM, Schumacher BL, Sah RL: Bioengineering joints: the synovial fluid. *Trans Orthop Res Soc* 32:1506, 2007.

Blewis ME, Lao BJ, Schmidt TA, Derfus GE, Antonacci JM, Schumacher BL, Sah RL: Bioengineering joints: the synovial fluid. *Trans Orthop Res Soc* 32:1506, 2007.

ABSTRACT OF THE DISSERTATION

BIOENGINEERING SYNOVIAL FLUID WITH
THEORETICAL AND EXPERIMENTAL MODELS OF
THE SYNOVIAL JOINT

by

Megan E. Blewis

Doctor of Philosophy in Bioengineering

University of California, San Diego, 2008

Professor Robert L. Sah, Chair

Synovial fluid (SF) in native joints functions as a biomechanical lubricant, lowering the friction and wear of articulating cartilage in synovial joints. SF lubricant macromolecules, including hyaluronan (HA) and proteoglycan 4 (PRG4), are secreted by synoviocytes lining the joint and chondrocytes in cartilage, and concentrated in SF due to the retaining property of the semi-permeable synovium. A bioengineered SF recapitulating the properties of native SF may be beneficial in tissue engineering articular cartilage and synovial joints for the treatment of arthritis, as an appropriate lubricating environment may be critical to maintain the low-friction, low-wear properties of articulating cartilage surfaces undergoing joint-like motion in bioreactors. The ability to generate such a fluid may have additional applications in

developing arthritis therapies targeted at restoration of failed joint lubrication, such as viscosupplements and molecules that regulate lubricant secretion, and may also further our understanding of in vivo SF lubricant regulation. Thus, the overall motivation for this dissertation was to develop and integrate theoretical and experimental models of the synovial joint. More specifically, the goals were to (1) incorporate biophysical features of the joint into a theoretical model of the SF compartment, and (2) recapitulate these features in a biomimetic bioreactor system to produce a bioengineered SF with lubricant composition and function similar to that of native SF.

Theoretical modeling of the dynamics of SF lubricant composition in native joints predicted steady-state lubricant concentrations within physiological ranges, marked alteration in these concentrations with chemical regulation, and distinct kinetics for HA and PRG4 in SF. Cytokine regulation of lubricant secretion by synoviocytes showed distinct regulation of HA and PRG4 secretion rates, with certain cytokines synergistically interacting to markedly increase HA secretion rates and regulate the molecular weight (MW) of secreted HA to resemble that present in native SF. Assessment of the ability of semi-permeable membranes to retain lubricant molecules demonstrated a selective retention of HA and PRG4 as a function of membrane pore size, lubricant MW, and the presence of a cell layer adherent on the membrane. Finally, it was shown that a bioengineered SF with lubricant composition and function similar to that of native SF could be generated in a novel bioreactor system at the tissue explant scale by incorporating biomimetic features of the synovial joint, including lubricant secreting cell types, a lubricant retaining membrane, and cytokine regulatory factors. Application of the theoretical model to this system predicted lubricant concentrations in bioengineered SF that were similar to those

observed experimentally, and kinetics that varied with lubricant structure and membrane pore size.

This work has contributed to a greater understanding of the dynamics of in vivo SF lubricant composition that may occur in health, injury, and disease, and it may also aid in the development of novel arthritis therapies targeted at restoration of failed joint lubrication. Specifically, the ability to bioengineer a functional SF may have applications in developing viscosupplements, evaluating the effects of potential therapeutic agents on SF lubricant composition, and in providing an appropriate lubricating environment to whole joints being tissue engineered and mechanically stimulated in bioreactors for biological joint replacement.

CHAPTER 1:

INTRODUCTION

1.1   General Introduction to the Dissertation

Synovial fluid (SF) functions as a biomechanical lubricant, lowering the friction and wear of articulating cartilage in synovial joints. SF lubricant macromolecules, including hyaluronan (HA) and proteoglycan 4 (PRG4), are secreted by synoviocytes lining the joint and chondrocytes in cartilage, and concentrated in SF due to the retaining property of the semi-permeable synovium. Incorporation of these biophysical features into a theoretical model of the SF compartment of synovial joints may allow SF lubricant composition to be described and predicted, while recapitulation of these features in a biomimetic bioreactor system may produce a bioengineered SF with lubricant composition and function similar to that of native SF.

Synovial joint models such as these may contribute to a greater understanding of in vivo SF lubricant regulation, and may have applications in developing novel arthritis therapies aimed at restoration of failed joint lubrication. Certain biomimetic features of the synovial joint have been incorporated into various experimental systems to examine the biology and mechanobiology of synovium and cartilage; however, a system that combines these lubricant secreting cell types with a lubricant-retaining membrane to generate a SF-like compartment has yet to be established.

Biophysical features of the joint, particularly related to the synovium, have been applied to general models of fluid and solute transport to describe entry and exit of albumin in SF; however, this type of model has not been utilized to describe SF lubricant dynamics.

Thus, the aim of this dissertation work was to develop and integrate theoretical and experimental models of the synovial joint to biomimetically bioengineer a functional SF (**Figure 1.1**). Toward this goal, (1) a mathematical model of the synovial joint was developed to describe the dynamics of SF lubricant composition in native and bioengineered joints, (2) key model parameters including cytokine-regulated lubricant secretion rates and lubricant structure were experimentally determined, (3) lubricant retention by semi-permeable membranes of various pore sizes was assessed, and (4) a novel bioreactor system was developed at the tissue explant scale with biomimetic features of the synovial joint in which a bioengineered SF was generated with lubricant composition and function similar to that of native SF. This work has allowed a greater understanding of lubricant regulation that may affect in vivo SF lubricant composition in health, injury, and disease. It may also contribute to the development of novel arthritis therapies targeted at restoration of failed joint lubrication. Specifically, it provides motivation for bioengineering SF in bioreactors at the whole joint scale, wherein mechanical stimuli may be applied to tissue engineered joints in an appropriate lubricating environment for the ultimate arthritis therapy of biological joint replacement.
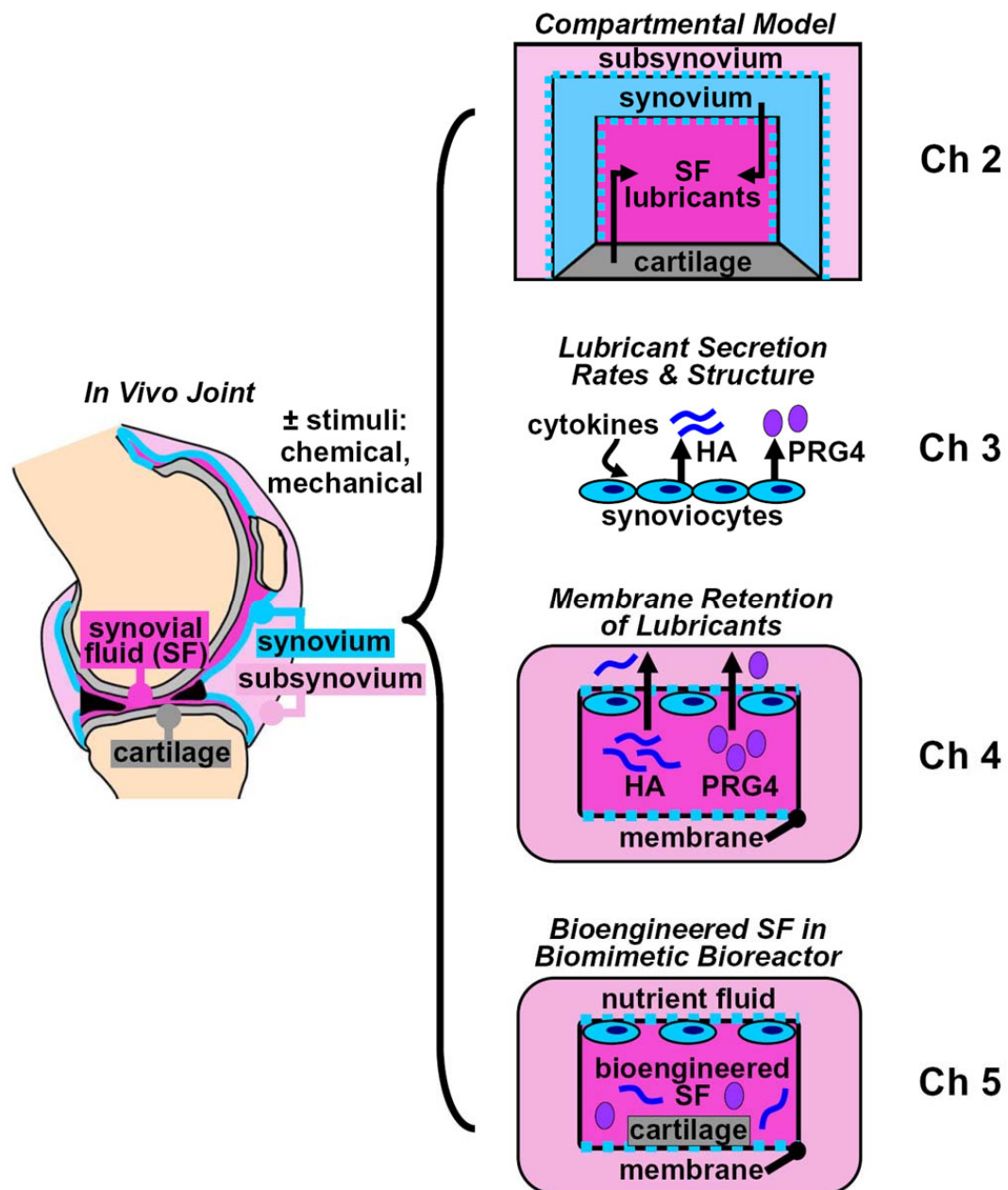
Figure 1.1: Overall aims of the dissertation involving development of biomimetic models to theoretically describe SF lubricant composition, and to experimentally generate a bioengineered synovial fluid with composition and friction-lowering function similar to that of native SF.

This chapter begins with a review of the synovial joint system, focusing on the key components and their composition, structure, and function. A review of SF lubricant homeostasis, dynamics, and imbalance in health and disease is then given. Finally, existing theoretical and experimental models that incorporate some features of the synovial joint are discussed to further motivate the current work.

Chapter 2, published in *European Cells and Materials*, describes the mathematical model of the synovial joint that was developed to describe and predict the concentration of HA and PRG4 in SF of native and bioengineered joints with different chemical regulators of lubricant secretion and with therapeutic interventions. This model predicted steady-state lubricant concentrations that were within physiologically observed ranges and that were markedly altered with chemical regulation. The model also predicted distinct kinetics for HA and PRG4 and a clearance rate of HA after therapeutic injection that was consistent with the experimentally observed half-life in SF.

Chapter 3, submitted to *Arthritis Research & Therapy*, addresses lubricant secretion by human synoviocytes with application of the cytokines IL-1β, IL-17, IL-32, TGF-β1, and TNF-α, individually and in combination. Results showed that individual and synergistic effects of certain cytokines regulated HA secretion over a range of rates spanning two orders of magnitude, while PRG4 secretion rates were regulated in a counter-balancing manner by certain cytokines and over a smaller spanning range. The results also showed that the molecular weight distribution of secreted HA was regulated by certain cytokine combinations to resemble that present in native SF, while PRG4 molecular weight was not observed to be regulated but was also similar to that present in native SF.

Chapter 4 addresses the ability of synoviocytes to maintain a lubricant-secreting phenotype when cultured on semi-permeable expanded polytetrafluoroethylene (ePTFE) membranes, and the ability of these membranes to retain lubricant molecules. Results showed that secretion of HA and PRG4 is regulated by cytokines in a similar manner on the membranes as on standard tissue culture substrates. The results also demonstrate selective retention of lubricant molecules by the membranes as a function of membrane pore size, the molecular weight of the lubricant molecule, and the presence of an adherent cell layer on the membrane.

Chapter 5 describes the biomimetic bioreactor system that was developed and which incorporated lubricant secreting cell types, lubricant retaining membranes characterized in Chapter 4, and cytokine regulatory factors to bioengineer a mechanically functional SF. Results demonstrate that the lubricant concentration and lubricating function of bioengineered SF generated using membranes of 50 nm pore size approached that of native SF, and was significantly greater than that generated with membranes of 3 μm pore size. A strong correlation between composition and function of bioengineered SF was also revealed. Application of the theoretical model describing SF lubricant dynamics developed in Chapter 2 provided predictions of lubricant concentrations in bioengineered SF that were similar to those observed experimentally and kinetics that varied with lubricant structure and membrane pore size.

Finally, Chapter 6 summarizes the major conclusions from this work and discusses future directions for these projects.

1.2   Synovial Joint Components and Structure

The synovial joint is a low-friction, low-wear load-bearing system that includes articular cartilage, synovial fluid (SF), and synovium components. Articular cartilage is composed of chondrocytes within a dense extracellular matrix, and bears load and slides relative to an apposing surface with low-friction and low-wear properties. The SF acts biomechanically as a lubricant for articular cartilage, while containing a complex milieu of lubricating molecules, regulatory cytokines, and other factors. The synovium is the thin, flexible lining of the joint composed of synoviocytes and extracellular matrix components, with capillaries present beneath the cell layer. A key function of the synovium is to serve as a semi-permeable membrane for exchange of solutes from SF (such as nutrients, waste products, and cytokines), but offers sufficient outflow resistance to retain high molecular weight macromolecules, such as lubricants, in SF.

The synovial joint has distinct structural properties that are critical for its normal function (**Table 1.1**). The total cartilage surface area in the human knee joint is, on average, 120 cm^2 while that of the human ankle joint is ~32 cm^2 [21, 22]. Estimates of synovium surface area in humans are ~277 cm^2 for the knee joint and ~45 cm^2 for the ankle joint [21]. Thus, an average ratio of synovium: cartilage surface area is ~2. The synovium is ~50 μm thick [80] in humans and has an estimated pore size of 20-90 nm [16, 17, 30, 92], while mature human articular cartilage is ~2-5 mm thick [22]. The SF volume enclosed by these tissue surfaces is ~1-2 ml in a normal human knee joint [84]. An impressive parameter of the synovial joint to consider is the approximate ratio of SF volume to synovium surface area, which is ~2 cm^3 : 200 cm^2, or ~0.01 cm.

It may be noted that while SF, cartilage, and synovium are key components of synovial joints, ligaments are also present in all synovial joints. However, ligaments may often be extracapsular and thus not within the synovium-enclosed SF compartment. In a similar manner, menisci structures are present only in certain joints and are thus not a general synovial joint component within the SF compartment.

Table 1.1: Structural properties of key components of the synovial joint.

Component	Surface area (cm^2)	Thickness (mm)	Pore size (nm)	Volume (ml)
synovium	280	0.05-0.06	20-90	1-2
cartilage	100-160	2-5	2-6	16-34
synovial fluid				1-2

1.3 Synovial Fluid: Complex Milieu of Lubricants & Chemical Factors

SF is an ultrafiltrate of blood plasma, and also includes lubricating molecules and a complex milieu of chemical regulatory factors. Nutrients and ions enter SF through capillaries present in the synovium, while lubricating molecules are synthesized and secreted into SF by cells present in cartilage and synovium. Chemical factors may enter through capillaries or may be secreted by these or other cell types residing in the joint tissues.

Lubricating molecules in SF include hyaluronan (HA) and proteoglycan 4 (PRG4). HA is a glycosaminoglycan polymer, comprised of the repeating disaccharide unit of D-glucuronic acid and D-N-acetylglucosamine. PRG4 is a 12 exon protein encoded by the PRG4 gene, with an expansive and lubricating mucin-like domain in exon 6 consisting of O-linked glycosylations [36]. PRG4 is also commonly referred to as lubricin and superficial zone protein (SZP) due to its function and source. HA is present in SF at a concentration of ~1-4 mg/ml, while PRG4 is present at 0.05-0.5 mg/ml [8, 9, 20, 65, 88]. These lubricants are both high molecular weight molecules (MW), with the MW of HA in normal SF reported to be ~70% ≥4000 kDa with the remaining ~30% distributed at lower MWs in the range of <4000 kDa to ~100-200 kDa, and the MW of PRG4 reported to be primarily ~0.3 MDa [8, 9, 20, 52, 54].

SF also contains a complex milieu of chemical regulatory factors, including cytokines, binding molecules, and enzymes. Cytokines in SF include TGF-β1, IL-1β, TNF-α, IL-17, IL-8, and IL-6, in addition to many others [2, 11, 29, 43, 45, 48, 51, 64, 101]. Natural antagonists of certain cytokines are also present in SF and have inhibitory effects on cytokine activity, including the IL-1β/α specific IL-1β/α receptor antagonist (IL-1ra) [64]. Another component of SF includes proteins that bind to

lubricant molecules, such as tumor necrosis factor-stimulated gene 6 (TSG-6) [48] and the inter-alpha trypsin inhibitor (IαI) family of molecules, both of which bind HA to stabilize it and prevent its depolymerization in SF [35]. Extracellular matrix degrading enzymes, such as collagenases and MMPs, may also be present in SF [1, 12].

1.4   Articular Cartilage: Load Bearing Material & Source of Lubricants

Articular cartilage is the low-friction, wear-resistant, load-bearing tissue at the ends of bones in synovial joints [98]. Articular cartilage bears load and slides relative to an opposing tissue surface with low-friction and low wear. This is due, in part, to the lubricating molecules present in SF that contribute to both boundary mode and fluid film lubrication [5, 105]. In boundary mode lubrication, load is supported by surface-to-surface contact of apposing cartilage surfaces, and the associated frictional properties are determined by lubricant molecules bound to the cartilage surface. In fluid film lubrication, load is supported as a result of pressurization of the interstitial fluid within cartilage due to the biphasic nature of the tissue. Together, both modes of lubrication contribute to the low-friction, wear-resistant properties of articular cartilage.

Articular cartilage is typically classified into 3 zones, superficial, middle, and deep, resulting from depth-associated variation in cell and extracellular matrix properties [37]. In the superficial zone of mature articular cartilage (0-10% depth from articular surface), cell density is relatively high and cells are arranged in clusters parallel to the surface. Cell density is lower in the middle zone (10-40%), and there, cells appear more rounded and randomly dispersed. In the deep zone (40-100%), cells

are present at an even lower density and have a columnar organization [34]. Chondrocytes in the superficial zone secrete PRG4 [89, 39], while chondrocytes from the middle and deep zones of articular cartilage secrete very little of this lubricant molecule, but produce the glycosaminoglycan (GAG) component of the extracellular matrix at a relatively high rate [7].

1.5 Synovium: Semi-Permeable Membrane, and Source of Lubricants & Lubricant-Modifying Molecules

The synovium is the thin lining of the joint comprised of macrophage-like A cells and fibroblast-like B cells [6, 82, 102], with fenestrated capillaries present beneath the cell layer [50]. The cells in the synovium form a nearly continuous layer separated by intercellular gaps of several microns in width [50, 66]. The extracellular matrix in these gaps contains collagen types I, III, and V [4, 83], hyaluronan [103], chondroitin sulphate [79, 104], biglycan and decorin proteoglycans [14], and fibronectin [78].

The synovium matrix provides the permeable pathway through which exchange of molecules occurs [59], but also offers sufficient outflow resistance [14, 95] to retain high molecular weight macromolecules in SF. Lubricant transport through the synovium occurs around the spaces, or volume fractions, occupied by synoviocytes, collagen fibrils, and glycosaminoglycan chains, and is further limited by the tortuosity of the pathway imposed by the cells and collagen fibrils [59]. Molecules that travel through these pores enter the underlying subsynovium, a thicker, loose connective tissue (~100 μm), where an extensive system of lymphatics exists to clear transported molecules [41, 56, 57].

Type B fibroblast-like synoviocytes, rather than type A macrophage-like synoviocytes, secrete the lubricant molecules HA [33, 96] and PRG4 [40, 90] into SF. Both cell types, however, may be sources of lubricant-modifying molecules. Cytokines such as IL-1β and TNF-α are secreted into SF by the macrophage-like cells [43, 44], while fibroblast-like synoviocytes in the synovium (abbreviated in this thesis from this point forward as "synoviocytes") secrete IL-6, granulocyte-macrophage colony-stimulating factor (GM-CSF), IL-8, FGF, and TGF-β1 [1, 2, 25]. Synoviocytes also secrete the HA-binding protein TSG-6 [48], and enzymes such as collagenases and MMPs involved in joint destruction [1, 12]. T cells that may also be present in the synovium (to varying degrees depending on joint conditions) secrete cytokines that contribute to the milieu of SF, including IL-17 and IFN-γ [97, 106]. Cytokines present in SF may have individual, additive, or synergistic effects, and may also act through autocrine and paracrine mechanisms.

1.6   Synovial Fluid Lubricant Homeostasis, Dynamics, and Imbalance

The mechanobiology of joints and SF constitutes a complex, low-friction, low-wear system that is normally in homeostasis. A normal steady-state lubricant concentration is maintained in SF due to a balance of the dynamic processes of lubricant synthesis, lubricant flux across the synovium, and lubricant degradation in SF. Imbalances in these processes may occur in injury and disease to alter SF lubricant composition.

Lubricant Synthesis by Joint Components

Chondrocytes in articular cartilage and synoviocytes isolated from synovium secrete basal levels of lubricant molecules in vitro when cultured in media with varying concentrations of serum or albumin, but certain cytokines present in SF induce alterations in lubricant secretion from basal levels (**Table 1.2**). IL-1β, TGF-β1, and TNF-α each increase HA secretion rates by synoviocytes [13, 33, 81]. IL-1β has also been reported to increase the molecular weight (MW) of secreted HA compared to basal conditions [33, 46]. Individually applied TGF-β1 increases total PRG4 secretion by synoviocytes, while IL-1β decreases secretion [42, 70]. PRG4 secretion by other tissues, such as the meniscus and ligament, are also regulated by these cytokines in a similar manner [55].

Various mechanical stimuli also have a regulatory effect on lubricant secretion (**Table 1.2**). Static compression of cartilage explants decreases PRG4 secretion [74], while dynamic shear stimulation increases PRG4 secretion [73], compared to unloaded controls. Applied surface motion of chondrocyte-seeded scaffolds against a ceramic hip ball results in increased PRG4 mRNA expression, compared to statically compressed controls [27, 28, 63]. Continuous passive motion of whole joints in a joint-scale bioreactor similarly increases PRG4 secretion in regions of cartilage continuously or intermittently sliding against another tissue surface [72]. HA secretion by synoviocytes is also mechanosensitive, as stretching of synoviocytes cultured on a flexible substrate [69] and also stretching of intact synovium by expansion of the joint with fluid both increase HA secretion [18].

Table 1.2: Chemical and mechanical regulation of lubricant synthesis.

Source	Lubricant	Chemical factor			Mechanical factor			
		IL-1β	TGF-β1	TNF-α	Comp.	Shear	CPM[a]	Stretch
synoviocyte	HA	↑	↑	↑			↑	↑
	PRG4	↓	↑	↓				
chondrocyte	PRG4	↓	↑	↓	↓	↑	↑	

[a]Cyclic or continuous passive motion

Lubricant Efflux Across the Synovium

The synovium matrix provides the permeable pathway through which exchange of molecules occurs [59], including the lubricants PRG4 and HA, but also offers sufficient outflow resistance [14, 95] to retain macromolecules within the joint cavity. Transport of solutes from SF is dependent upon processes of diffusion and convective fluid flow [59], and molecules that traverse the synovium enter the underlying subsynovium where they are drained away by an extensive system of lymphatics [41, 56, 57].

The diffusive flux of a lubricant through the synovium is a function of its permeability through the synovium and the synovium surface area, and is driven by the concentration gradient of lubricant between SF and subsynovium compartment. Lubricant transport through the synovium occurs around the spaces occupied by synoviocytes and extracellular matrix components, and through the voids in the glycosaminoglycan (GAG) network. Restricted diffusion of lubricants thus occurs within the synovium and is dependent upon the diffusion of lubricant in free solution, the volume fraction of the GAG component, the radius of GAG chains, and the effective radius of the solute [75]. The diffusive flux of a lubricant molecule is further dependent upon the volume fractions and tortuosity of collagen and cellular components of the tissue occurs [59], the area of the synovium, and the lubricant concentration gradient between the SF and subsynovium compartments.

The convective flux of a lubricant through the synovium is a function of the velocity of fluid flow out of the membrane, the reflection coefficient of the membrane (i.e. the parameter that describes maximum reflection of a molecule by a semi-permeable membrane), and the concentration gradient between SF and subsynovium compartments [19, 76], and is driven by joint motion during flexion and extension.

The velocity of fluid flow is dependent upon the hydrostatic pressure difference and osmotic pressure difference between SF and subsynovium compartments, and also the hydraulic conductance of the synovium [47]. At physiological concentrations of lubricants in SF, convective fluid flow may be attenuated due to the high osmotic pressure and an associated concentration polarization phenomenon that occurs for the high molecular weight macromolecules, particularly HA [67, 86, 93]. This phenomenon has been experimentally observed when the opposition to fluid filtration across the synovium increases in proportion to the applied pressure, and postulated to be a result of HA ultrafiltration by the synovium and creation of a highly concentrated HA "filter–cake" at the synovial surface [68]. Quantitative models of this hypothesis suggest that the osmotic pressure of the concentrated HA layer at the fluid/tissue interface provides the force that opposes joint fluid pressure and water outflow [16]. The reflection coefficient for HA, or the maximum reflection of HA by the synovium, has been estimated at ~0.91 for physiologically normal MWs [86].

Lubricant Degradation Mechanisms

The degradation rate of lubricants in SF is dependent upon the concentration and activity of degradative species that are present. PRG4 may be targeted by various enzymes, and in particular has been shown to be degraded by elastase [24]. HA may be targeted by hyaluronidase enzymes [23], or degradative oxygen-derived free radicals [32], although the interaction of HA-binding proteins with HA may serve to counterbalance such degradation [35].

Lubricant Homeostasis and Dynamics in Health

Lubricant homeostasis, or maintenance of steady-state lubricant composition in SF, is a result of a balance between the dynamic processes of lubricant synthesis, degradation, and flux. In normal human knee joints, the volume of SF is ~1-2 ml [84], and the concentrations of PRG4 and HA are <0.5 mg/ml [88] and ~1-4 mg/ml [8, 9, 20, 65], respectively. Lubricant secretion rates, which are key parameters contributing to these steady-state concentration, have been studied in vitro for both HA and PRG4, with lubricant secretion rates spanning over a wide range depending on applied chemical and mechanical stimuli. Lubricant residence time in SF is interrelated to lubricant synthesis, degradation, and flux, and in normal joints the half-life of HA has been reported to be on the order of ~24 hours [18, 53, 87].

Lubricant Imbalance in Disease & Injury

In naturally occurring or animal models of osteoarthritis, rheumatoid arthritis, and injury, alterations in SF composition and volume may occur from that of normal conditions as a result of imbalances in lubricant dynamics. The volume of SF in normal knee joints is ~1-2 ml, but increases ~10-25 fold in inflamed or diseased joints [3, 38, 84]; in the latter case, HA and PRG4 concentrations are decreased, but only to 30-50% of normal levels [3, 8-10]. Thus, the total mass of HA in SF (volume multiplied by concentration) may be substantially greater in inflamed or diseased joints. Additional changes that often occur in SF composition during pathology include a decrease in the molecular weight (MW) of HA [8, 9, 20] and increases in the concentrations of certain SF cytokines, including IL-1β, IL-17, IL-32, TGF-β1, and TNF-α [11, 43, 51, 64, 101].

Changes to the articular cartilage tissue, particularly in the superficial zone, often occur in conditions of injury or disease and may lead to altered SF lubricant composition. Fibrillation and erosion result in a loss of the superficial zone of cartilage, thus decreasing the quantity of PRG4-secreting chondrocytes. Lubricant secretion by remaining chondrocytes may be affected by changes in chemical and mechanical stimuli, such as an altered cytokine milieu or altered joint loading and biomechanics [31].

The synovium often experiences altered structural properties and biosynthetic activity in pathological conditions that may similarly contribute to altered SF lubricant composition. Altered content and organization of the synovium extracellular matrix can markedly affect its permeability to solutes. For example, digestion of selected matrix components, such as certain glycosaminoglycans, non-collagenous proteins, and HA, has been shown to increase the hydraulic permeability of the synovium [15, 91]. Such increased permeability may contribute to the observed decrease in HA half-life in SF in arthritic joints compared to normal joints (~12 hours vs. ~24 hours) [18, 26, 53, 87]. In a similar manner to chondrocytes in cartilage, lubricant secretion by synoviocytes in pathological conditions may be affected by changes in chemical and mechanical stimuli, such as an altered cytokine milieu or altered joint loading and biomechanics [31].

1.7   Vision and Application of Synovial Joint Models

The whole synovial joint, including cartilage, synovium and SF, presents complexities that make it difficult to continuously measure in vivo SF composition

and function, and also the main determinants of their dynamics in health, injury, and disease. Models that theoretically describe or experimentally mimic the synovial joint may thus be of great value for understanding joint pathophysiology. In particular, models that describe or mimic the SF compartment of joints may contribute to an understanding of in vivo SF lubricant regulation in health, injury, and disease, and may lead to the development of arthritis therapies targeted at restoration of failed joint lubrication.

Current Theoretical and Experimental Models of the Synovial Joint

A mathematical model describing the dynamics of SF lubricant composition in native joints has not yet been established; however, the concept of combining theory of mass balance with knowledge of fluid and solute transport through the synovium has been introduced as an approach for determining the concentration of a molecule in SF, such as a lubricant [60]. In addition, an extensive model has been developed to describe the transport of albumin from synovial capillaries into SF and out through the synovium [59], utilizing general models of fluid flow and solute transport through a matrix (reviewed in [19, 58]) and also experimentally-determined model parameters [59, 61, 62, 79, 80, 85, 94]. A similar approach may be taken to mathematically model HA and PRG4 transport across the synovium and associated lubricant concentration in SF.

Several in vitro experimental culture systems exist that have incorporated certain biomimetic features of the synovial joint to examine the biology and mechanobiology of synovium and its interaction with articular cartilage, but an experimental model that includes a SF-like compartment has not yet been established. For example, a three-dimensional synovial-like tissue similar to native synovium has

been generated in vitro to study the function and behavior of synoviocytes in organizing the synovium [49]. Chondrocyte and synoviocyte co-culture systems have been utilized to assess modulation of cartilage matrix metabolism as a result of cellular interaction [71, 77]. Mechanical regulation of articular cartilage with attached subchondral bone has been examined not only for osteochondral fragments [99, 100], but also for whole knee joints utilizing a joint-scale bioreactor [72]. However, an experimental system that combines lubricant secreting cell types with a lubricant-retaining membrane to generate a bioengineered SF with lubricant composition and function similar to that of native SF has yet to be established.

Vision and Application of Models with a Synovial Fluid-Like Compartment

The vision of this dissertation was to develop theoretical and experimental models of the synovial joint to describe the dynamics of lubricant concentration in SF, and to biomimetically generate a mechanically functional bioengineered SF.

It was hypothesized that incorporation of the biophysical features of the synovial joint into a theoretical model of the SF compartment would allow SF lubricant composition to be described and predicted. This type of model may have applications in predicting transient and steady-state SF lubricant concentration in native joints under physiological and pathophysiological conditions, with various regulators of chondrocyte and synoviocyte lubricant secretion, and with different therapeutic interventions. The model may similarly be applied to experimental models of the joint, at tissue scale or whole joint scale, to describe a bioengineered SF compartment.

It was also hypothesized that recapitulation of the biophysical features of the synovial joint in a biomimetic bioreactor system would produce a bioengineered SF

with lubricant composition and function similar to that of native SF. A bioengineered SF may be beneficial in tissue engineering articular cartilage and synovial joints for the treatment of arthritis, as an appropriate lubricating environment may be critical to maintain the low-friction, low-wear properties of articulating cartilage surfaces undergoing joint-like motion in bioreactors. The ability to generate such a fluid may have additional applications in developing arthritis therapies targeted at restoration of failed joint lubrication, such as viscosupplements and molecules that regulate lubricant secretion, and may also further our understanding of in vivo SF lubricant regulation.

1.8   References

1. Alvaro-Gracia JM, Zvaifler NJ, Brown CB, Kaushansky K, Firestein GS: Cytokines in chronic inflammatory arthritis. VI. Analysis of the synovial cells involved in granulocyte-macrophage colony-stimulating factor production and gene expression in rheumatoid arthritis and its regulation by IL-1 and tumor necrosis factor-alpha. *J Immunol* 146:3365-71, 1991.

2. Alvaro-Gracia JM, Zvaifler NJ, Firestein GS: Cytokines in chronic inflammatory arthritis. V. Mutual antagonism between interferon-gamma and tumor necrosis factor-alpha on HLA-DR expression, proliferation, collagenase production, and granulocyte macrophage colony-stimulating factor production by rheumatoid arthritis synoviocytes. *J Clin Invest* 86:1790-8, 1990.

3. Asari A, Miyauchi S, Sekiguchi T, Machida A, Kuriyama S, Miyazaki K, Namiki O: Hyaluronan, cartilage destruction and hydrarthrosis in traumatic arthritis. *Osteoarthritis Cartilage* 2:79-89, 1994.

4. Ashhurst DE, Bland YS, Levick JR: An immunohistochemical study of the collagens of rabbit synovial interstitium. *J Rheumatol* 18:1669-72, 1991.

5. Ateshian GA, Mow VC: Friction, lubrication, and wear of articular cartilage and diarthrodial joints. In: *Basic Orthopaedic Biomechanics and Mechano-Biology,* ed. by VC Mow, Huiskes R, Lippincott Williams & Wilkins, Philadelphia, 2005, 447-94.

6. Athanasou NA, Quinn J: Immunocytochemical analysis of human synovial lining cells: phenotypic relation to other marrow derived cells. *Ann Rheum Dis* 50:311-5, 1991.

7. Aydelotte MB, Greenhill RR, Kuettner KE: Differences between sub-populations of cultured bovine articular chondrocytes. II. Proteoglycan metabolism. *Connect Tissue Res* 18:223-34, 1988.

8. Balazs EA: The physical properties of synovial fluid and the special role of hyaluronic acid. In: *Disorders of the knee,* ed. by AJ Helfet, Lippincott Co., Philadelphia, 1974, 63-75.

9. Balazs EA, Watson D, Duff IF, Roseman S: Hyaluronic acid in synovial fluid. I. Molecular parameters of hyaluronic acid in normal and arthritis human fluids. *Arthritis Rheum* 10:357-76, 1967.

10. Belcher C, Yaqub R, Fawthrop F, Bayliss M, Doherty M: Synovial fluid chondroitin and keratan sulphate epitopes, glycosaminoglycans, and hyaluronan in arthritic and normal knees. *Ann Rheum Dis* 56:299-307, 1997.

11. Bertone AL, Palmer JL, Jones J: Synovial fluid cytokines and eicosanoids as markers of joint disease in horses. *Vet Surg* 30:528-38, 2001.

12. Chabaud M, Garnero P, Dayer JM, Guerne PA, Fossiez F, Miossec P: Contribution of interleukin 17 to synovium matrix destruction in rheumatoid arthritis. *Cytokine* 12:1092-9, 2000.

13. Chenevier-Gobeaux C, Morin-Robinet S, Lemarechal H, Poiraudeau S, Ekindjian JC, Borderie D: Effects of pro- and anti-inflammatory cytokines and nitric oxide donors on hyaluronic acid synthesis by synovial cells from patients with rheumatoid arthritis. *Clin Sci (Lond)* 107:291-6, 2004.

14. Coleman P, Kavanagh E, Mason RM, Levick JR, Ashhurst DE: The proteoglycans and glycosaminoglycan chains of rabbit synovium. *Histochem J* 30:519-24, 1998.

15. Coleman PJ, Scott D, Abiona A, Ashhurst DE, Mason RM, Levick JR: Effect of depletion of interstitial hyaluronan on hydraulic conductance in rabbit knee synovium. *J Physiol* 509 (Pt 3):695-710, 1998.

16. Coleman PJ, Scott D, Mason RM, Levick JR: Characterization of the effect of high molecular weight hyaluronan on trans-synovial flow in rabbit knees. *J Physiol* 514 (Pt 1):265-82, 1999.

17. Coleman PJ, Scott D, Mason RM, Levick JR: Role of hyaluronan chain length in buffering interstitial flow across synovium in rabbits. *J Physiol* 526 Pt 2:425-34, 2000.

18. Coleman PJ, Scott D, Ray J, Mason RM, Levick JR: Hyaluronan secretion into the synovial cavity of rabbit knees and comparison with albumin turnover. *J Physiol* 503 (Pt 3):645-56, 1997.

19. Curry F: Mechanics and thermodynamics of transcapillary exchange. In: *Handbook of Physiology,* ed. by ERaC Michel, American Physiological Society, Bethesda, 1984, 309-74.

20. Dahl LB, Dahl IM, Engstrom-Laurent A, Granath K: Concentration and molecular weight of sodium hyaluronate in synovial fluid from patients with rheumatoid arthritis and other arthropathies. *Ann Rheum Dis* 44:817-22, 1985.

21. Davies DV: Synovial membrane and synovial fluid of joints. *Lancet* 248:815-22, 1946.

22. Eckstein F, Winzheimer M, Hohe J, Englmeier KH, Reiser M: Interindividual variability and correlation among morphological parameters of knee joint cartilage plates: analysis with three-dimensional MR imaging. *Osteoarthritis Cartilage* 9:101-11, 2001.

23. El Hajjaji H, Cole AA, Manicourt DH: Chondrocytes, synoviocytes and dermal fibroblasts all express PH-20, a hyaluronidase active at neutral pH. *Arthritis Res Ther* 7:R756-68, 2005.

24. Elsaid KA, Jay GD, Warman ML, Rhee DK, Chichester CO: Association of articular cartilage degradation and loss of boundary-lubricating ability of synovial fluid following injury and inflammatory arthritis. *Arthritis Rheum* 52:1746-55, 2005.

25. Fossiez F, Djossou O, Chomarat P, Flores-Romo L, Ait-Yahia S, Maat C, Pin JJ, Garrone P, Garcia E, Saeland S, Blanchard D, Gaillard C, Das Mahapatra B, Rouvier E, Golstein P, Banchereau J, Lebecque S: T cell interleukin-17 induces stromal cells to produce proinflammatory and hematopoietic cytokines. *J Exp Med* 183:2593-603, 1996.

26. Fraser JR, Kimpton WG, Pierscionek BK, Cahill RN: The kinetics of hyaluronan in normal and acutely inflamed synovial joints: observations with experimental arthritis in sheep. *Semin Arthritis Rheum* 22:9-17, 1993.

27. Grad S, Gogolewski S, Alini M, Wimmer MA: Effects of simple and complex motion patterns on gene expression of chondrocytes seeded in 3D scaffolds. *Tissue Eng* 12:3171-9, 2006.

28. Grad S, Lee CR, Wimmer MA, Alini M: Chondrocyte gene expression under applied surface motion. *Biorheology* 43:259-69, 2006.

29. Granet C, Maslinski W, Miossec P: Increased AP-1 and NF-kappaB activation and recruitment with the combination of the proinflammatory cytokines IL-1beta, tumor necrosis factor alpha and IL-17 in rheumatoid synoviocytes. *Arthritis Res Ther* 6:R190-8, 2004.

30. Granger HJ, Taylor AE: Permeability of connective tissue linings isolated from implanted capsules; implications for interstitial pressure measurements. *Circ Res* 36:222-8, 1975.

31. Gratz KR, Wong BL, Bae WC, Sah RL: The effects of focal articular defects on intra-tissue strains in the surrounding and opposing cartilage. *Biorheology* 45:193-207, 2008.

32. Greenwald RA, Moi WW: Effect of oxygen-derived free radicals on hyaluronic acid. *Arthritis Rheum* 23:455-63, 1980.

33. Haubeck H-D, Kock R, Fischer D-C, van de Leur E, Hoffmeister K, Greiling H: Transforming growth factor ß1, a major stimulator of hyaluronan synthesis in human synovial lining cells. *Arthritis Rheum* 38:669-77, 1995.

34. Hunziker EB, Quinn TM, Hauselmann HJ: Quantitative structural organization of normal adult human articular cartilage. *Osteoarthritis Cartilage* 10:564-72, 2002.

35. Hutadilok N, Ghosh P, Brooks PM: Binding of haptoglobin, inter-alpha-trypsin inhibitor, and alpha 1 proteinase inhibitor to synovial fluid hyaluronate and the influence of these proteins on its degradation by oxygen derived free radicals. *Ann Rheum Dis* 47:377-85, 1988.

36. Ikegawa S, Sano M, Koshizuka Y, Nakamura Y: Isolation, characterization and mapping of the mouse and human PRG4 (proteoglycan 4) genes. *Cytogenet Cell Genet* 90:291-7, 2000.

37. Jadin KD, Wong BL, Bae WC, Li KW, Williamson AK, Schumacher BL, Price JH, Sah RL: Depth-varying density and organization of chondrocyte in immature and mature bovine articular cartilage assessed by 3-D imaging and analysis. *J Histochem Cytochem* 53:1109-19, 2005.

38. Jawed S, Gaffney K, Blake DR: Intra-articular pressure profile of the knee joint in a spectrum of inflammatory arthropathies. *Ann Rheum Dis* 56:686-9, 1997.

39. Jay GD: Lubricin and surfacing of articular joints. *Curr Opin Orthop* 15:355-9, 2004.

40. Jay GD, Britt DE, Cha D-J: Lubricin is a product of megakaryocyte stimulating factor gene expression by human synovial fibroblasts. *J Rheumatol* 27:594-600, 2000.

41. Jensen LT, Henriksen JH, Olesen HP, Risteli J, Lorenzen I: Lymphatic clearance of synovial fluid in conscious pigs: the aminoterminal propeptide of type III procollagen. *Eur J Clin Invest* 23:778-84, 1993.

42. Jones AR, Flannery CR: Bioregulation of lubricin expression by growth factors and cytokines. *Eur Cell Mater* 13:40-5; discussion 5, 2007.

43. Joosten LA, Netea MG, Kim SH, Yoon DY, Oppers-Walgreen B, Radstake TR, Barrera P, van de Loo FA, Dinarello CA, van den Berg WB: IL-32, a proinflammatory cytokine in rheumatoid arthritis. *Proc Natl Acad Sci USA* 103:3298-303, 2006.

44. Jovanovic DV, Di Battista JA, Martel-Pelletier J, Jolicoeur FC, He Y, Zhang M, Mineau F, Pelletier JP: IL-17 stimulates the production and expression of proinflammatory cytokines, IL-beta and TNF-alpha, by human macrophages. *J Immunol* 160:3513-21, 1998.

45. Katz Y, Nadiv O, Beer Y: Interleukin-17 enhances tumor necrosis factor alpha-induced synthesis of interleukins 1,6, and 8 in skin and synovial fibroblasts: a possible role as a "fine-tuning cytokine" in inflammation processes. *Arthritis Rheum* 44:2176-84, 2001.

46. Kawakami M, Suzuki K, Matsuki Y, Ishizuka T, Hidaka T, Konishi T, Matsumoto M, Kataharada K, Nakamura H: Hyaluronan production in human rheumatoid fibroblastic synovial lining cells is increased by interleukin 1 beta but inhibited by transforming growth factor beta 1. *Ann Rheum Dis* 57:602-5, 1998.

47. Kedem O, Katchalsky A: Thermodynamic analysis of the permeability of biological membranes to non-electrolytes. *Biochim Biophys Acta* 27:229-46, 1958.

48. Kehlen A, Pachnio A, Thiele K, Langner J: Gene expression induced by interleukin-17 in fibroblast-like synoviocytes of patients with rheumatoid arthritis: upregulation of hyaluronan-binding protein TSG-6. *Arthritis Res Ther* 5:R186-92, 2003.

49. Kiener HP, Lee DM, Agarwal SK, Brenner MB: Cadherin-11 induces rheumatoid arthritis fibroblast-like synoviocytes to form lining layers in vitro. *Am J Pathol* 168:1486-99, 2006.

50. Knight AD, Levick JR: Morphometry of the ultrastructure of the blood-joint barrier in the rabbit knee. *Q J Exp Physiol* 69:271-88, 1984.

51. Kotake S, Udagawa N, Takahashi N, Matsuzaki K, Itoh K, Ishiyama S, Saito S, Inoue K, Kamatani N, Gillespie MT, Martin TJ, Suda T: IL-17 in synovial fluids from patients with rheumatoid arthritis is a potent stimulator of osteoclastogenesis. *J Clin Invest* 103:1345-52, 1999.

52. Kvam C, Granese D, Flaibani A, Zanetti F, Paoletti S: Purification and characterization of hyaluronan from synovial fluid. *Anal Biochem* 211:44-9, 1993.

53. Laurent UB, Fraser JR, Engstrom-Laurent A, Reed RK, Dahl LB, Laurent TC: Catabolism of hyaluronan in the knee joint of the rabbit. *Matrix* 12:130-6, 1992.

54. Lee HG, Cowman MK: An agarose gel electrophoretic method for analysis of hyaluronan molecular weight distribution. *Anal Biochem* 219:278-87, 1994.

55. Lee SY, Niikura T, Reddi AH: Superficial Zone Protein (Lubricin) in the Different Tissue Compartments of the Knee Joint: Modulation by Transforming Growth Factor Beta 1 and Interleukin-1 Beta. *Tissue Eng Part A*, 2008.

56. Levick JR: Absorption of artificial effusions from synovial joints: an experimental study in rabbits. *Clin Sci (Lond)* 59:41-8, 1980.

57. Levick JR: Contributions of the lymphatic and microvascular systems to fluid absorption from the synovial cavity of the rabbit knee. *J Physiol* 306:445-61, 1980.

58. Levick JR: Flow through interstitium and other fibrous matrices. *Q J Exp Physiol* 72:409-37, 1987.

59. Levick JR: An analysis of the interaction between interstitial plasma protein, interstitial flow, and fenestral filtration and its application to synovium. *Microvasc Res* 47:90-125, 1994.

60. Levick JR: A method for estimating macromolecular reflection by human synovium, using measurements of intra-articular half-lives. *Ann Rheum Dis* 57:339-44, 1998.

61. Levick JR, McDonald JN: Synovial capillary distribution in relation to altered pressure and permeability in knees of anaesthetized rabbits. *J Physiol* 419:477-92, 1989.

62. Levick JR, McDonald JN: Ultrastructure of transport pathways in stressed synovium of the knee in anaesthetized rabbits. *J Physiol* 419:493-508, 1989.

63. Li Z, Yao S, Alini M, Grad S: Different response of articular chondrocyte subpopulations to surface motion. *Osteoarthritis Cartilage* 15:1034-41, 2007.

64. Marks PH, Donaldson ML: Inflammatory cytokine profiles associated with chondral damage in the anterior cruciate ligament-deficient knee. *Arthroscopy* 21:1342-7, 2005.

65. Mazzucco D, Scott R, Spector M: Composition of joint fluid in patients undergoing total knee replacement and revision arthroplasty: correlation with flow properties. *Biomaterials* 25:4433-45, 2004.

66. McDonald JN, Levick JR: Morphology of surface synoviocytes in situ at normal and raised joint pressure, studied by scanning electron microscopy. *Ann Rheum Dis* 47:232-40, 1988.

67. McDonald JN, Levick JR: Evidence for simultaneous bidirectional fluid flux across synovial lining in knee joints of anaesthetized rabbits. *Exp Physiol* 77:513-5, 1992.

68. McDonald JN, Levick JR: Effect of intra-articular hyaluronan on pressure-flow relation across synovium in anaesthetized rabbits. *J Physiol* 485 (Pt 1):179-93, 1995.

69. Momberger TS, Levick JR, Mason RM: Hyaluronan secretion by synoviocytes is mechanosensitive. *Matrix Biol* 24:510-9, 2005.

70. Niikura T, Reddi AH: Differential regulation of lubricin/superficial zone protein by transforming growth factor beta/bone morphogenetic protein superfamily members in articular chondrocytes and synoviocytes. *Arthritis Rheum* 56:2312-21, 2007.

71. Nixon AJ, Haupt JL, Frisbie DD, Morisset SS, McIlwraith CW, Robbins PD, Evans CH, Ghivizzani S: Gene-mediated restoration of cartilage matrix by combination insulin-like growth factor-I/interleukin-1 receptor antagonist therapy. *Gene Ther* 12:177-86, 2005.

72. Nugent-Derfus GE, Takara T, O'Neill J K, Cahill SB, Gortz S, Pong T, Inoue H, Aneloski NM, Wang WW, Vega KI, Klein TJ, Hsieh-Bonassera ND, Bae WC, Burke JD, Bugbee WD, Sah RL: Continuous passive motion applied to whole joints stimulates chondrocyte biosynthesis of PRG4. *Osteoarthritis Cartilage* 15:566-74, 2007.

73. Nugent GE, Aneloski NM, Schmidt TA, Schumacher BL, Voegtline MS, Sah RL: Dynamic shear stimulation of bovine cartilage biosynthesis of proteoglycan 4 (PRG4). *Arthritis Rheum* 54:1888-96, 2006.

74. Nugent GE, Schmidt TA, Schumacher BL, Voegtline MS, Bae WC, Jadin KD, Sah RL: Static and dynamic compression regulate cartilage metabolism of proteoglycan 4 (PRG4). *Biorheology* 43:191-200, 2006.

75. Ogston AG, Preston BN, Wells JD: On the transport of compact particles through solutions of chain-polymers. *Proc Roy Soc Lond A* 333:297-316, 1973.

76. Patlak CS, Goldstein DA, Hoffman JF: The flow of solute and solvent across a two-membrane system. *J Theor Biol* 5:426-42, 1963.

77. Patwari P, Norris SA, Kumar S, Lark MW, Grodzinsky AJ: Inhibition of bovine cartilage biosynthesis by coincubation of joint capsule tissue is mediated by an interleukin-1-independent signalling pathway. *Trans Orthop Res Soc* 28:158, 2003.

78. Poli A, Mason RM, Levick JR: Effects of Arg-Gly-Asp sequence peptide and hyperosmolarity on the permeability of interstitial matrix and fenestrated endothelium in joints. *Microcirculation* 11:463-76, 2004.

79. Price FM, Levick JR, Mason RM: Glycosaminoglycan concentration in synovium and other tissues of rabbit knee in relation to synovial hydraulic resistance. *J Physiol (Lond)* 495:803-20, 1996.

80. Price FM, Mason RM, Levick JR: Radial organization of interstitial exchange pathway and influence of collagen in synovium. *Biophys J* 69:1429-39, 1995.

81. Recklies AD, White C, Melching L, Roughley PJ: Differential regulation and expression of hyaluronan synthases in human articular chondrocytes, synovial cells and osteosarcoma cells. *Biochem J* 354:17-24, 2001.

82. Revell PA: Synovial lining cells. *Rheumatol Int* 9:49-51, 1989.

83. Rittig M, Tittor F, Lutjen-Drecoll E, Mollenhauer J, Rauterberg J: Immunohistochemical study of extracellular material in the aged human synovial membrane. *Mech Ageing Dev* 64:219-34, 1992.

84. Ropes MW, Rossmeisl EC, Bauer W: The origin and nature of normal human synovial fluid. *J Clin Invest* 19:795-9, 1940.

85. Sabaratnam S, Arunan V, Coleman PJ, Mason RM, Levick JR: Size selectivity of hyaluronan molecular sieving by extracellular matrix in rabbit synovial joints. *J Physiol* 567:569-81, 2005.

86. Sabaratnam S, Mason RM, Levick JR: Filtration rate dependence of hyaluronan reflection by joint-to-lymph barrier: evidence for concentration polarisation. *J Physiol* 557:909-22, 2004.

87. Sakamoto T, Mizono, S, Miyazaki, K, Yamaguchi, T, Toyoshima, H, Namiki, O.: Biological fate of sodium hyaluronate (SPH): Studies on the distribution, metabolism, and excretion of ^{14}C-SPH in rabbits after intra-articular administration. *Pharmacometrics* 28:375-87, 1984.

88. Schmid T, Lindley K, Su J, Soloveychik V, Block J, Kuettner K, Schumacher B: Superficial zone protein (SZP) is an abundant glycoprotein in human synovial fluid and serum. *Trans Orthop Res Soc* 26:82, 2001.

89. Schumacher BL, Block JA, Schmid TM, Aydelotte MB, Kuettner KE: A novel proteoglycan synthesized and secreted by chondrocytes of the superficial zone of articular cartilage. *Arch Biochem Biophys* 311:144-52, 1994.

90. Schumacher BL, Hughes CE, Kuettner KE, Caterson B, Aydelotte MB: Immunodetection and partial cDNA sequence of the proteoglycan, superficial zone protein, synthesized by cells lining synovial joints. *J Orthop Res* 17:110-20, 1999.

91. Scott D, Coleman PJ, Mason RM, Levick JR: Glycosaminoglycan depletion greatly raises the hydraulic permeability of rabbit joint synovial lining. *Exp Physiol* 82:603-6, 1997.

92. Scott D, Coleman PJ, Mason RM, Levick JR: Action of polysaccharides of similar average mass but differing molecular volume and charge on fluid drainage through synovial interstitium in rabbit knees. *J Physiol* 528:609-18, 2000.

93. Scott D, Coleman PJ, Mason RM, Levick JR: Interaction of intraarticular hyaluronan and albumin in the attenuation of fluid drainage from joints. *Arthritis Rheum* 43:1175-82, 2000.

94. Scott D, Levick JR, Miserocchi G: Non-linear dependence of interstitial fluid pressure on joint cavity pressure and implications for interstitial resistance in rabbit knee. *Acta Physiol Scand* 179:93-101, 2003.

95. Scott DL, Shipley M, Dawson A, Edwards S, Symmons DP, Woolf AD: The clinical management of rheumatoid arthritis and osteoarthritis: strategies for improving clinical effectiveness. *Br J Rheumatol* 37:546-54, 1998.

96. Smith MM, Ghosh P: The synthesis of hyaluronic acid by human synovial fibroblasts is influenced by the nature of the hyaluronate in the extracellular environment. *Rheumatol Int* 7:113-22, 1987.

97. Steiner G, Tohidast-Akrad M, Witzmann G, Vesely M, Studnicka-Benke A, Gal A, Kunaver M, Zenz P, Smolen JS: Cytokine production by synovial T cells in rheumatoid arthritis. *Rheumatology (Oxford)* 38:202-13, 1999.

98. Stockwell RA. Biology of Cartilage Cells. New York: Cambridge University Press; 1979.

99. Thibault M, Poole AR, Buschmann MD: Cyclic compression of cartilage/bone explants in vitro leads to physical weakening, mechanical breakdown of collagen and release of matrix fragments. *J Orthop Res* 20:1265-73, 2002.

100. Visser NA, van Kampen GPJ, Dekoning MHMT, van der Korst JK: The effects of loading on the synthesis of biglycan and decorin in intact mature articular cartilage in vitro. *Connect Tissue Res* 30:241-50, 1994.

101. Wei X, Messner K: Age- and injury-dependent concentrations of transforming growth factor-beta 1 and proteoglycan fragments in rabbit knee joint fluid. *Osteoarthritis Cartilage* 6:10-8, 1998.

102. Wilkinson LS, Pitsillides AA, Worrall JG, Edwards JC: Light microscopic characterization of the fibroblast-like synovial intimal cell (synoviocyte). *Arthritis Rheum* 35:1179-84, 1992.

103. Worrall JG, Bayliss MT, Edwards JC: Morphological localization of hyaluronan in normal and diseased synovium. *J Rheumatol* 18:1466-72, 1991.

104. Worrall JG, Wilkinson LS, Bayliss MT, Edwards JC: Zonal distribution of chondroitin-4-sulphate/dermatan sulphate and chondroitin-6-sulphate in normal and diseased human synovium. *Ann Rheum Dis* 53:35-8, 1994.

105. Wright V, Dowson D: Lubrication and cartilage. *J Anat* 121:107-18, 1976.

106. Yao Z, Painter SL, Fanslow WC, Ulrich D, Macduff BM, Spriggs MK, Armitage RJ: Human IL-17: a novel cytokine derived from T cells. *J Immunol* 155:5483-6, 1995.

CHAPTER 2:

A MODEL OF SYNOVIAL FLUID LUBRICANT COMPOSITION IN NORMAL AND INJURED JOINTS

2.1   Abstract

The synovial fluid (SF) of joints normally functions as a biological lubricant, providing low-friction and low-wear properties to articulating cartilage surfaces through the putative contributions of proteoglycan 4 (PRG4), hyaluronan (HA), and surface active phospholipids (SAPL). These lubricants are secreted by chondrocytes in articular cartilage and synoviocytes in synovium, and concentrated in the synovial space by the semi-permeable synovial lining. A deficiency in this lubricating system may contribute to the erosion of articulating cartilage surfaces in conditions of arthritis. A quantitative intercompartmental model was developed to predict in vivo SF lubricant concentration in the human knee joint. The model consists of a SF compartment that (a) is lined by cells of appropriate types, (b) is bound by a semi-permeable membrane, and (c) contains factors that regulate lubricant secretion. Lubricant concentration was predicted with different chemical regulators of chondrocyte and synoviocyte secretion, and also with therapeutic interventions of joint lavage and HA injection. The model predicted steady-state lubricant concentrations that were within physiologically observed ranges, and which were

markedly altered with chemical regulation. The model also predicted that when starting from a zero lubricant concentration after joint lavage, PRG4 reaches steady-state concentration ~10-40 times faster than HA. Additionally, analysis of the clearance rate of HA after therapeutic injection into SF predicted that the majority of HA leaves the joint after ~1-2 days. This quantitative compartmental model allows integration of biophysical processes to identify both environmental factors and clinical therapies that affect SF lubricant composition in whole joints.

2.2 Introduction

The synovial fluid (SF) of natural joints normally functions as a biological lubricant as well as a biochemical pool through which nutrients and regulatory cytokines traverse. SF contains molecules that provide low-friction and low-wear properties to articulating cartilage surfaces. Molecules postulated to play a key role, alone or in combination, in lubrication are proteoglycan 4 (PRG4) [93] present in SF at a concentration of 0.05-0.35 mg/ml [79], hyaluronan (HA) [64] at 1-4 mg/ml [53], and surface-active phospholipids (SAPL) [86] at 0.1 mg/ml [53]. Synoviocytes secrete PRG4 [32, 83] and are the major source of SAPL [18, 31, 85], as well as HA [29, 57], in SF. Other cells also secrete PRG4, including chondrocytes in the superficial layer of articular cartilage [80, 82] and, to a much lesser extent, cells in the meniscus [84].

As a biochemical depot, SF is an ultrafiltrate of plasma that is concentrated by virtue of its filtration through the synovial membrane. The synovium is a thin lining (~50-60 μm in humans) comprised of tissue macrophage A cells, fibroblast-derived B cells [3, 72, 103], and fenestrated capillaries [37]. It is backed by a thick layer (~100 μm) of loose connective tissue called the subsynovium (SUB) that includes an extensive system of lymphatics for clearance of transported molecules. The cells in the synovium form a discontinuous layer separated by intercellular gaps of several microns in width [37, 54]. The extracellular matrix in these gaps contains collagen types I, III, and V [2, 73], hyaluronan [104], chondroitin sulphate [69, 105], biglycan and decorin proteoglycans [12], and fibronectin [68]. The synovial matrix provides the permeable pathway through which exchange of molecules occurs [44], including the lubricants PRG4 and HA, but also offers sufficient outflow resistance [12, 90] to retain large solutes of SF within the joint cavity. Together, the appropriate reflection

of secreted lubricants by the synovial membrane and the appropriate lubricant secretion by cells are necessary for development of a mechanically functional SF.

The mechanobiology of joints and SF constitutes a complex, low-friction, low-wear system that is normally in homeostasis. However, in arthritis, injury, and artificial joint failure, there is increased friction between the articulating surfaces and concomitant erosion of the load bearing elements [9]. This increase in friction is associated with altered SF composition. Specifically, the SF PRG4 concentration decreases following acute injury, as does the friction-lowering property of such SF [20], while PRG4 concentration increases in patients undergoing arthrocentesis procedures [79]. HA [7] and SAPL [71] also exhibit decreased concentrations in osteoarthritis, and HA is also decreased with failure of artificial joints [53]. The mechanisms by which altered SF lubricant composition occur are unknown.

Joint injury and arthritis may additionally result in dramatic changes in the concentration of some cytokines in SF [8, 10, 21, 22, 58, 65, 102]. A complex milieu of regulatory cytokines exist in SF, including TGF-β, IGF-1, TNF-α, IL-1, and IL-6 [22, 35, 78, 99, 102]. The cytokines TGF-β and IL-1 can have significant effects on secretion of lubricants by both chondrocytes and synoviocytes. IL-1 downregulates PRG4 secretion by chondrocytes, while TGF-β upregulates PRG4 secretion [23, 81]. Additionally, both TGF-β and IL-1 result in increased HA secretion by synoviocytes [29, 57]. Thus, the changing chemical environment with injury and arthritis may have significant effects on lubricant secretion by cells, and, consequently, SF lubricant composition.

A variety of treatments have been developed to biologically alter the synovial joint environment in injury and arthritis. Some pharmaceutical agents are capable of reducing pain and inflammation [27, 60]. HA injections have been purported to affect

the biology of the joint in order to restore the viscosity and protective functions of the synovial fluid [59, 98]. Therapeutic joint lavage has been used to cleanse the joint of cartilage degradation products, proinflammatory cells, and destructive enzymes associated with arthritis [4], and can be performed alone or in combination with anti-inflammatory steroids [26, 96]. These treatments have not specifically targeted restoration of lubrication in joints, and treatment effects on SF lubricant composition have not yet been examined.

The whole synovial joint, including cartilage, synovium and SF (**Figure 2.1**), presents complexities that make it difficult to measure continuously the *in vivo* SF lubricant composition, and also the main determinants of dynamics in this composition. General models of fluid flow and solute transport through a matrix (reviewed in [15, 42]) have been developed, and extensive analysis of the synovium structure has been performed to obtain values for functional parameters that control its transport properties [44, 46, 47, 69, 70, 75, 89]. Knowledge of the structure of synovium, along with related published data, has been applied to the models of fluid and solute transport to specifically model the flow of albumin from synovial capillaries into SF and out through the synovium membrane [44]. Additionally, the concept of combining the theory of mass balance with the data on fluid and solute transport through the synovium has been introduced as an approach for determining the concentration of a molecule in SF, such as a lubricant [45].
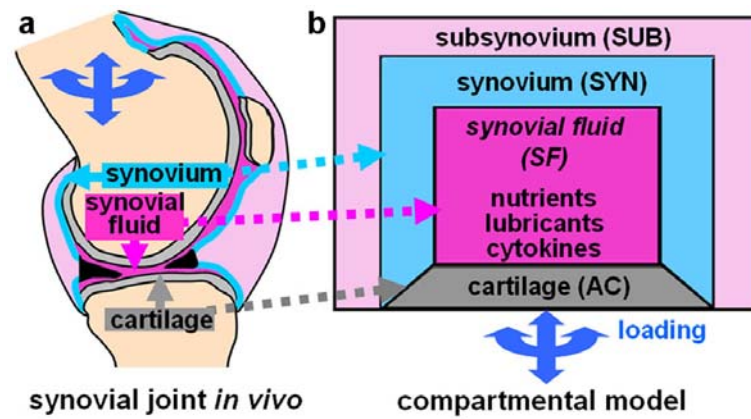
Figure 2.1: (A) Synovial joints are generally composed of cartilage, synovium, and SF, (B) modeled by communicating compartments in which chemical and mechanical factors regulate lubricant secretion.

Thus, the objective of this study was to develop a mathematical model to analyze lubricant composition in SF of whole human knee joints, expanding upon the approaches taken in previous studies and utilizing relevant published functional parameters. The model was applied to determine theoretically (1) the steady-state lubricant concentration in SF under normal and altered chemical environments in the synovial joint that may occur with injury and disease, (2) the kinetics associated with attaining these steady-state concentrations from a zero starting concentration after simulated joint lavage, and (3) the clearance rate of HA from the joint after simulated therapeutic HA injection. The validity of the model was assessed by comparison of the lubricant concentrations predicted at steady-state with those observed *in vivo*.

2.3   Model

The model consists of a SF compartment surrounded by articular cartilage and a semi-permeable synovial membrane that separates the SF from an underlying subsynovium (SUB) compartment (**Figure 2.2**). Lubricants are secreted into the SF by chondrocytes in articular cartilage (AC) and synoviocytes in the synovium (SYN). Some lubricants are lost from the SF by either degradation or flux through the membrane into the SUB; however, the synovium offers sufficient outflow resistance to retain a large pool of lubricant macromolecules in the SF. Transient accumulation of lubricants exists in the SF compartment until the system reaches a steady-state lubricant composition. A complete list of variables and parameters included in the model are shown in **Table 2.1**.
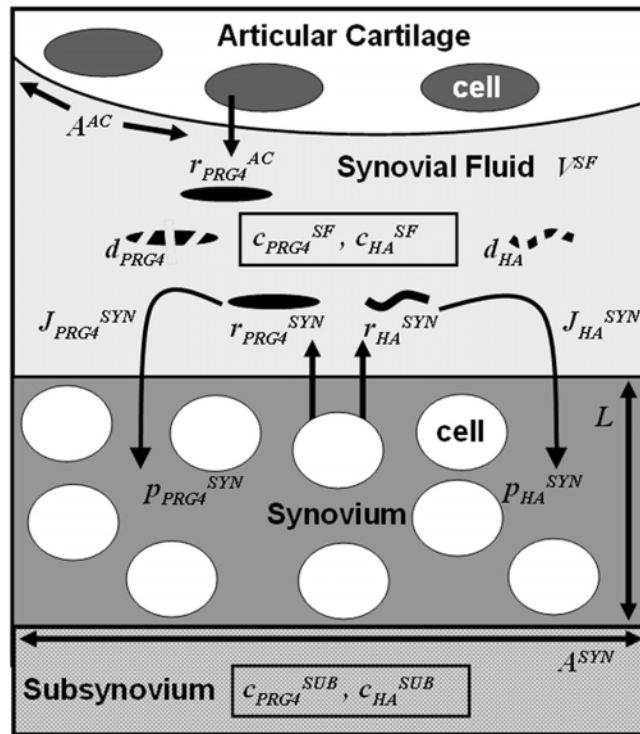
Figure 2.2: Schematic of synovial fluid composition model. Cartilage and synovium form a compartment around the synovial fluid, where lubricants secreted by the chondrocytes and synoviocytes are retained by the semi-permeable synovium. See **Table 2.1** for a complete list of variables.

Table 2.1: List of model variables and parameters.

Variable or parameter	Units	Description
i		PRG4, HA
c_i^{SF}	mg/ml	Concentration of i in synovial fluid
c_i^{SUB}	mg/ml	Concentration of i in subsynovium
J_i^{SYN}	mg/s	Total flux of i through membrane area
$J_{i,diff}^{SYN}$	mg/s	Flux of i due to diffusion
$J_{i,conv}^{SYN}$	mg/s	Flux of i due to fluid convection
J_v^{SYN}	ml/s	Fluid flow rate out of the synovium
p_i^{SYN}	cm/s	Permeability of i through synovium
p_i^{INT}	cm/s	Permeability of i through interstial space
$\Delta\pi_i$	cm H$_2$0	Osmotic pressure diff. of SF and SUB
ΔP^{SYN}	cm H$_2$0	Hydrostatic pressure diff. of SF and SUB
k_i	cm/(s•cm H$_2$0)	Hydraulic conductance of synovium
r_i^{SYN}	mg/(cm^2•s)	Secretion rate of i by synoviocytes (SYN)
r_i^{AC}	mg/(cm^2•s)	Secretion rate of i by articular cartilage (AC)
d_i	mg/s	Degradation rate of i in synovial fluid
A^{SYN}	cm^2	Area of synovial membrane
A^{AC}	cm^2	Area of cartilage surfaces
L	cm	Membrane thickness
t	s	Time
α		Environmental factor
V^{SF}	ml	Volume of synovial fluid
D_i	cm^2/s	Diffusion coefficient of i in free solution
ζ_{col}	cm^2/s	Restricted diffusion coeff. of i in synovium
ϕ_i		Partition coefficient of i for synovium
σ_i		Reflection coefficient of i for synovium
θ_{cell}		Volume fraction of cells in synovium
θ_{col}		Volume fraction of collagen in synovium
θ_{GAG}		Polymer volume fraction in GAG matrix
ρ_i	mg/ml	Density of i
a_{GAG}	nm	Radius of GAG chains in synovium
a_i	nm	Radius of i
ζ_{col}		Tortuosity due to collagen fibrils
ζ_{cell}		Tortuosity due to cells

Governing Equations

The rate of change in mass of lubricant i (i=PRG4, HA, or SAPL) that has a concentration of c_i^{SF} in a SF volume of V^{SF} is assumed to depend on the secretion rate of i by AC (r_i^{AC}) and SYN (r_i^{SYN}) of areas A^{AC} and A^{SYN}, the degradation rate of i in SF (d_i^{SF}), and the flux of i across the synovial membrane area (J_i^{SYN}). All parameters are also a function of time, t, and the environment, which is described by the parameter α and includes chemical and mechanical factors.

A mass balance applied to the SF compartment results in:

$$\frac{\partial[V^{SF}(t,\alpha)\cdot c_i^{SF}(t,\alpha)]}{\partial t} = r_i^{SYN}(t,\alpha)\cdot A^{SYN}(t,\alpha) + r_i^{AC}(t,\alpha)\cdot A^{AC}(t,\alpha) - d_i(t,\alpha) - J_i^{SYN}(t,\alpha) \quad \textbf{(1)}$$

The degradation rate of i (d_i) is dependent upon the concentration and activity of degradative enzyme in SF. For example, the protein PRG4 may be targeted by various enzymes, and in particular has been shown to be degraded by elastase [20]. As shown by that study in a rabbit knee model of acute injury, injured SF had an elastase activity level of 1-4 μunits/ml, or about 0.2-0.6 pg/ml of elastase (1 mg = ~6.8 units) Application of 7 μg of elastase to 5 μg of PRG4 resulted in complete degradation of PRG4 within 2-6 hours. Thus, d_i can be of the form:

$$d_i(t,\alpha) = X(t,\alpha)\cdot Y(t,\alpha)\cdot c_i^{SF}(t,\alpha)\cdot V^{SF}(t,\alpha) \quad \textbf{(2)}$$

where X is the ratio of concentration of degradative enzyme in SF to the concentration of lubricant in SF, and Y is the mass of substrate degraded per mass of enzyme per unit time. A similar analysis can be performed for other degradative enzymes that target PRG4, and also for enzymes present in SF that degrade HA, such as hyaluronidase.

The flux of lubricants (J_i^{SYN}) across the membrane is a sum of the solute flux due to diffusion ($J_{i,diff}^{SYN}$) and the solute flux due to convective fluid flow ($J_{i,conv}^{SYN}$):

$$J_i^{SYN} = J_{i,diff}^{SYN} + J_{i,conv}^{SYN} \tag{3}$$

$J_{i,diff}^{SYN}$ is dependent upon the permeability ($p_{i,}^{SYN}$) and area (A^{SYN}) of the synovial membrane and the concentration gradient between the *SF* and *SUB* compartments:

$$J_{i,diff}^{SYN}(t,\alpha) = p_i^{SYN}(t,\alpha) \cdot [c_i^{SF}(t,\alpha) - c_i^{SUB}(t,\alpha)] \cdot A^{SYN}(t,\alpha) \tag{4}$$

$J_{i,conv}^{SYN}$ is dependent upon the fluid flow out of the membrane (J_v^{SYN}), the reflection coefficient of the membrane (σ_i), and the concentration of i in SF (c_i^{SF}) [15, 66]:

$$J_{i,conv}^{SYN} = J_v^{SYN}(1 - \sigma_i) \cdot c_i^{SF} \tag{5}$$

J_v^{SYN} can be described by the following expression for fluid flow across a leaky membrane [36]:

$$J_v^{SYN} = k[\Delta P^{SYN}(t,\alpha) - \sigma_i(t,\alpha)\Delta\pi_i(t,\alpha)] \cdot A^{SYN}(t,\alpha) \tag{6}$$

where ΔP^{SYN} is the hydrostatic pressure difference and $\Delta\pi_i$ is the osmotic pressure difference between SF and SUB compartments, respectively, and k is the hydraulic conductance of the synovium.

Membrane Permeability

Lubricant transport through the synovium occurs around the spaces, or volume fractions, occupied by synoviocytes (θ_{cell}) and collagen fibrils (θ_{col}), and around the polymer volume fraction of glycosaminoglycans (θ_{GAG}), and is further limited by the tortuosity of the pathway imposed by the cells (ζ_{cell}) and collagen fibrils (ζ_{col}) [44]. Thus, there is restricted diffusion of lubricants within the synovium compared to diffusion in free solution. The restricted diffusion coefficient (D_i^{SYN}) for a globular solute within the GAG matrix of synovium is related to the diffusion coefficient in free solution (D_i), θ_{GAG}, the radius of GAG chains (a_{GAG}), and the effective radius of the solute (a_i) [63]:

$$D_i^{SYN}(t,\alpha) = D_i \cdot e^{\{-\sqrt{\theta_{GAG}(t,\alpha)} \cdot (1+\frac{a_i}{a_{GAG}})\}} \tag{7}$$

The a_i can be taken as the Stokes-Einstein equivalent radius of a solute, estimated from its molecular weight (MW) and density (ρ), according to the following, where N_a is Avogadro's number [97]:

$$a_i = \left(\frac{3 \cdot MW}{4 \cdot \pi \cdot \rho \cdot N_a} \right)^{1/3} \tag{8}$$

The permeability associated with the interstitial, or extracellular, space (p_i^{INT}) is a function of the restricted diffusion coefficient of the lubricant in the matrix (D_i^{SYN}), the partition coefficient (ϕ_i), the volume fraction (θ_{col}) and tortuosity (ζ_{col}) of the impenetrable collagen matrix components, and the thickness of the membrane (L) [44]:

$$p_i^{INT}(t,\alpha) = \frac{D_i^{SYN}(t,\alpha) \cdot \phi_i(t,\alpha) \cdot [1 - \theta_{col}(t,\alpha)] \cdot \zeta_{col}(t,\alpha)}{L}$$

(9)

The ϕ_i of the lubricant in the matrix represents the ratio of the available solute space to the space occupied by the GAGs. The fractional space available to the solute (K_{AV}) is given by the Ogston relation [63].

$$K_{AV}(t,\alpha) = e^{\left\{ -\frac{\theta_{GAG}(t,\alpha)}{a_{GAG}^2}\cdot(a_{GAG}+a_i)^2 \right\}}$$

(10)

The ϕ_i is related to K_{AV} by the following [15]:

$$\phi_i(t,\alpha) = \frac{K_{AV}(t,\alpha)}{e^{-\theta_{GAG}}}$$

(11)

Finally, the permeability of the entire synovium (p_i^{SYN}) to the lubricant i is a function of the interstitial permeability (p_i^{INT}), and also the volume fraction (θ_{cell}) and tortuosity (ζ_{cell}) imposed by the impenetrable synoviocytes in the membrane [44]:

$$p_i^{SYN}(t,\alpha) = p_i^{INT}(t,\alpha) \cdot [1 - \theta_{cell}(t,\alpha)] \cdot \zeta_{cell}(t,\alpha)$$

(12)

Non-Dimensional Equations

The governing equations of the model can be non-dimensionalized by defining non-dimensional concentration ($c_i^{,SF}$), secretion rates ($r_i^{,SYN}$, $r_i^{,AC}$), degradation rate (d_i') and time (t'):

$$c_i'^{SF} = \frac{c_i^{SF}}{c_{i,basal}^{SF}} \tag{13}$$

$$r_i'^{SYN} = \frac{r_i^{SYN}}{r_{i,basal}^{SYN}} \tag{14}$$

$$r_i'^{AC} = \frac{r_i^{AC}}{r_{i,basal}^{AC}} \tag{15}$$

$$d_i' = \frac{d_i}{d_{i,basal}} \tag{16}$$

$$t_i' = \frac{t}{\tau_i} \tag{17}$$

After substitution and simplification, a non-dimensional mass balance governing equation results:

$$\frac{\partial c_i'^{SF}}{\partial t'} = k_1 r_i'^{SYN} + k_2 r_i'^{AC} - k_3 d_i' - c_i'^{SF} \tag{18}$$

The non-dimensional parameters, k_1, k_2, k_3, and τ_i are defined below:

$$k_1 = \frac{r_{i,basal}^{SYN}}{p_i^{SYN} c_{i,basal}^{SF}} \tag{19}$$

$$k_2 = \frac{A^{AC} r_{i,basal}{}^{AC}}{A^{SYN} p_i{}^{SYN} c_{i,basal}{}^{SF}} \tag{20}$$

$$k_3 = \frac{d_{i,basal}}{A^{SYN} p_i{}^{SYN} c_{i,basal}} \tag{21}$$

$$\tau_i = \frac{V^{SF}}{p_i{}^{SYN} A^{SYN}} \tag{22}$$

Model Assumptions

General assumptions. It is assumed that the only parameters in the model that are altered with changes in the chemical environment (i.e. are a function of α) are the lubricant secretion rates and the dependent lubricant concentration. It is also assumed that the concentration of lubricants in the SUB compartment is zero for all situations, as transported fluid and solutes drain away via the system of lymphatics along intermuscular connective tissue planes [34, 39, 40].

$$c_i{}^{SUB}(t,\alpha) = 0 \tag{23}$$

SF volume is kept in a steady-state, as the filtration of fluid across the capillary wall into SF occurs at a rate equal to that of lymph flow [42]. It is also assumed that the degradation of lubricants is negligible compared to cellular secretion rates:

$$d_i(t,\alpha) = 0 \tag{24}$$

Additionally, the flux of lubricants due to fluid convection is also considered negligible compared to the flux due to diffusion, as the ratio of convective transport of solute to diffusive transport of solute was estimated for albumin to be $\ll 1$ [56]:

$$J_{i,conv}(t,\alpha) = 0 \tag{25}$$

Further support for this assumption comes from the fact that convective fluid flow out of the joint cavity may be attenuated by SF osmotic pressure at high lubricant concentrations, and also by a concentration polarization phenomenon for large molecules in SF such as HA [55, 76, 88].

Case 1: Steady-state. The concentration of lubricants at steady-state will not change with time:

$$\frac{\partial c_i^{SF}}{\partial t}(t = \infty, \alpha) = 0 \tag{26}$$

Case 2: Joint lavage. After joint lavage, the concentration of lubricants in the SF will be effectively reduced to zero:

$$c_i^{SF}(t = 0, \alpha) = 0 \tag{27}$$

The secretion rates with no chemical stimulation will be considered to be basal levels. Also, the volume of SF will be unaffected by the lavage procedure as any volume of fluid that remains in the joint and exceeds normal SF volume will be removed quickly. The transynovial flow rate of water is normally ~5-10 µl/min at an

intraarticular pressure of ~2 cmH$_2$O (flexed knee joint), but under raised intraarticular pressures of ~20 cmH$_2$O (chronic joint effusion) that occur with large increases in SF volume, is ~20-40 µl/min [13, 87]. Thus, the SF volume of 1 ml in normal human knee joints turns over in ~1-2 hrs, and portions of volumes in excess of this would likely equilibrate in <1 hr.

Case 3: HA injection. Prior to the injection, the concentration of HA in SF will be equal to that achieved at steady-state:

$$c_{HA}^{SF}(t = 0^-, \alpha) = c_{HA}^{SF}(t = \infty, \alpha) \tag{28}$$

HA injections are generally on the order of 20 mg [98], and this will represent the bolus of HA introduced into the joint.

$$c_{HA}^{SF}(t = 0^+, \alpha) = c_{HA}^{SF}(t = 0^-, \alpha) + \frac{20mg}{V^{SF}} \tag{29}$$

The volume of SF will also be unaffected by this procedure due to the relatively high transynovial flow rate of water, particularly at raised intraarticular pressures and volumes. With a flow rate of ~20-40 µl/min [13, 87], a typical injection of 2 ml buffer solution would drain in ~1-2 hr.

Model Parameters

Values for parameters used in the model are based on published values in the literature. The properties of cartilage, synovium, and synoval fluid utilized in the

model include cartilage and synovium surface area, synovial fluid volume, and organization of the synovium relating to transynovial transport. The total surface area in the human knee joint is 121 cm^2 for cartilage [19] and 277 cm^2 for synovium [17], and the synovial fluid volume enclosed by these surfaces is 1.1 ml [74]. The synovium, which is 50 µm thick in humans [70], has a cell volume fraction varying from 0.42 at the surface to 0.67 in deeper layers and a tortuosity due to the cells of 0.69 [46, 47]. The volume fraction due to collagen is 0.2 [44] and the tortuosity is 0.70 [50, 92]. The portion of synovium through which lubricants travel contains GAG chains with radii of 0.56 nm [63] and a volume fraction of 0.0075 [75, 89].

The molecular weight forms of PRG4 that have been isolated from SF and cartilage exist in the range of 220 kDa [95] to 345 kDa [82], while HA exists in the range of 2000-6000 kDa [25]. The mass density for both PRG4 and HA is 1.45 g/ml [49, 51, 94]. These parameters were used together to calculate a range of PRG4 and HA radii, assuming the idealized case that they exist in SF as globular solutes.

Diffusion coefficients have been determined for PRG4 and HA in free solution, and are 1.11 x 10^{-7} cm^2/s [94] and 9.8 x 10^{-8} cm^2/s [48], respectively. These free diffusion coefficients were used with the above parameter values of tissue and lubricant properties to calculate restricted diffusion and also permeability of lubricants through synovium.

Secretion rates used in the model depend on the regulatory factors present in the system, and are different under basal, TGF-β (10 ng/ml), and IL-1 (10 ng/ml) conditions. IL-1 downregulates PRG4 secretion by chondrocytes from 2.89 x 10^{-7} mg/(cm^2·s) to 1.16 x 10^{-7} mg/(cm^2·s), while TGF-β upregulates PRG4 secretion to 1.16 x 10^{-6} mg/(cm^2·s) [23, 81]. Synoviocyte PRG4 secretion is similarly regulated by these cytokines, as IL-1 downregulates secretion from 4.05 x 10^{-9} mg/(cm^2·s) to 2.43 x

10^{-9} mg/(cm^2·s), and TGF-β upregulates secretion to 2.23 x 10^{-8} mg/(cm^2·s) (unpublished data). TGF-β and IL-1 result in increased HA secretion by synoviocytes, rising from 2.84 x 10^{-9} mg/(cm^2·s) to 6.72 x 10^{-8} mg/(cm^2·s) and 9.95 x 10^{-8} mg/(cm^2·s), respectively [29]. Cellular secretion rates for synoviocytes were converted to tissue secretion rates using a ~0.8 surface area fraction of synovium occupied by synoviocytes [70] and assuming a typical cell diameter of ~16 μm.

Solutions

Using the parameter values above and listed in **Table 2.2**, the first-order system of ordinary differential equations were solved numerically using Matlab 7.0 (The MathWorks, Natick, MA). Results are given for both the low and high end of the predicted concentration range for each lubricant. General concentration profiles are also presented as a function of the non-dimensional constants and τ_i.

Table 2.2: Values used in the model. TGF-β and IL-1 values are for a concentration of 10 ng/ml.

Variable	Units	Value (basal)	(TGF-β)	(IL-1)	References
D_{HA}	cm²/s	9.80×10^{-8}			Lu, 2005
D_{PRG4}	cm²/s	1.11×10^{-7}			Swann, 1981
r_{HA}^{SYN}	mg/(cm²•s)	2.84×10^{-9}	6.72×10^{-8}	9.95×10^{-8}	Haubeck, 1995
r_{PRG4}^{AC}	mg/(cm²•s)	2.89×10^{-7}	1.16×10^{-6}	1.16×10^{-7}	Schmidt, 2005
r_{PRG4}^{SYN}	mg/(cm²•s)	4.05×10^{-9}	2.23×10^{-8}	2.43×10^{-9}	unpublished data
A^{AC}	cm²	121			Eckstein, 2001
A^{SYN}	cm²	277			Davies, 1946
V^{SF}	ml	1.1			Ropes, 1940
L	cm	0.005			Price, 1995
θ_{cell}		0.42-0.67			Levick, 1989a,b
θ_{col}		0.2			Levick, 1994
θ_{GAG}		0.0075			Sabaratnam, 2005 Scott, 2003
ζ_{col}		0.7			Maroudas, 1970, Sullivan, 1942
ζ_{cell}		0.69			Levick, 1989a,b
a_{GAG}	nm	0.56			Ogston, 1973
ρ_{HA}	g/ml	1.45			Mahlbacher, 1992 Mason, 1982
ρ_{PRG4}	g/ml	1.45			Swann, 1981
MW_{HA}	kDa	2000-6000			Fraser, 1997
MW_{PRG4}	kDa	220-345			Swann, 1977 Schumacher, 1994

2.4 Results

Case 1: Steady-state Lubricant Concentration

The form of the solution for c_i^{SF} at steady-state is determined from equations 13-18,

$$c_i^{SF}(t=\infty,\alpha)=c_{i,basal}^{SF}\{k_1\cdot\frac{r_i^{SYN}(\alpha)}{r_{i,basal}^{SYN}}+k_2\cdot\frac{r_i^{AC}(\alpha)}{r_{i,basal}^{AC}}\}\tag{30}$$

or equivalently, from equations 1 and 4:

$$c_i^{SF}(t=\infty,\alpha)=\frac{r_i^{SYN}(\alpha)+r_i^{AC}(\alpha)\cdot\frac{A^{AC}}{A^{SYN}}}{p_i^{SYN}}\tag{31}$$

The form of the equations shows that increases in r_i^{AC} and r_i^{SYN} result in increases in c_i^{SF}. Increases in k_1 and k_2 also cause increases in c_i^{SF}, and can be achieved by decreases in p_i^{SYN} or increases in the ratio of A^{AC} to A^{SYN}.

A range of values has been noted for some of the parameters used in the model (**Table 2.2**), and thus there was a range of model predictions for lubricant concentrations in SF. Permeability ranged from 6.79 x 10^{-7} cm/s - 1.56 x 10^{-6} cm/s for PRG4 and 1.73 x 10^{-8} cm/s - 1.84 x 10^{-7} cm/s for HA. The range of predictions for c_{PRG4}^{SF} and c_{HA}^{SF} at steady-state under basal conditions were 0.08-0.19 mg/ml and 0.02-0.16 mg/ml, respectively. With TGF-β stimulation, c_{PRG4}^{SF} increased to 0.34-0.77 mg/ml and c_{HA}^{SF} increased to 0.36-3.89 mg/ml, while with IL-1 c_{PRG4}^{SF} decreased to 0.03-0.08 mg/ml but c_{HA}^{SF} increased to 0.54-5.77 mg/ml (**Table 2.3**).

Table 2.3: Steady-state model predictions of ranges of synovial fluid lubricant composition under basal conditions or with 10 ng/ml of TGF-β or IL-1.

	Condition	Concentration range [mg/ml]	
		PRG4	HA
	physiological	0.05 – 0.35	1 – 4
predicted	basal	0.08 – 0.19	0.02 – 0.16
predicted	TGF-β	0.34 – 0.77	0.36 – 3.89
predicted	IL-1	0.03 – 0.08	0.54 – 5.77

Transient Changes in Lubricant Concentration

The form of the solution for transient changes in c_i^{SF} is determined from equations 13-18,

$$\frac{\partial c_i^{SF}(\alpha,t)}{\partial t} = \frac{c_{i,basal}^{SF}}{\tau_i} \left\{ k_1 \frac{r_i^{SYN}(\alpha)}{r_{i,basal}^{SYN}} + k_2 \frac{r_i^{AC}(\alpha)}{r_{i,basal}^{AC}} - \frac{c_i^{SF}(\alpha,t)}{c_{i,basal}^{SF}} \right\} \tag{32}$$

or equivalently, from equations 1 and 4:

$$\frac{\partial c_i^{SF}(\alpha,t)}{\partial t} = \frac{r_i^{SYN}(\alpha) \cdot A^{SYN} + r_i^{AC}(\alpha) \cdot A^{AC} - p_i^{SYN} \cdot c_i^{SF}(\alpha,t) \cdot A^{SYN}}{V^{SF}} \tag{33}$$

General curves with concentration plotted against time for conditions of joint lavage and HA injection are shown in **Figure 2.3.** This general case illustrates that steady state lubricant concentration levels are governed the non-dimensional constants k_1 and k_2 and secretion rates, while the temporal effects are governed by τ_i. The parameter τ_i describes the kinetics of lubricant concentration in SF, and represents the time to reach 63% of the steady state concentration after joint lavage, or time for 63% of injected HA to be cleared from the SF. The form of τ_i shows that increases in p_i^{SYN} and A^{SYN} result in decreases in τ_i, while increases in V^{SF} cause increases in τ_i. Numerical values for transient and steady state lubricant concentrations in the different cases are discussed below.
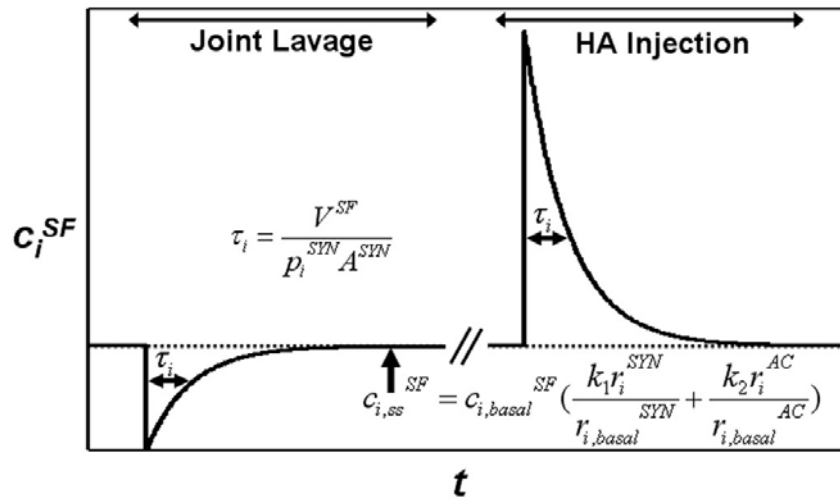
Figure 2.3: General curves of concentration plotted against time for conditions of joint lavage and HA injection, illustrating that steady state lubricant concentration levels are governed the non-dimensional constants k_1 and k_2 and secretion rates, while the temporal effects are governed by τ_i.

Case 2: Joint Lavage

After joint lavage, the starting concentration of lubricants in SF was decreased in a step-wise manner to 0 mg/ml at t=0 and returned to the predicted steady-state concentration with kinetics that were markedly different for PRG4 and HA. The range of time constants, which indicate the time to reach 63% of steady-state concentration of lubricant in SF were 0.03-0.07 days for PRG4 (**Figure 2.4A,B**) and 0.25-2.66 days for HA (**Figure 2.4C,D**). Chemical stimulation with TGF-β and IL-1 is not predicted to alter the kinetics of lubricant restoration following joint lavage; however, as noted for steady-state predictions, TGF-β and IL-1 dictated the magnitude attained at steady-state.

Case 3: Therapeutic HA Injection.

After an HA injection of 20 mg, the concentration of HA in SF increased by 18.2 mg/ml and then returned to steady-state concentration after a duration of time (**Figure 2.5A,B**). The time for 63% of the injected HA to be cleared from the joint, was 0.25-2.66 days. As stated above, chemical stimulation with TGF-β and IL-1 did not alter the kinetics associated with HA injection, but dictated the magnitude of the final steady-state concentration.
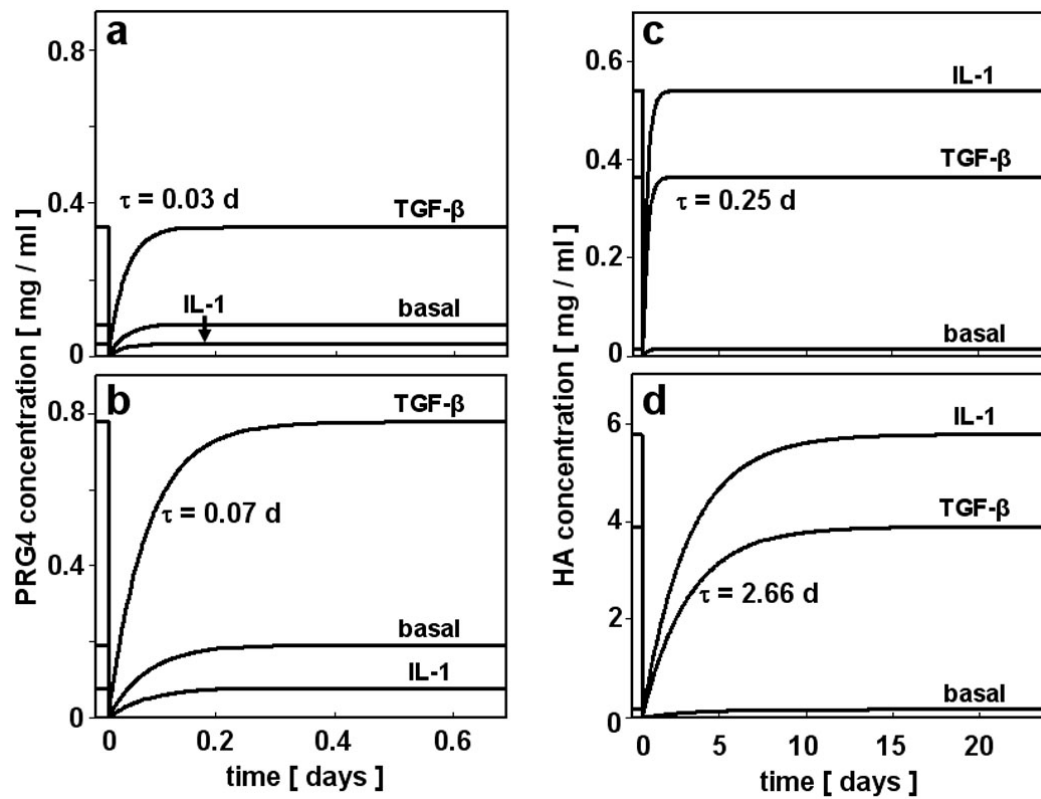
Figure 2.4: Transient rise in synovial fluid lubricant concentration after joint lavage, with or without chemical regulatory factors, and associated time constants, τ. (**A**) low end PRG4 predictions, (**B**) high end PRG4 predictions, (**C**) low end HA predictions, and (**D**) high end HA predictions.
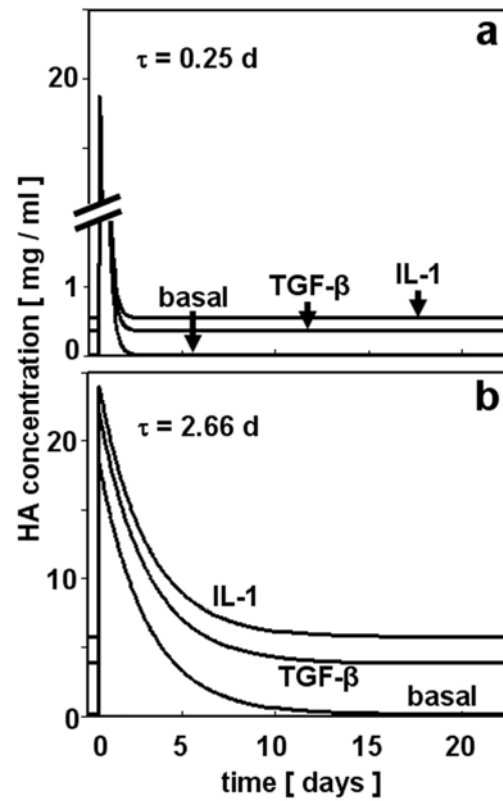
Figure 2.5: Transient changes in synovial fluid lubricant concentration after therapeutic HA injection, with or without chemical regulatory factors, and associated time constants, τ. (**A**) low end HA predictions and (**B**) high end HA predictions.

2.5   Discussion

This study describes some essential features of steady-state and kinetic SF lubricant composition in whole joints under normal or altered chemical environments, and also with different therapeutic interventions. The model predicts steady-state lubricant concentrations that are consistent with physiologically observed concentrations. Further, chemical alterations in the synovial joint environment that may occur in injury and disease were predicted to alter lubricant concentration. The kinetics associated with joint lavage predicted that PRG4 and HA achieve steady-state concentration on distinct time scales. Finally, therapeutic injection of HA into SF was predicted to cause an immediate increase in HA concentration, which returns to steady-state concentration after ~1-2 days.

The quantitative intercompartmental model developed in this study included several assumptions that allowed for a straightforward analysis that could be expanded upon. For example, the model could be extended by including additional environmental factors and allowing a number of parameters to change with the environment and time. Some parameters in the model are also described in bulk and spatially averaged terms rather than on multiple scale levels. Finally, physical and chemical interactions of lubricants with their environment were not considered in the model, and may affect the free concentration of lubricants in SF.

While lubricant secretion rates were the sole variables in the model that were assumed to be dependent on chemical factors, other variables and parameters included in the model may also be affected by these and other environmental factors. Such environmental factors can include mechanical stimuli that are also known to regulate lubricant secretion by both chondrocytes and synoviocytes. Compressive forces

downregulate PRG4 secretion by chondrocytes, while shear forces upregulate PRG4 secretion [61, 62]. Mechanical stretching of synovium results in increased HA secretion by synoviocytes [57]. Both chemical and mechanical factors may affect not only lubricant secretion, but also parameters that influence permeability of the synovial membrane. For example, different cytokines may have anabolic or catabolic effects on the extracellular matrix of synovium and thus alter its composition and organization. The increased permeability of the synovium in rheumatoid arthritis may possibly reflect such a phenomenon [41]. Joint motion involving stretching of the synovium may result in changes in thickness and area of the membrane, leading to altered permeability. Chemical and mechanical factors may also affect synovium permeability by regulating aspects of lubricant metabolism, such as the molecular weight form of lubricant that is secreted. In the SF of arthritic joints, HA exists at a lower molecular weight [5, 16], while in normal SF, PRG4 may exist in both monomeric and multimeric forms [67]. Changes in any of these parameters that affect permeability to lubricants may also alter the rate at which fluid is transported across the synovial membrane. The direction, i.e. entry or exit, of this fluid transport may similarly be controlled by chemical and mechanical factors, such as osmotic pressure exerted by SF molecules and hydrostatic pressure due to joint flexion and extension. Thus, changes in parameters that affect permeability may subsequently lead to changes in SF volume. Such concomitant alterations in membrane area and permeability, SF volume, and the turnover of SF are observed in cases of joint swelling associated with injury or disease [43, 100].

The parameters of the compartmental model may be taken as a macroscopic representation of processes occurring on multiple scales, each of which may have distinct spatial and temporal characteristics. For example, the matrix composition of

the synovium may be affected by cytokines that alter the content of a specific collagen type. The current model reflects this change only in the lumped parameters that represent total collagen volume fraction and tortuosity, and thus does not attempt to discriminate details on this scale. The model also does not reflect alterations in gene expression for either lumped or specific components. At each of these scales, tissue properties may vary throughout the total area or volume, and triggered events may occur over distinct time scales for different components.

Interactions of lubricants with themselves, other lubricants, or with surrounding tissues could also be included in the model. For example, PRG4 may interact with itself, as both monomeric and multimeric forms have been observed [67]. HA may also be influenced by its own presence, as secretion by synoviocytes can depend upon the concentration and molecular weight form of HA in the environment of the synoviocytes [91]. Lubricant molecules may also interact with each other. In particular, the putative lubricant surface active phospholipid (SAPL) may bind to HA or PRG4 and be carried in SF by these molecules [30]. It should be noted that SAPL was not examined in this model as there is conflicting evidence on its role in joint lubrication [31, 33]. However, its behavior indicates that interactions between molecules in SF do exist. Electrostatic interactions between lubricants and the extracellular matrix of synovium, and binding of lubricants to tissues in the joint may also be important processes affecting SF lubricant composition.

Steady-state lubricant concentrations predicted by the model were generally consistent with those observed physiologically. The concentration of PRG4 in human SF ranges from 52-350 µg/ml in normal joints post-mortem, and increases to 276-762 µg/ml in SF obtained from patients undergoing arthrocentesis procedures [79]. In acute injury in a rabbit knee model, PRG4 concentration decreased from 280 µg/ml to

20-100 µg/ml [20]. Model predictions of $c_{PRG4}{}^{SF}$ at steady-state under basal conditions were comparable to that observed in normal SF *in vivo*. The model predicted an increased PRG4 concentration with TGF-β stimulation but decreased concentration with IL-1, which may reflect distinct changes in the SF chemical environment that occur with different types of injury and disease. The concentration of HA in human SF ranges from 1-4 mg/ml in healthy individuals [6, 11, 53, 101], and decreases after effusive joint injury [1] and in arthritic disease to ~0.1-1.3 mg/ml [16, 53]. Model predictions of $c_{HA}{}^{SF}$ under basal conditions were considerably below normal SF concentration. Stimulation with either TGF-β or IL-1 increased $c_{HA}{}^{SF}$ to the upper range of *in vivo* levels, which may indicate that a certain concentration of these cytokines is required in normal SF to achieve physiological concentrations of HA. The discrepancy between observed HA concentration in diseased joints and model predictions in an environment of increased cytokine concentration that may exist in injury and disease might result from allowing only lubricant secretion rates in the model to change as a function of the environment. As discussed previously, chemical stimuli may exert their effects on SF lubricant composition by altering the permeability of the synovium which may dominate over alterations in lubricant secretion rates.

The distinct kinetics of PRG4 and HA restoration after joint lavage have implications for disease and clinical therapies. For example, in acute injury, both PRG4 and HA concentrations are observed to decrease [1, 20]. Model predictions suggest that after the inflammation of an acute injury has cleared, the concentration of PRG4 may be restored relatively rapidly compared to the concentration of HA. The minimum concentration of lubricants in SF that is required to create a mechanically functional fluid is unknown. However, decreasing doses of SF and the PRG4 and HA

constituents results in increased friction between articulating cartilage surfaces in a cartilage-on-cartilage friction test (unpublished data, Schmidt 2006). If the joint lavage procedure challenges the low-friction, low-wear environment of synovial joints in the short term, it may prove beneficial to provide adjunctive therapies to normalize lubricant concentrations. Steroid supplementation is commonly given with joint lavage to help reduce inflammation [26, 96], and more recently, HA supplementation has been given to enhance lubrication in the joint and decrease post-procedure pain [52]. The model predictions in this study support the use of lubricant supplementation to temporarily increase lubricant concentration in SF.

The clearance rate of HA predicted by the model after therapeutic injection is generally consistent with experimental reports, suggesting that this approach of analysis may be useful for putative therapies involving delivery of PRG4. The half-life of HA in SF has been studied in rabbit and sheep models, and is on the order of ~24 hours for normal joints [14, 38, 77], but decreases to ~12 hours in the case of induced arthritis in the sheep model [24]. In the present study, simulated therapeutic delivery of HA into SF resulted in a large instantaneous rise in concentration over the steady-state levels, but the model predicted that the injected HA appreciably cleared (i.e. 63% cleared) after 0.25-2.66 days. This rate of clearance is also consistent with the periodic weekly injection of HA into diseased joints [98]. Clinical results of therapeutic HA injection can be highly dependent upon the molecular weight of HA [28, 59], possibly reflecting changes in synovium permeability and the half-life of this molecule in SF. Thus, the present model may have applications in comparing the kinetics of molecular concentrations with associated clinical outcomes.

The quantitative intercompartmental model of SF lubricant composition developed in this study may also have applications to a variety of current and future

joint therapies. In partial or total knee arthroplasty, removal of the cartilage surface areas may affect lubricant concentration. In cell injection or transplantation therapies, the model may elucidate the effects of the cell sources on lubricant concentration. In engineering whole biological joints, the model may facilitate development of a mechanically functional bioengineered SF in a closed volume. Such bioengineering of fluid, as opposed to the traditional engineering of tissues, may be a critical component of a whole joint bioreactor system for creation of large contoured orthotopic tissue blocks for biological arthroplasty.

2.6   Acknowledgments

2.7   References

1. Asari A, Miyauchi S, Sekiguchi T, Machida A, Kuriyama S, Miyazaki K, Namiki O: Hyaluronan, cartilage destruction and hydrarthrosis in traumatic arthritis. *Osteoarthritis Cartilage* 2:79-89, 1994.

2. Ashhurst DE, Bland YS, Levick JR: An immunohistochemical study of the collagens of rabbit synovial interstitium. *J Rheumatol* 18:1669-72, 1991.

3. Athanasou NA, Quinn J: Immunocytochemical analysis of human synovial lining cells: phenotypic relation to other marrow derived cells. *Ann Rheum Dis* 50:311-5, 1991.

4. Ayral X: Arthroscopy and joint lavage. *Best Pract Res Clin Rheumatol* 19:401-15, 2005.

5. Balazs E, Briller SO, Denlinger JL: Na-hyaluronate molecular size variations in equine and human arthritis synovial fluids and the effect on phagocytic cells. *Osteoarth Symp Semin Arthritis Rheum* Suppl:141-3, 1980.

6. Balazs EA: The physical properties of synovial fluid and the special role of hyaluronic acid. In: *Disorders of the knee,* ed. by AJ Helfet, Lippincott Co., Philadelphia, 1974, 63-75.

7. Belcher C, Yaqub R, Fawthrop F, Bayliss M, Doherty M: Synovial fluid chondroitin and keratan sulphate epitopes, glycosaminoglycans, and hyaluronan in arthritic and normal knees. *Ann Rheum Dis* 56:299-307, 1997.

8. Bertone AL, Palmer JL, Jones J: Synovial fluid cytokines and eicosanoids as markers of joint disease in horses. *Vet Surg* 30:528-38, 2001.

9. Buckwalter JA, Mankin HJ: Articular cartilage. Part II: degeneration and osteoarthrosis, repair, regeneration, and transplantation. *J Bone Joint Surg Am* 79-A:612-32, 1997.

10. Cameron ML, Fu FH, Paessler HH, Schneider M, Evans CH: Synovial fluid cytokine concentrations as possible prognostic indicators in the ACL-deficient knee. *Knee Surg Sports Traumatol Arthrosc* 2:38-44, 1994.

11. Chmiel IH, Walitza E. On the rehology of blood and synovial fluids. New York: Research Studies Press; 1980.

12. Coleman P, Kavanagh E, Mason RM, Levick JR, Ashhurst DE: The proteoglycans and glycosaminoglycan chains of rabbit synovium. *Histochem J* 30:519-24, 1998.

13. Coleman PJ, Scott D, Abiona A, Ashhurst DE, Mason RM, Levick JR: Effect of depletion of interstitial hyaluronan on hydraulic conductance in rabbit knee synovium. *J Physiol* 509 (Pt 3):695-710, 1998.

14. Coleman PJ, Scott D, Ray J, Mason RM, Levick JR: Hyaluronan secretion into the synovial cavity of rabbit knees and comparison with albumin turnover. *J Physiol* 503 (Pt 3):645-56, 1997.

15. Curry F: Mechanics and thermodynamics of transcapillary exchange. In: *Handbook of Physiology,* ed. by ERaC Michel, American Physiological Society, Bethesda, 1984, 309-74.

16. Dahl LB, Dahl IM, Engstrom-Laurent A, Granath K: Concentration and molecular weight of sodium hyaluronate in synovial fluid from patients with rheumatoid arthritis and other arthropathies. *Ann Rheum Dis* 44:817-22, 1985.

17. Davies DV: Synovial membrane and synovial fluid of joints. *Lancet* 248:815-22, 1946.

18. Dobbie JW, Hind C, Meijers P, Bodart C, Tasiaux N, Perret J, Anderson JD: Lamellar body secretion: ultrastructural analysis of an unexplored function of synoviocytes. *Br J Rheumatol* 34:13-23, 1995.

19. Eckstein F, Winzheimer M, Hohe J, Englmeier KH, Reiser M: Interindividual variability and correlation among morphological parameters of knee joint cartilage plates: analysis with three-dimensional MR imaging. *Osteoarthritis Cartilage* 9:101-11, 2001.

20. Elsaid KA, Jay GD, Warman ML, Rhee DK, Chichester CO: Association of articular cartilage degradation and loss of boundary-lubricating ability of synovial fluid following injury and inflammatory arthritis. *Arthritis Rheum* 52:1746-55, 2005.

21. Fahlgren A, Andersson B, Messner K: TGF-beta1 as a prognostic factor in the process of early osteoarthrosis in the rabbit knee. *Osteoarthritis Cartilage* 9:195-202, 2001.

22. Fava R, Olsen N, Keski-Oja J, Mose H, Pincus T: Active and latent forms of transforming growth factor ß activity in synovial effusions. *J Exp Med* 169:291-6, 1989.

23. Flannery CR, Hughes CE, Schumacher BL, Tudor D, Aydelotte MB, Kuettner KE, Caterson B: Articular cartilage superficial zone protein (SZP) is homologous to megakaryocyte stimulating factor precursor and Is a multifunctional proteoglycan with potential growth-promoting, cytoprotective, and lubricating properties in cartilage metabolism. *Biochem Biophys Res Commun* 254:535-41, 1999.

24. Fraser JR, Kimpton WG, Pierscionek BK, Cahill RN: The kinetics of hyaluronan in normal and acutely inflamed synovial joints: observations with experimental arthritis in sheep. *Semin Arthritis Rheum* 22:9-17, 1993.

25. Fraser JR, Laurent TC, Laurent UB: Hyaluronan: its nature, distribution, functions and turnover. *J Intern Med* 242:27-33, 1997.

26. Frias G, Caracuel MA, Escudero A, Rumbao J, Perez-Gujo V, del Carmen Castro M, Font P, Gonzalez J, Collantes E: Assessment of the efficacy of joint lavage versus joint lavage plus corticoids in patients with osteoarthritis of the knee. *Curr Med Res Opin* 20:861-7, 2004.

27. Furst DE: Anakinra: review of recombinant human interleukin-I receptor antagonist in the treatment of rheumatoid arthritis. *Clin Ther* 26:1960-75, 2004.

28. Ghosh P, Guidolin D: Potential mechanism of action of intra-articular hyaluronan therapy in osteoarthritis: are the effects molecular weight dependent? *Semin Arthritis Rheum* 32:10-37, 2002.

29. Haubeck H-D, Kock R, Fischer D-C, van de Leur E, Hoffmeister K, Greiling H: Transforming growth factor ß1, a major stimulator of hyaluronan synthesis in human synovial lining cells. *Arthritis Rheum* 38:669-77, 1995.

30. Hills BA: Boundary lubrication in vivo. *Proc Inst Mech Eng [H]* 214:83-94, 2000.

31. Hills BA, Crawford RW: Normal and prosthetic synovial joints are lubricated by surface-active phospholipid: a hypothesis. *J Arthroplasty* 18:499-505, 2003.

32. Jay GD, Britt DE, Cha D-J: Lubricin is a product of megakaryocyte stimulating factor gene expression by human synovial fibroblasts. *J Rheumatol* 27:594-600, 2000.

33. Jay GD, Cha D-J: The effect of phospholipase digestion upon the boundary lubricating activity of synovial fluid. *J Rheumatol* 26:2454-7, 1999.

34. Jensen LT, Henriksen JH, Olesen HP, Risteli J, Lorenzen I: Lymphatic clearance of synovial fluid in conscious pigs: the aminoterminal propeptide of type III procollagen. *Eur J Clin Invest* 23:778-84, 1993.

35. Kaneyama K, Segami N, Sun W, Sato J, Fujimura K: Analysis of tumor necrosis factor-alpha, interleukin-6, interleukin-1beta, soluble tumor necrosis factor receptors I and II, interleukin-6 soluble receptor, interleukin-1 soluble receptor type II, interleukin-1 receptor antagonist, and protein in the synovial fluid of patients with temporomandibular joint disorders. *Oral Surg Oral Med Oral Pathol Oral Radiol Endod* 99:276-84, 2005.

36. Kedem O, Katchalsky A: Thermodynamic analysis of the permeability of biological membranes to non-electrolytes. *Biochim Biophys Acta* 27:229-46, 1958.

37. Knight AD, Levick JR: Morphometry of the ultrastructure of the blood-joint barrier in the rabbit knee. *Q J Exp Physiol* 69:271-88, 1984.

38. Laurent UB, Fraser JR, Engstrom-Laurent A, Reed RK, Dahl LB, Laurent TC: Catabolism of hyaluronan in the knee joint of the rabbit. *Matrix* 12:130-6, 1992.

39. Levick JR: Absorption of artificial effusions from synovial joints: an experimental study in rabbits. *Clin Sci (Lond)* 59:41-8, 1980.

40. Levick JR: Contributions of the lymphatic and microvascular systems to fluid absorption from the synovial cavity of the rabbit knee. *J Physiol* 306:445-61, 1980.

41. Levick JR: Permeability of rheumatoid and normal human synovium to specific plasma proteins. *Arthritis Rheum* 24:1550-60, 1981.

42. Levick JR: Flow through interstitium and other fibrous matrices. *Q J Exp Physiol* 72:409-37, 1987.

43. Levick JR: The clearance of macromolecular substances such as cartilage markers from synovial fluid and serum. In: *Methods in Cartilage Research,* ed. by A Maroudas, Kuettner KE, Academic Press, New York, 1990, 352-7.

44. Levick JR: An analysis of the interaction between interstitial plasma protein, interstitial flow, and fenestral filtration and its application to synovium. *Microvasc Res* 47:90-125, 1994.

45. Levick JR: A method for estimating macromolecular reflection by human synovium, using measurements of intra-articular half-lives. *Ann Rheum Dis* 57:339-44, 1998.

46. Levick JR, McDonald JN: Synovial capillary distribution in relation to altered pressure and permeability in knees of anaesthetized rabbits. *J Physiol* 419:477-92, 1989.

47. Levick JR, McDonald JN: Ultrastructure of transport pathways in stressed synovium of the knee in anaesthetized rabbits. *J Physiol* 419:493-508, 1989.

48. Lu Y, Levick JR, Wang W: The mechanism of synovial fluid retention in pressurized joint cavities. *Microcirculation* 12:581-95, 2005.

49. Mahlbacher V, Sewing A, Elsasser HP, Kern HF: Hyaluronan is a secretory product of human pancreatic adenocarcinoma cells. *Eur J Cell Biol* 58:28-34, 1992.

50. Maroudas A: Distribution and diffusion of solutes in articular cartilage. *Biophys J* 10:365-79, 1970.

51. Mason RM, Kimura JH, Hascall VC: Biosynthesis of hyaluronic acid in cultures of chondrocytes from the swarm rat chondrosarcoma. *J Biol Chem* 257:2236-45, 1982.

52. Mathies B: Effects of Viscoseal, a synovial fluid substitute, on recovery after arthroscopic partial meniscectomy and joint lavage. *Knee Surg Sports Traumatol Arthrosc* 14:32-9, 2006.

53. Mazzucco D, Scott R, Spector M: Composition of joint fluid in patients undergoing total knee replacement and revision arthroplasty: correlation with flow properties. *Biomaterials* 25:4433-45, 2004.

54. McDonald JN, Levick JR: Morphology of surface synoviocytes in situ at normal and raised joint pressure, studied by scanning electron microscopy. *Ann Rheum Dis* 47:232-40, 1988.

55. McDonald JN, Levick JR: Evidence for simultaneous bidirectional fluid flux across synovial lining in knee joints of anaesthetized rabbits. *Exp Physiol* 77:513-5, 1992.

56. McDonald JN, Levick JR: Effect of extravascular plasma protein on pressure-flow relations across synovium in anaesthetized rabbits. *J Physiol* 465:539-59, 1993.

57. Momberger TS, Levick JR, Mason RM: Hyaluronan secretion by synoviocytes is mechanosensitive. *Matrix Biol* 24:510-9, 2005.

58. Moos V, Fickert S, Muller B, Weber U, Sieper J: Immunohistological analysis of cytokine expression in human osteoarthritic and healthy cartilage. *J Rheumatol* 26:870-9, 1999.

59. Moreland LW: Intra-articular hyaluronan (hyaluronic acid) and hylans for the treatment of osteoarthritis: mechanisms of action. *Arthritis Res Ther* 5:54-67, 2003.

60. Moreland LW: Drugs that block tumour necrosis factor: experience in patients with rheumatoid arthritis. *Pharmacoeconomics* 22:39-53, 2004.

61. Nugent GE, Aneloski NM, Schmidt TA, Schumacher BL, Voegtline MS, Sah RL: Dynamic shear stimulation of bovine cartilage biosynthesis of proteoglycan 4 (PRG4). *Arthritis Rheum* 54:1888-96, 2006.

62. Nugent GE, Schmidt TA, Schumacher BL, Voegtline MS, Bae WC, Jadin KD, Sah RL: Static and dynamic compression regulate cartilage metabolism of proteoglycan 4 (PRG4). *Biorheology* 43:191-200, 2006.

63. Ogston AG, Preston BN, Wells JD: On the transport of compact particles through solutions of chain-polymers. *Proc Roy Soc Lond A* 333:297-316, 1973.

64. Ogston AG, Stanier JE: The physiological function of hyaluronic acid in synovial fluid: viscous, elastic and lubricant properties. *J Phys* 119:244-52, 1953.

65. Okazaki R, Sakai A, Uezono Y, Ootsuyama A, Kunugita N, Nakamura T, Norimura T: Sequential changes in transforming growth factor (TGF)-beta1 concentration in synovial fluid and mRNA expression of TGF-beta1 receptors in chondrocytes after immobilization of rabbit knees. *J Bone Miner Metab* 19:228-35, 2001.

66. Patlak CS, Goldstein DA, Hoffman JF: The flow of solute and solvent across a two-membrane system. *J Theor Biol* 5:426-42, 1963.

67. Plaas A, Chekerov I, Zheng Y, Schmidt T, Sah R, Carter J, Sandy J: Disulfide-bonded multimers of lubricin (LGP-1, PRG4) glycovariants in cartilage, synovium and synovial fluid. *Trans Orthop Res Soc* 52:1422, 2006.

68. Poli A, Mason RM, Levick JR: Effects of Arg-Gly-Asp sequence peptide and hyperosmolarity on the permeability of interstitial matrix and fenestrated endothelium in joints. *Microcirculation* 11:463-76, 2004.

69. Price FM, Levick JR, Mason RM: Glycosaminoglycan concentration in synovium and other tissues of rabbit knee in relation to synovial hydraulic resistance. *J Physiol (Lond)* 495:803-20, 1996.

70. Price FM, Mason RM, Levick JR: Radial organization of interstitial exchange pathway and influence of collagen in synovium. *Biophys J* 69:1429-39, 1995.

71. Rabinowitz JL, Gregg JR, Nixon JE: Lipid composition of the tissues of human knee joints. II. Synovial fluid in trauma. *Clin Orthop Rel Res*:292-8, 1984.

72. Revell PA: Synovial lining cells. *Rheumatol Int* 9:49-51, 1989.

73. Rittig M, Tittor F, Lutjen-Drecoll E, Mollenhauer J, Rauterberg J: Immunohistochemical study of extracellular material in the aged human synovial membrane. *Mech Ageing Dev* 64:219-34, 1992.

74. Ropes MW, Rossmeisl EC, Bauer W: The origin and nature of normal human synovial fluid. *J Clin Invest* 19:795-9, 1940.

75. Sabaratnam S, Arunan V, Coleman PJ, Mason RM, Levick JR: Size selectivity of hyaluronan molecular sieving by extracellular matrix in rabbit synovial joints. *J Physiol* 567:569-81, 2005.

76. Sabaratnam S, Mason RM, Levick JR: Filtration rate dependence of hyaluronan reflection by joint-to-lymph barrier: evidence for concentration polarisation. *J Physiol* 557:909-22, 2004.

77. Sakamoto T, Mizono, S, Miyazaki, K, Yamaguchi, T, Toyoshima, H, Namiki, O.: Biological fate of sodium hyaluronate (SPH): Studies on the distribution, metabolism, and excretion of ^{14}C-SPH in rabbits after intra-articular administration. *Pharmacometrics* 28:375-87, 1984.

78. Schalkwijk J, Joosten LAB, van den Berg WB, van Wyk JJ, van de Putte LBA: Insulin-like growth factor stimulation of chondrocyte proteoglycan synthesis by human synovial fluid. *Arthritis Rheum* 32:66-71, 1989.

79. Schmid T, Lindley K, Su J, Soloveychik V, Block J, Kuettner K, Schumacher B: Superficial zone protein (SZP) is an abundant glycoprotein in human synovial fluid and serum. *Trans Orthop Res Soc* 26:82, 2001.

80. Schmid T, Soloveychik V, Kuettner K, Schumacher B: Superficial zone protein (SZP) from human cartilage has lubrication activity. *Trans Orthop Res Soc* 26:178, 2001.

81. Schmidt TA, Schumacher BL, Han EH, Klein TJ, Voegtline MS, Sah RL: Chemomechanical coupling in articular cartilage: IL-1α and TGF-ß1 regulate chondrocyte synthesis and secretion of proteoglycan 4. In: *Physical Regulation of Skeletal Repair,* ed. by RK Aaron, Bolander ME, American Academy of Orthopaedic Surgeons, Chicago, 2005, 151-61.

82. Schumacher BL, Block JA, Schmid TM, Aydelotte MB, Kuettner KE: A novel proteoglycan synthesized and secreted by chondrocytes of the superficial zone of articular cartilage. *Arch Biochem Biophys* 311:144-52, 1994.

83. Schumacher BL, Hughes CE, Kuettner KE, Caterson B, Aydelotte MB: Immunodetection and partial cDNA sequence of the proteoglycan, superficial zone protein, synthesized by cells lining synovial joints. *J Orthop Res* 17:110-20, 1999.

84. Schumacher BL, Schmidt TA, Voegtline MS, Chen AC, Sah RL: Proteoglycan 4 (PRG4) synthesis and immunolocalization in bovine meniscus. *J Orthop Res* 23:562-8, 2005.

85. Schwarz IM, Hills BA: Synovial surfactant: lamellar bodies in type B synoviocytes and proteolipid in synovial fluid and the articular lining. *Br J Rheumatol* 35:821-7, 1996.

86. Schwarz IM, Hills BA: Surface-active phospholipids as the lubricating component of lubricin. *Br J Rheumatol* 37:21-6, 1998.

87. Scott D, Coleman PJ, Mason RM, Levick JR: Glycosaminoglycan depletion greatly raises the hydraulic permeability of rabbit joint synovial lining. *Exp Physiol* 82:603-6, 1997.

88. Scott D, Coleman PJ, Mason RM, Levick JR: Interaction of intraarticular hyaluronan and albumin in the attenuation of fluid drainage from joints. *Arthritis Rheum* 43:1175-82, 2000.

89. Scott D, Levick JR, Miserocchi G: Non-linear dependence of interstitial fluid pressure on joint cavity pressure and implications for interstitial resistance in rabbit knee. *Acta Physiol Scand* 179:93-101, 2003.

90. Scott DL, Shipley M, Dawson A, Edwards S, Symmons DP, Woolf AD: The clinical management of rheumatoid arthritis and osteoarthritis: strategies for improving clinical effectiveness. *Br J Rheumatol* 37:546-54, 1998.

91. Smith MM, Ghosh P: The synthesis of hyaluronic acid by human synovial fibroblasts is influenced by the nature of the hyaluronate in the extracellular environment. *Rheumatol Int* 7:113-22, 1987.

92. Sullivan R, Hertel, K.: The permeability method for determining specific surface of fibers and powders. *Adv Colloid Sci* 1:37-80, 1942.

93. Swann DA, Silver FH, Slayter HS, Stafford W, Shore E: The molecular structure and lubricating activity of lubricin isolated from bovine and human synovial fluids. *Biochem J* 225:195-201, 1985.

94. Swann DA, Slayter HS, Silver FH: The molecular structure of lubricating glycoprotein-I, the boundary lubricant for articular cartilage. *J Biol Chem* 256:5921-5, 1981.

95. Swann DA, Sotman S, Dixon M, Brooks C: The isolation and partial characterization of the major glycoprotein (LGP-I) from the articular lubricating fraction of synovial fluid. *Biochem J* 161:473-85, 1977.

96. Tanaka N, Sakahashi H, Hirose K, Ishima T, Ishii S: Volume of a wash and the other conditions for maximum therapeutic effect of arthroscopic lavage in rheumatoid knees. *Clin Rheumatol* 25:65-9, 2006.

97. Tanford C. Physical Chemistry of Macromolecules. New York: John Wiley & Sons; 1961.

98. Tehranzadeh J, Booya F, Root J: Cartilage metabolism in osteoarthritis and the influence of viscosupplementation and steroid: a review. *Acta Radiol* 46:288-96, 2005.

99. Van Obberghen-Schilling E, Roche NS, Flanders KC, Sporn MB, Roberts AB: Transforming growth factor beta 1 positively regulates its own expression in normal and transformed cells. *J Biol Chem* 263:7741-6, 1988.

100. Wallis WJ, Simkin PA, Nelp WB: Protein traffic in human synovial effusions. *Arthritis Rheum* 30:57-63, 1987.

101. Watterson JR, Esdaile JM: Viscosupplementation: therapeutic mechanisms and clinical potential in osteoarthritis of the knee. *J Am Acad Orthop Surg* 8:277-84, 2000.

102. Wei X, Messner K: Age- and injury-dependent concentrations of transforming growth factor-beta 1 and proteoglycan fragments in rabbit knee joint fluid. *Osteoarthritis Cartilage* 6:10-8, 1998.

103. Wilkinson LS, Pitsillides AA, Worrall JG, Edwards JC: Light microscopic characterization of the fibroblast-like synovial intimal cell (synoviocyte). *Arthritis Rheum* 35:1179-84, 1992.

104. Worrall JG, Bayliss MT, Edwards JC: Morphological localization of hyaluronan in normal and diseased synovium. *J Rheumatol* 18:1466-72, 1991.

105. Worrall JG, Wilkinson LS, Bayliss MT, Edwards JC: Zonal distribution of chondroitin-4-sulphate/dermatan sulphate and chondroitin-6-sulphate in normal and diseased human synovium. *Ann Rheum Dis* 53:35-8, 1994.

CHAPTER 3:

INTERACTIVE CYTOKINE REGULATION OF

SYNOVIOCYTE SECRETION OF

SYNOVIAL FLUID LUBRICANTS,

HYALURONAN AND PROTEOGLYCAN 4

3.1   Abstract

Introduction: The regulation by cytokines of secretion of synovial fluid (SF) lubricants, hyaluronan (HA) and proteoglycan 4 (PRG4), is important in health, injury, and disease of synovial joints, and also in developing approaches for controlling lubricant secretion in synovial joint bioreactors. The objective of this study was to determine the levels of lubricant secretion by synoviocytes, as well as the structure of secreted HA and PRG4, in response to IL-1β, IL-17, IL-32, TGF-β1, and TNF-α, applied individually and in combination.

Methods: Human synoviocytes were treated with IL-1β, IL-17, IL-32, TGF-β1 (0.1, 1, 10 ng/ml), and TNF-α (1, 10, 100 ng/ml) individually, and in all combinations (using highest concentration). Synoviocyte secretion of HA and PRG4 were assessed by quantifying levels of these molecules in conditioned medium using ELISA and

binding assays, and assessing the molecular weight (MW) by gel electrophoresis and Western blotting.

Results: HA secretion rates were increased ~40-fold over control levels by IL-1β and to a lesser extent by TNF-α or TGF-β1, and increased synergistically to ~80-fold by the combination of IL-1β+TGF-β1, or of TNF-α+IL-17. PRG4 secretion rates were increased ~80-fold over control levels by TGF-β1, and this effect was counterbalanced by IL-1β and TNF-α. Secreted HA was distributed primarily in the <1 MDa MW range under control conditions and after stimulation by individual cytokines, but distributed in the >1 MDa MW range and concentrated at >3 MDa, more closely resembling the MW distribution of HA in normal human SF, after stimulation by IL-1β+TGF-β1+TNF-α. The MW of secreted PRG4 was not affected by cytokines, and similar to that of the high MW PRG4 in human SF.

Conclusions: The results of this study provide information on cytokine regulation of HA and PRG4 secretion rates and structure, and contribute to an understanding of the relationship between alterations in SF cytokine and lubricant content that occur in injury and disease. The results also provide approaches for using individual and combinations of cytokines to modulate HA and PRG4 secretion rates and HA MW over a range of magnitudes, which may allow achievement of desired lubricant composition of fluid generated in synovial joint bioreactors.

3.2   Introduction

The synovial joint is a low-friction, low-wear load-bearing system that includes articular cartilage, synovial fluid (SF), and synovium components. Articular cartilage is composed of chondrocytes within a dense extracellular matrix, and bears load and slides relative to an apposing surface with low-friction and low-wear properties. The SF acts biomechanically on articular cartilage as a lubricant, containing a number of lubricating molecules, as well as regulatory cytokines, nutrients, and other components. The lubricating molecule hyaluronan (HA) in SF is produced predominantly by fibroblast-like synoviocytes in synovium (abbreviated in this paper as "synoviocytes") [21, 49], while the lubricating molecule proteoglycan 4 (PRG4) is secreted by synoviocytes as well as chondrocytes in the superficial layer of articular cartilage [25, 47, 48]. The rate of synthesis of these lubricating molecules, and the structure of the molecules synthesized, is important because the balance between the rate of synthesis and the rate of loss of these molecules, by degradation and transport through the semi-permeable synovium, dictate their concentration in SF [10, 36].

In naturally occurring or animal models of osteoarthritis, rheumatoid arthritis, and injury, the concentration of HA and PRG4 in SF are often decreased, as is the molecular weight (MW) of HA [5-8, 13, 16]. However, the volume of SF is often increased proportionately more [5, 24, 46], leading to an overall net increase in total lubricant content in SF. These changes in lubricant content and volume in SF are often accompanied by increases in the concentrations of certain cytokines in SF. However, the relationship between altered cytokine concentrations and altered lubricant content remain to be established.

Experimental biomimetic culture systems have been developed to examine the biology and mechanobiology of synovium and its interaction with articular cartilage. For example, a three-dimensional synovial-like tissue has been generated in vitro to study the function and behavior of synoviocytes in organizing the synovial tissue [32]. Chondrocyte and synoviocyte co-culture systems have been utilized to assess the interactive modulation of cartilage matrix metabolism [41, 43]. Mechanical regulation of articular cartilage with attached subchondral bone has been examined not only for osteochondral fragments [54, 55], but also for knee joints utilizing a joint-scale bioreactor [42]. Although these types of culture systems include certain biomimetic features of the synovial joint, the presence of a lubricating fluid similar to that of native SF has not yet been incorporated. An appropriate lubricating environment may be particularly important for a mechano-biological bioreactor system where cartilaginous surfaces articulate and undergo joint-like motion [17, 18, 42]. The secretion rates of lubricants and structure of the secreted lubricants would be key parameters affecting the lubricant composition of fluid in such a system (**Figure 3.1**). The ability to generate a lubricating fluid could also have application to arthritis therapies, such as novel viscosupplements.

A number of cytokines are candidates for the regulation of lubricant secretion by synoviocytes and chondrocytes. Native SF contains a complex milieu of cytokines, and the cytokines IL-1β, IL-17, IL-32, TGF-β1, and TNF-α play an important role in joint homeostasis and disease pathogenesis. These cytokines are often present at elevated levels in disease and injury, are involved in synoviocyte activation, and demonstrate certain synergistic interactions [2, 3, 9, 19, 27, 28, 30, 33, 37, 56]. The individual effects of some of these cytokines on lubricant secretion have been studied, but interactive effects that likely occur in vivo remain to be established. IL-1β, TGF-

β1, and TNF-α induce increased HA secretion rates by synoviocytes [11, 21, 45]. IL-1β has also been reported to induce secretion of HA of higher molecular weight (MW) compared to basal controls [21, 29]. Individually applied TGF-β1 stimulates PRG4 secretion by synoviocytes, while IL-1β inhibits secretion, although quantitative rates have not been reported [26, 40]. A combinatorial approach to evaluate the interactive effects of cytokines could provide a better understanding of cytokine-regulated lubricant secretion.

The objective of this study was to determine the secretion rates of HA and PRG4 by human synoviocytes, as well as the MW of these secreted molecules, as regulated by the cytokines IL-1β, IL-17, IL-32, TGF-β1, and TNF-α applied individually and in combination.
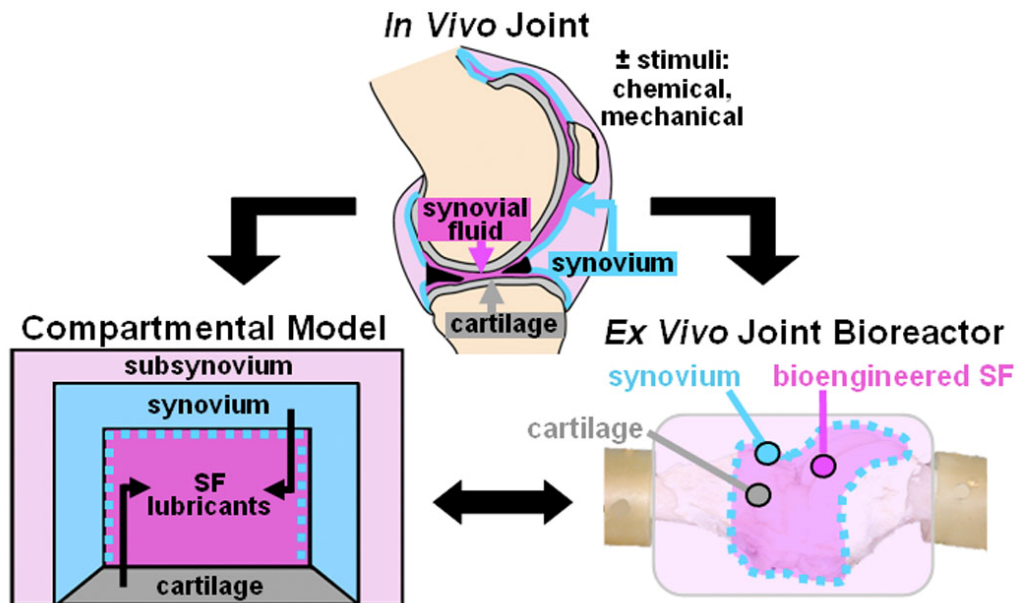
Figure 3.1: Synovial joints may be modeled theoretically with a compartmental approach, and experimentally in a bioreactor with key components that include lubricant-secreting cell types, a SF compartment, and a lubricant-retaining semi-permeable membrane. Chemical and mechanical stimuli are key parameters that may regulate lubricant secretion and structure, and affect lubricant composition in native and bioengineered SF.

3.3   Materials and Methods

Synoviocyte and Synovial Fluid Isolation

Human synovial tissue and SF samples were collected with IRB approval and informed donor consent. All studies were approved by the University of California, San Diego Human Subjects Research Protection Program.

Synovial tissue was obtained from patients with osteoarthritis (OA) and rheumatoid arthritis (RA) at the time of joint replacement with patient consent, as described previously [3]. The diagnosis of RA conformed to the 1987 revised American College of Rheumatology criteria [4]. Synovial tissues were minced and incubated with 1 mg/ml collagenase in serum free DMEM with additives (100 U/ml penicillin, 100 µg/ml streptomycin, 0.25 µg/ml Fungizone, 0.1 mM MEM non-essential amino acids, 10 mM HEPES, 0.4 mM L-proline, 2 mM L-glutamine) for 2 hr at 37ºC, filtered through a nylon mesh, extensively washed, and cultured in DMEM supplemented with 10% fetal bovine serum. After overnight culture, nonadherent cells were removed. Adherent cells were later trypsinized, split at a 1:3 ratio, and cultured in DMEM+10% FBS. Synoviocytes were used from passages 3 through 9 when they are a homogeneous population of fibroblast-like synoviocytes (<1% CD11b, <1% phagocytic, and <1% FcgRII positive [3]).

Normal human SF was obtained from the normal knee (as assessed by X-ray) of subjects with intra-articular fractures in the contralateral knee, with informed consent. Collected SF was clarified of cells and debris by centrifugation (3,000 g, 30 min, 4ºC), and the resultant samples were stored at −70°C before analysis.

Synoviocyte Culture and Cytokine Treatment

For all experiments, synoviocytes were seeded at 10,000 cells/cm^2 and cultured in DMEM+10% FBS until confluent. Confluent synoviocytes were subsequently incubated under basal conditions of DMEM+0.5% FBS for 2 days and then with the addition of cytokines individually or in combination for 3 days. All subsequent analyses were performed on either cell layers or conditioned media during the 3 day cytokine treatment. Donor tissue for each experiment consisted of 6 different donors, with 3 OA sources (66 ± 20 yr, 6 donors) and 3 RA sources (60 ± 11 yr, 6 donors). Cell cultures for each donor and each experimental group were performed in duplicate and the cell layers and conditioned media from the 3 day cytokine treatment were pooled for analysis from duplicate cultures. As the effects of individual and combinations of cytokines did not statistically differ for OA and RA groups in the analyses, the data is presented and discussed collectively.

Individual Cytokine Treatment. Individual cytokines were applied over a range of concentrations to assess dose responses: IL-1β, IL-17, IL-32, TGF-β1 (0.1, 1, 10 ng/ml), and TNF-α (1, 10, 100 ng/ml).

Combination Cytokine Treatment. A fully factorial experimental design of cytokine combinations (32 groups total) was used to elucidate additive and/or synergistic effects of IL-1β, IL-17, IL-32, TGF-β1 (10 ng/ml), and TNF-α (100 ng/ml). As certain combinations of cytokines at high concentrations, but not low concentrations, resulted in synergistic regulation of lubricant secretion in preliminary experiments, all experiments in this study were carried out using high cytokine concentrations.

DNA Content

Net cell proliferation was assessed as the ratio of day 3 DNA to day 0 DNA. Cell layers were solubilized on days 0 and 3 with 0.5 mg/ml proteinase K (Roche, Indianapolis, IN), harvested, and analyzed for DNA using PicoGreen® [38] (Molecular Probes, Eugene, OR).

Lubricant Secretion Rates

Secretion of HA and PRG4 was assessed after the 3 day cytokine treatment by analyzing conditioned medium for PRG4 by ELISA using mAb GW4.23 (gift from Dr. Klaus Kuettner [53]), and for HA by an enzyme-linked binding assay using HA binding protein [1]. Secretion rates (r_{HA}, r_{PRG4}) were determined by normalizing total mass of secreted lubricant to cell number on day 3 as estimated from DNA, and to culture duration.

Molecular Weight Distribution of Secreted HA

The molecular weight (MW) distribution of HA secreted by synoviocytes was performed using an agarose gel electrophoresis technique [34], with several modifications. Conditioned media samples (pooled from 6 donors for each cytokine condition, and from individual donors for selected conditions), normal human synovial fluid (SF) and HA standards in the MW range 0.16-4.0 MDa (Associates of Cape Cod Inc., East Falmouth, MA) were treated with ± *Streptomyces* hyaluronidase (10 U/ml) (Seikagaku Corp., Tokyo, Japan) overnight at 37C and then subsequently with + proteinase K (0.5 mg/ml) overnight at 37ºC. Samples with HA mass of 200-500 ng were applied to 1% agarose gels (Lonza, Rockland, ME), separated by horizontal electrophoresis at 100V for 110 minutes in TAE buffer (0.4 M Tris-acetate, 0.01 M EDTA, pH 8.3), and visualized after incubation with 0.1% Stainsall reagent (Sigma,

St. Louis, MO). Gel images were digitized with a D80 digital camera (Nikon, Melville, NY) and also processed to determine HA distribution by subtracting the intensities of hyaluronidase-treated samples from that of non-hyaluronidase-treated samples, and then displaying on a relative scale (0 to 1) to show relative HA content between 0.1 and 7.0 MDa. Also, the distribution of HA within the MW ranges of 0.1 - 1 MDa, 1 - 3 MDa, and >3 MDa were calculated.

Structure of PRG4

The structure of PRG4 secreted by synoviocytes was determined for samples showing upregulation by Western blot. Conditioned media was concentrated with a 30 kDa MWCO centrifugal filtration device (Millipore, Billerica, MA), and then these samples (0.15 μg PRG4 equivalent) and also normal human SF (0.5 μl) were treated with 10 U/ml *Streptomyces* hyaluronidase (Seikagaku Corp., Tokyo, Japan) overnight at 37ºC. Samples were then applied to precast 3-8% acrylamide Tris-acetate gels, and separated by electrophoresis at 150V for 1 hr in Tris-acetate SDS running buffer (50 mM Tricine, 50 mM Tris base, 0.1% SDS, pH 8.24), blotted onto PVDF membranes (Amersham, Piscataway, NJ) at 30V for 1 hr in transfer buffer (25 mM Bicine, 25 mM Bis-Tris, 1 mM EDTA, pH 7.20). The membranes were then blocked for 1 hr in 5% normal goat serum in PBS + 0.1% Tween 20 (pH 7.4), reacted with mAb GW4.23 to PRG4 (or non-specific mouse IgG as a control (Pierce, Rockford, IL)) at 0.5 μg/ml in 1% BSA in PBS + 0.1% Tween 20 for 1 hr, and then a goat anti-mouse secondary antibody conjugated to horse radish peroxidase. Immunoreactivity was detected by ECL-Plus chemiluminescence (Amersham Biosciences, Piscataway, NJ), recorded with a Storm Imager (GMI, Ramsey, Minnesota).

Statistical Analysis

Data are expressed as mean ± SEM. Data were log transformed to improve normality. For individual cytokines, effects on DNA and secretion rates were analyzed by 1-way ANOVA and Dunnett's post-hoc test to assess differences from controls. For combinations of cytokines, a 5-way ANOVA (factors: IL-1β, IL-17, IL-32, TGF-β1, and TNF-α) was used to assess interactive (i.e., non-additive) effects of cytokines on DNA and secretion rates. For analysis of HA MW, effects of cytokines were analyzed by 1-way ANOVA and Tukey post-hoc test to assess differences among samples in the percentage of total HA present in the MW ranges of <1 MDa, 1-3 MDa, and >3 MDa.

3.4   Results

DNA Analysis

Overall cell proliferation was low during the 3 day cytokine treatment. Relative proliferation was (~1-1.5-fold), consistent with the high cell density of monolayers on the initial day of cytokine treatment and the short culture duration. There was a slight stimulatory effect (~+30%) of TGF-β1, IL-1β, and TNF-α ($p<0.05$) (**Figure 3.2A, 3.3A**).
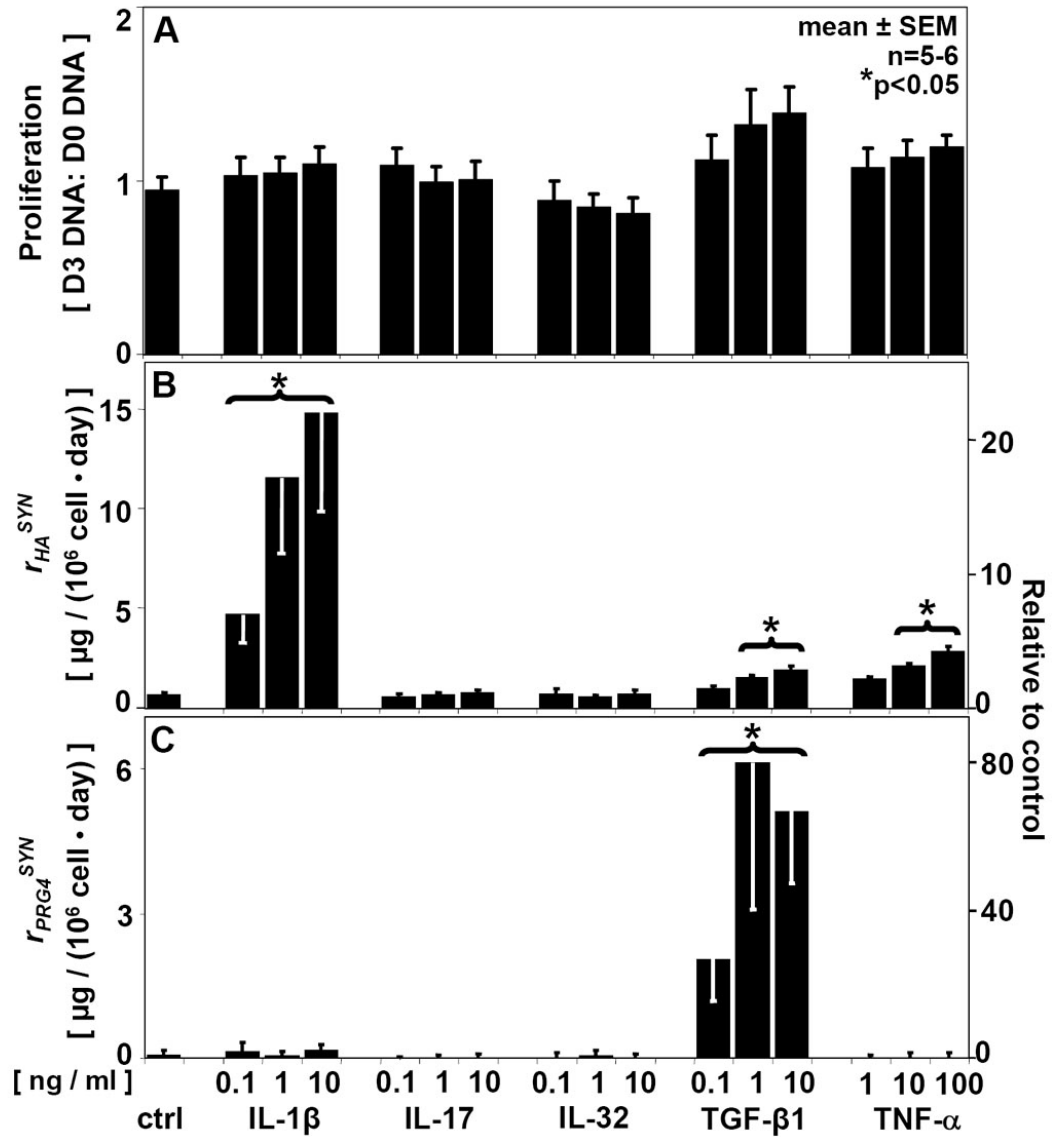
Figure 3.2: Regulatory effects of the individual cytokines IL-1β, IL-17, IL-32, TGF-β1, and TNF-α at a range of concentrations on (**A**) Proliferation, (**B**) HA secretion, and (**C**) PRG4 secretion by human synoviocytes.

Lubricant Secretion Rates

r_{HA} and r_{PRG4} were differentially regulated by individually applied cytokines (**Figure 3.2B,C**). The r_{HA} of control cultures was increased ~22x by IL-1β ($p<0.05$). Less stimulatory to r_{HA} were TNF-α and TGF-β1, causing increases to ~4.2x and ~2.8x, respectively (each, $p<0.05$) (**Figure 3.2B**). In contrast, r_{PRG4} was affected only by TGF-β1, increased to ~78x over the control rate ($p<0.05$) (**Figure 3.2C**). r_{HA} and r_{PRG4} were not significantly affected by the addition of IL-17 or IL-32 individually.

Synergistic interactions of certain combinations of cytokines increased r_{HA} markedly over the additive effects of individual cytokines (**Figure 3.3B**). TNF-α acted synergistically with multiple cytokines, including IL-1β, IL-17, and TGF-β1, increasing r_{HA} to ~1.3x, ~6.3x, and ~2.3x over the predicted additive effects of these cytokines, respectively (each, $p<0.05$). IL-1β also acted synergistically with IL-17 and TGF-β1, increasing r_{HA} ~1.2x and ~2.1x over the predicted additive effects (each, $p<0.05$). r_{HA} was not significantly affected by the addition of IL-32 to any other cytokine, including these synergistic combinations.

Counterbalancing effects with certain combinations of cytokines were apparent for regulation of PRG4 secretion (**Figure 3.3C**). The stimulatory effect of individually applied TGF-β1 was counterbalanced by the addition of either IL-1β or TNF-α, decreasing r_{PRG4} to ~0.6x or ~0.8x, respectively ($p<0.05$). When applied together with TGF-β1, IL-1β and TNF-α further decreased r_{PRG4} ~0.3x. r_{PRG4} was unchanged by the addition of IL-17 or IL-32 to any condition.

Figure 3.3: Regulatory effects of different combinations of the cytokines IL-1β, IL-17, IL-32, TGF-β1, and TNF-α on (**A**) Proliferation, (**B**) HA secretion, and (**C**) PRG4 secretion by human synoviocytes.

Effect of Cytokines on Lubricant Structure

The MW distribution of secreted HA was markedly regulated by individual and combinations of cytokines, and resembled that of normal human SF in some cases. For all samples, hyaluronidase treatment eliminated detection of signal in agarose gels, confirming that the protease-digested samples were stained specifically for HA (**Figure 3.4A**). The percentage of total HA present in the MW ranges of >3 MDa, 1-3 MDa, and <1 MDa for all cytokine conditions using samples pooled from multiple donors revealed an overall regulation by the cytokines IL-1β, TGF-β1, and TNF-α, applied individually and in combination (**Figure 3.5**) Selected regulatory conditions that were further analyzed from individual donors (**Figure 3.4B**) showed that for control and TGF-β1 conditions, the MW of HA was primarily in the <1 MDa range (~93% for ctrl and ~96% for TGF-β1). For individually-applied IL-1β, the MW profile of HA was more diffuse, with a larger percentage of HA in the 1-3 MDa range (~30% for IL-1β vs. ~5% for control and ~3% for TGF-β1, $p < 0.05$) and also >3 MDa range (~11% for IL-1β vs. ~2% for control and ~1% for TGF-β1, $p < 0.05$), although the majority of HA was still present at <1 MDa. The effect of TGF-β1 in combination with IL-1β shifted the MW distribution of HA to a higher percentage in the >3 MDa range (~34% vs. ~11% for IL-1β, $p < 0.05$). The effect of TNF-α in combination with TGF-β1 and IL-1β did not significantly alter the MW distribution from that of TGF-β1+IL-1β, but showed a trend of increasing percentage of HA in the >3 MDa range (~49% vs. ~34% for TGF-β1+IL-1β). This latter combination of cytokines generated a MW profile that most closely resembled that of normal human SF (~70% in the >3 MDa range).
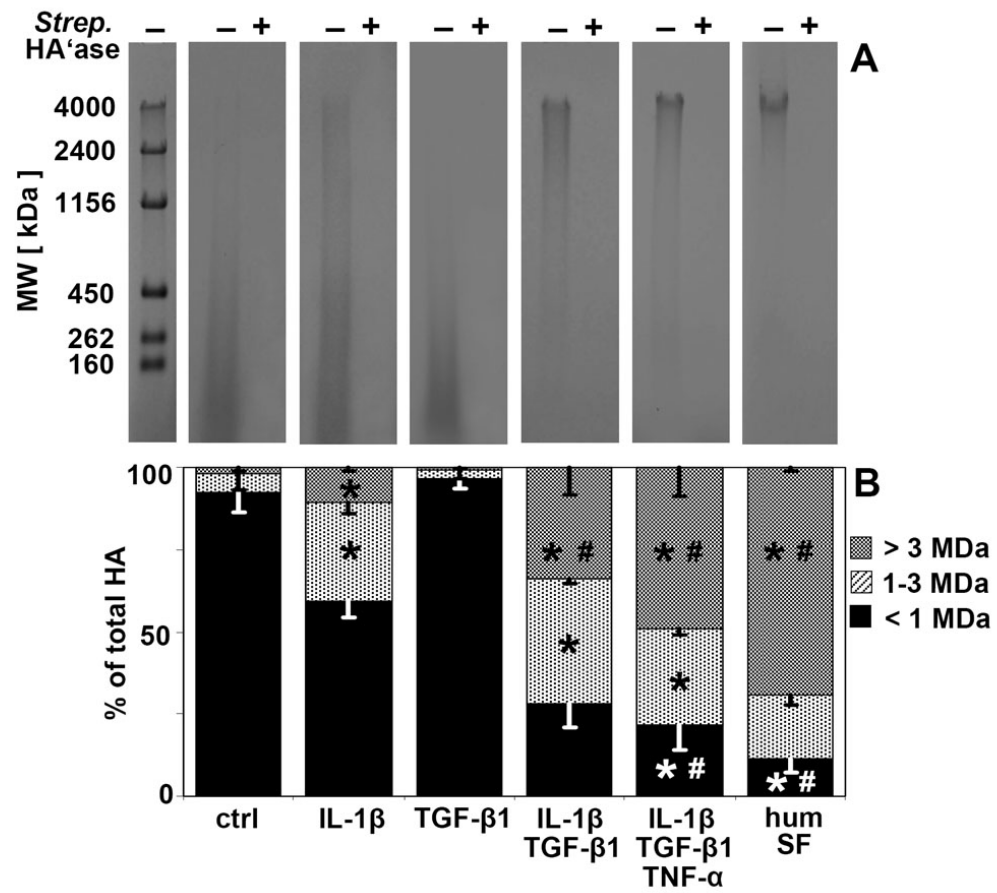
Figure 3.4: (**A**) Visualization of HA in conditioned media samples from selected regulatory cytokine treatments in the MW range of 0.1-7.0 MDa, an using agarose gel electrophoresis technique. (**B**) Percentage of total HA in the MW ranges of >3 MDa, 1-3 MDa, and < 1 MDa, averaged from relative intensities of samples in (**A**), mean ±SEM, n=2-4; *$p < 0.05$ vs. both control & TGF-β1, and #$p < 0.05$ vs. IL-1β.

A

relative amount of HA — 1 ... 0

MW [kDa]: 5000, 3000, 1000, 500, 100

Treatment matrix (rows): IL-1β, IL-17, IL-32, TGF-β1, TNF-α | control | ... | human SF

B — % of total in:

	> 3 MDa	1-3 MDa	< 1 MDa
control	2	8	90

> 3 MDa	9	2	1	2	5
1-3 MDa	32	5	6	7	13
< 1 MDa	59	93	93	91	82

> 3 MDa	11	6	27	31	6	1	11	<1	3	4
1-3 MDa	26	21	29	34	13	3	32	<1	3	17
< 1 MDa	63	73	44	35	81	96	57	99	94	79

> 3 MDa	8	23	32	16	20	40	1	13	39	15
1-3 MDa	23	36	30	32	29	29	23	27	39	27
< 1 MDa	69	41	38	52	51	31	96	60	32	58

> 3 MDa	22	28	43	40	31
1-3 MDa	36	28	27	29	32
< 1 MDa	42	44	30	31	37

	boxed	human SF
> 3 MDa	34	70
1-3 MDa	30	23
< 1 MDa	36	7

Figure 3.5: (**A**) Relative HA intensity profiles in the MW range of 0.1-7.0 MDa for all conditioned media samples (pooled from n=6) and normal human SF. (**B**) Percentage of total HA in the MW ranges of >3 MDa, 1-3 MDa, and < 1 MDa, calculated from relative intensities of samples in (**A**).
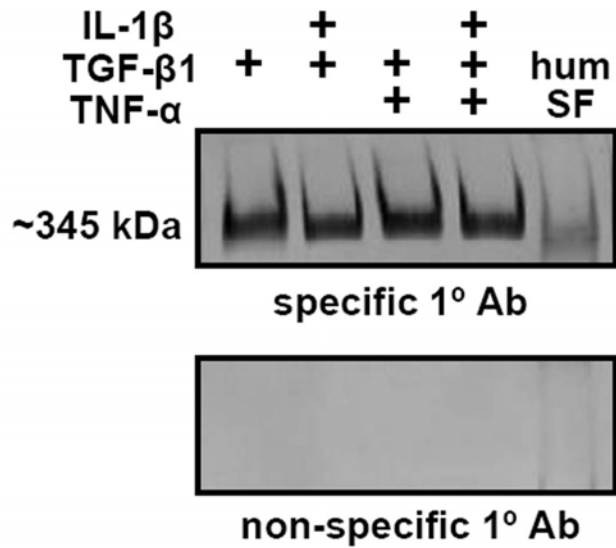
Figure 3.6: **(A)** Visualization of PRG4 from conditioned media with selected individual and combination cytokine treatments and also human SF, using techniques of gel electrophoresis, Western-blotting, and chemiluminescent detection.

The secreted PRG4 had a high MW structure that was not differentially regulated by any combination of cytokines analyzed, and also appeared similar to that present in normal human SF (**Figure 3.6**).

3.5   Discussion

This study examined the regulatory effects of selected cytokines, individually and in combination, on synoviocyte secretion of HA and PRG4, the primary boundary lubricant molecules of SF. Both the secretion rates and size of these lubricants were analyzed. Individually, IL-1β, and to a lesser extent TNF-α, increased HA secretion rates, although these same cytokines did not alter PRG4 secretion rates from basal levels (**Figure 3.2B,C**). With an effect similar to that of IL-1β and that of TNF-α, TGF-β1 induced a slight increase in HA secretion rate; however with an effect in contrast to that of IL-1β and of TNF-α, TGF-β1 markedly increased PRG4 secretion rate (**Figure 3.2B,C**). The combination of IL-1β and TGF-β1 synergistically increased HA secretion rates, up to two orders of magnitude higher than basal rates (**Figure 3.3B**); however, this cytokine combination decreased PRG4 secretion rates compared to individual TGF-β1 treatment (**Figure 3.3C**). The combination of TNF-α and IL-17 also synergistically increased HA secretion rates, but had no effect on PRG4 secretion rates. The HA MW distribution with the combination of IL-1β and TGF-β1 ± TNF-α approached that of normal SF where the majority of HA was present in the >1 MDa range and concentrated at >3 MDa; in contrast, the majority of HA in conditions with individual cytokines was present in the <1 MDa range (**Figure 3.4, 3.5**). Under all culture conditions examined, the PRG4 was detected at a high MW form similar to that present in normal human SF (**Figure 3.6**). The results of this study provide

information on cytokine regulation of lubricant secretion rates and structure that can be used to modulate lubricant secretion rates in synovial joint bioreactors and that may contribute to altered SF lubricant composition in disease and injury.

The interpretation of the data from the present study could apply to synoviocytes isolated from a normal joint, although the synoviocytes utilized in the present study were isolated from synovium of patients undergoing joint replacement due to either osteoarthritis or rheumatoid arthritis. Cells from both tissue sources were regulated in a similar manner by cytokines, suggesting that the responses delineated here are those typical of fibroblast-like synoviocytes. The consistent responses would be expected for the standardized in vitro microenvironment, where the cells have been passaged to allowed study of fibroblast-like synoviocytes without macrophage-like synoviocytes.

The effects of individually applied cytokines were consistent with and extended previous studies on the regulation of synoviocyte HA and PRG4 secretion. The observed stimulatory effects on HA secretion of individually applied IL-1β, TGF-β1, and TNF-α, and the synergistic effects of IL-1β and TGF-β1 have been previously demonstrated [11, 21, 45]. Similarly, the observed stimulatory effects of TGF-β1 on PRG4 secretion, and the counterbalancing effects of IL-1β and TNF-α are consistent with the reported individual effects of these cytokines [26, 31, 40]. The demonstrated effect of IL-1β to induce secreted HA to be distributed at higher MWs over basal controls also confirms previous reports, as does the observed high MW structure of PRG4 secreted with TGF-β1 stimulation.

In addition, the current study provides new information on the synergistic interaction between TNF-α and multiple cytokines on HA secretion. While synoviocyte synthesis of certain molecules, including IL-6, IL-8, and GM-CSF, is

synergistically stimulated by interaction of TNF-α with other cytokines [2, 19, 28], the present studies are the first report of such interactive regulation of lubricant secretion. The interaction of IL-17 with TNF-α suggests that T cells secreting IL-17 could play a role in the regulation of SF lubricant composition by their paracrine regulation of fibroblast-like synoviocytes. The synergistic effect of TNF-α with not only IL-17, but also IL-1β and TGF-β1 also suggests that therapies targeting TNF-α might have more potent effects than those expected based on the individual effects of TNF-α. Cytokine inhibitors of TNF-α and IL-1β are currently in clinical use for rheumatoid arthritis, and although both cytokines are heavily implicated as key mediators of inflammation in this disease, TNF-α therapies have demonstrated higher success [12, 14]. This might be due, in part, to the potent interaction of TNF-α with a number of cytokines present in the synovial joint milieu.

These synergistic effects of cytokines on HA secretion would likely lead to an increase in the total HA content in both native SF and the fluid in synovial joint bioreactors, with effects on concentration that are dependent on fluid volume. The volume of SF in normal knee joints is ~1-2 ml, but increased ~10-25 fold in inflamed or diseased joints [5, 24, 46]; in the latter case, HA concentration is decreased, but only to 30-50% of normal levels [5-8]. Thus, the total mass of HA in SF (volume multiplied by concentration) could be substantially greater in inflamed or diseased joints, and could be a result of upregulation of synoviocyte secretion, mediated by certain cytokines. The ability of cytokines acting individually or synergistically to regulate HA secretion rates by orders of magnitude could be particularly useful in synovial joint bioreactors to modulate the lubricity of the fluid component [42].

The observed cytokine regulation of the size of HA in the medium may involve a combination of synthesis, stabilization, or degradation processes. The

cytokines IL-1β, TNF-α, and IL-17 stimulate secretion of the HA-binding protein TSG-6 [30] that stabilize HA and prevent its depolymerization in SF [22]. Such stabilization could have occurred in this study to prevent the degradation of high MW HA. The cytokine conditions that most closely resembled normal human SF in HA MW distribution were generally ones in which IL-1β and TNF-α were present in combination, and thus may have had a greater concentration of HA-binding proteins. In contrast to this protective effect, IL-1β also induces secretion of the NP-20 hyaluronidase enzyme by synoviocytes [15], and could thereby regulate HA degradation. The net effect of a combination of cytokines on the size of HA is thus likely to be dependent on a variety of metabolic processes.

The size distribution of HA in SF is dependent upon not only synthesis and degradation processes, but also on HA retention. As transport of HA out of SF occurs through the voids of the synovium extracellular matrix [10, 35], alterations in the tissue structure or in the MW of secreted HA might affect the rate that HA permeates the tissue and is lost from SF. The effect of cytokine-regulated alterations in the size distribution of HA may be magnified by the size-dependent retention properties of the synovium, with the low MW forms of HA being lost quickly from SF and the high MW forms being selectively retained.

There are a number of mechanisms by which cytokines could have regulated the HA and PRG4 secretion as observed in this study. Marked increases in the mRNA expression of a specific HA synthase (HAS) enzyme, HAS1 (rather than HAS2 or HAS3), occurs in response to IL-1β, TGF-β1, or TNF-α, applied individually [51]. Small molecule inhibition of the MAP kinase molecules p38 and MEK inhibit TGF-β1-induced HAS1 mRNA [51], while COX inhibitors and the overexpression of NF-κB-associated molecules block the effects of IL-1β [50, 52]. The HAS enzymes might

also underlie the regulation of the size of HA, as HAS3-transfected fibroblasts synthesized HA of lower MW than HAS2 and HAS1 transfected cells [23]. Other potential mechanisms of cytokine regulation of HA include catabolism mediated by HA-degrading hyaluronidases, cellular trafficking of HAS proteins, activation of sugar nucleotide HA building blocks, and interactions between HAS enzymes and the nascent growing HA chains as they are extruded from the cell [20, 44]. Signaling mechanisms behind PRG4 regulation have been studied less extensively than that of HA, but have suggested the role of Smad2/3 in mediating TGF-β1 signaling [39]. Although these regulatory mechanisms of HA and PRG4 secretion by individual cytokines have been identified, it is unknown if regulation by cytokines in combination occurs through signaling pathways that are distinct or involve crosstalk.

The results of this study provide information on cytokine regulation of HA and PRG4 secretion rates and structure, and contribute to an understanding of the relationship between alterations in SF cytokine and lubricant content that occur in injury and disease. The results also provide approaches for using individual cytokines to differentially regulate HA and PRG4 secretion rates, and combinations of cytokines to modulate secretion rates and HA MW over a range of magnitudes. Application of this knowledge may allow achievement of desired lubricant composition of fluid generated in synovial joint bioreactors, which may be critical for providing an appropriate lubricating environment to cartilage surfaces articulating and undergoing joint-like motion. The ability to generate a fluid with modulated lubricant composition could also facilitate development of arthritis therapies, such as viscosupplements or molecules that regulate lubricant secretion.

3.6 Acknowledgments

3.7   References

1. Afify A, Lynne LC, Howell L: Correlation of cytologic examination with ELISA assays for hyaluronan and soluble CD44v6 levels in evaluation of effusions. *Diagn Cytopathol* 35:105-10, 2007.

2. Alvaro-Gracia JM, Zvaifler NJ, Brown CB, Kaushansky K, Firestein GS: Cytokines in chronic inflammatory arthritis. VI. Analysis of the synovial cells involved in granulocyte-macrophage colony-stimulating factor production and gene expression in rheumatoid arthritis and its regulation by IL-1 and tumor necrosis factor-alpha. *J Immunol* 146:3365-71, 1991.

3. Alvaro-Gracia JM, Zvaifler NJ, Firestein GS: Cytokines in chronic inflammatory arthritis. V. Mutual antagonism between interferon-gamma and tumor necrosis factor-alpha on HLA-DR expression, proliferation, collagenase production, and granulocyte macrophage colony-stimulating factor production by rheumatoid arthritis synoviocytes. *J Clin Invest* 86:1790-8, 1990.

4. Arnett FC, Edworthy SM, Bloch DA, McShane DJ, Fries JF, Cooper NS, Healey LA, Kaplan SR, Liang MH, Luthra HS: The American Rheumatism Association 1987 revised criteria for the classification of rheumatoid arthritis. *Arthritis Rheum* 31:315-24, 1988.

5. Asari A, Miyauchi S, Sekiguchi T, Machida A, Kuriyama S, Miyazaki K, Namiki O: Hyaluronan, cartilage destruction and hydrarthrosis in traumatic arthritis. *Osteoarthritis Cartilage* 2:79-89, 1994.

6. Balazs EA: The physical properties of synovial fluid and the special role of hyaluronic acid. In: *Disorders of the knee,* ed. by AJ Helfet, Lippincott Co., Philadelphia, 1974, 63-75.

7. Balazs EA, Watson D, Duff IF, Roseman S: Hyaluronic acid in synovial fluid. I. Molecular parameters of hyaluronic acid in normal and arthritis human fluids. *Arthritis Rheum* 10:357-76, 1967.

8. Belcher C, Yaqub R, Fawthrop F, Bayliss M, Doherty M: Synovial fluid chondroitin and keratan sulphate epitopes, glycosaminoglycans, and hyaluronan in arthritic and normal knees. *Ann Rheum Dis* 56:299-307, 1997.

9. Bertone AL, Palmer JL, Jones J: Synovial fluid cytokines and eicosanoids as markers of joint disease in horses. *Vet Surg* 30:528-38, 2001.

10. Blewis ME, Nugent-Derfus GE, Schmidt TA, Schumacher BL, Sah RL: A model of synovial fluid lubricant composition in normal and injured joints. *Eur Cell Mater* 13:26-39, 2007.

11. Chenevier-Gobeaux C, Morin-Robinet S, Lemarechal H, Poiraudeau S, Ekindjian JC, Borderie D: Effects of pro- and anti-inflammatory cytokines and nitric oxide donors on hyaluronic acid synthesis by synovial cells from patients with rheumatoid arthritis. *Clin Sci (Lond)* 107:291-6, 2004.

12. Christodoulou C, Choy EH: Joint inflammation and cytokine inhibition in rheumatoid arthritis. *Clin Exp Med* 6:13-9, 2006.

13. Dahl LB, Dahl IM, Engstrom-Laurent A, Granath K: Concentration and molecular weight of sodium hyaluronate in synovial fluid from patients with rheumatoid arthritis and other arthropathies. *Ann Rheum Dis* 44:817-22, 1985.

14. Edwards CJ: Immunological therapies for rheumatoid arthritis. *Br Med Bull* 73-74:71-82, 2005.

15. El Hajjaji H, Cole AA, Manicourt DH: Chondrocytes, synoviocytes and dermal fibroblasts all express PH-20, a hyaluronidase active at neutral pH. *Arthritis Res Ther* 7:R756-68, 2005.

16. Elsaid KA, Jay GD, Warman ML, Rhee DK, Chichester CO: Association of articular cartilage degradation and loss of boundary-lubricating ability of synovial fluid following injury and inflammatory arthritis. *Arthritis Rheum* 52:1746-55, 2005.

17. Grad S, Gogolewski S, Alini M, Wimmer MA: Effects of simple and complex motion patterns on gene expression of chondrocytes seeded in 3D scaffolds. *Tissue Eng* 12:3171-9, 2006.

18. Grad S, Lee CR, Gorna K, Gogolewski S, Wimmer MA, Alini M: Surface motion upregulates superficial zone protein and hyaluronan production in chondrocyte-seeded three-dimensional scaffolds. *Tissue Eng* 11:249-56, 2005.

19. Granet C, Maslinski W, Miossec P: Increased AP-1 and NF-kappaB activation and recruitment with the combination of the proinflammatory cytokines IL-1beta, tumor necrosis factor alpha and IL-17 in rheumatoid synoviocytes. *Arthritis Res Ther* 6:R190-8, 2004.

20. Hascall VC, Majors AK, De La Motte CA, Evanko SP, Wang A, Drazba JA, Strong SA, Wight TN: Intracellular hyaluronan: a new frontier for inflammation? *Biochim Biophys Acta* 1673:3-12, 2004.

21. Haubeck H-D, Kock R, Fischer D-C, van de Leur E, Hoffmeister K, Greiling H: Transforming growth factor ß1, a major stimulator of hyaluronan synthesis in human synovial lining cells. *Arthritis Rheum* 38:669-77, 1995.

22. Hutadilok N, Ghosh P, Brooks PM: Binding of haptoglobin, inter-alpha-trypsin inhibitor, and alpha 1 proteinase inhibitor to synovial fluid hyaluronate and the influence of these proteins on its degradation by oxygen derived free radicals. *Ann Rheum Dis* 47:377-85, 1988.

23. Itano N, Sawai T, Yoshida M, Lenas P, Yamada Y, Imagawa M, Shinomura T, Hamaguchi M, Yoshida Y, Ohnuki Y, Miyauchi S, Spicer AP, McDonald JA, Kimata K: Three isoforms of mammalian hyaluronan synthases have distinct enzymatic properties. *J Biol Chem* 274:25085-92, 1999.

24. Jawed S, Gaffney K, Blake DR: Intra-articular pressure profile of the knee joint in a spectrum of inflammatory arthropathies. *Ann Rheum Dis* 56:686-9, 1997.

25. Jay GD, Britt DE, Cha D-J: Lubricin is a product of megakaryocyte stimulating factor gene expression by human synovial fibroblasts. *J Rheumatol* 27:594-600, 2000.

26. Jones AR, Flannery CR: Bioregulation of lubricin expression by growth factors and cytokines. *Eur Cell Mater* 13:40-5; discussion 5, 2007.

27. Joosten LA, Netea MG, Kim SH, Yoon DY, Oppers-Walgreen B, Radstake TR, Barrera P, van de Loo FA, Dinarello CA, van den Berg WB: IL-32, a proinflammatory cytokine in rheumatoid arthritis. *Proc Natl Acad Sci USA* 103:3298-303, 2006.

28. Katz Y, Nadiv O, Beer Y: Interleukin-17 enhances tumor necrosis factor alpha-induced synthesis of interleukins 1,6, and 8 in skin and synovial fibroblasts: a possible role as a "fine-tuning cytokine" in inflammation processes. *Arthritis Rheum* 44:2176-84, 2001.

29. Kawakami M, Suzuki K, Matsuki Y, Ishizuka T, Hidaka T, Konishi T, Matsumoto M, Kataharada K, Nakamura H: Hyaluronan production in human rheumatoid fibroblastic synovial lining cells is increased by interleukin 1 beta but inhibited by transforming growth factor beta 1. *Ann Rheum Dis* 57:602-5, 1998.

30. Kehlen A, Pachnio A, Thiele K, Langner J: Gene expression induced by interleukin-17 in fibroblast-like synoviocytes of patients with rheumatoid arthritis: upregulation of hyaluronan-binding protein TSG-6. *Arthritis Res Ther* 5:R186-92, 2003.

31. Khalafi A, Schmid TM, Neu C, Reddi AH: Increased accumulation of superficial zone protein (SZP) in articular cartilage in response to bone morphogenetic protein-7 and growth factors. *J Orthop Res* 25:293-303, 2007.

32. Kiener HP, Lee DM, Agarwal SK, Brenner MB: Cadherin-11 induces rheumatoid arthritis fibroblast-like synoviocytes to form lining layers in vitro. *Am J Pathol* 168:1486-99, 2006.

33. Kotake S, Udagawa N, Takahashi N, Matsuzaki K, Itoh K, Ishiyama S, Saito S, Inoue K, Kamatani N, Gillespie MT, Martin TJ, Suda T: IL-17 in synovial fluids from patients with rheumatoid arthritis is a potent stimulator of osteoclastogenesis. *J Clin Invest* 103:1345-52, 1999.

34. Lee HG, Cowman MK: An agarose gel electrophoretic method for analysis of hyaluronan molecular weight distribution. *Anal Biochem* 219:278-87, 1994.

35. Levick JR: An analysis of the interaction between interstitial plasma protein, interstitial flow, and fenestral filtration and its application to synovium. *Microvasc Res* 47:90-125, 1994.

36. Levick JR: A method for estimating macromolecular reflection by human synovium, using measurements of intra-articular half-lives. *Ann Rheum Dis* 57:339-44, 1998.

37. Marks PH, Donaldson ML: Inflammatory cytokine profiles associated with chondral damage in the anterior cruciate ligament-deficient knee. *Arthroscopy* 21:1342-7, 2005.

38. McGowan KB, Kurtis MS, Lottman LM, Watson D, Sah RL: Biochemical quantification of DNA in human articular and septal cartilage using PicoGreen and Hoechst 33258. *Osteoarthritis Cartilage* 10:580-7, 2002.

39. Neu CP, Khalafi A, Komvopoulos K, Schmid TM, Reddi AH: Mechanotransduction of bovine articular cartilage superficial zone protein by transforming growth factor beta signaling. *Arthritis Rheum* 56:3706-14, 2007.

40. Niikura T, Reddi AH: Differential regulation of lubricin/superficial zone protein by transforming growth factor beta/bone morphogenetic protein superfamily members in articular chondrocytes and synoviocytes. *Arthritis Rheum* 56:2312-21, 2007.

41. Nixon AJ, Haupt JL, Frisbie DD, Morisset SS, McIlwraith CW, Robbins PD, Evans CH, Ghivizzani S: Gene-mediated restoration of cartilage matrix by

combination insulin-like growth factor-I/interleukin-1 receptor antagonist therapy. *Gene Ther* 12:177-86, 2005.

42. Nugent-Derfus GE, Takara T, O'Neill J K, Cahill SB, Gortz S, Pong T, Inoue H, Aneloski NM, Wang WW, Vega KI, Klein TJ, Hsieh-Bonassera ND, Bae WC, Burke JD, Bugbee WD, Sah RL: Continuous passive motion applied to whole joints stimulates chondrocyte biosynthesis of PRG4. *Osteoarthritis Cartilage* 15:566-74, 2007.

43. Patwari P, Norris SA, Kumar S, Lark MW, Grodzinsky AJ: Inhibition of bovine cartilage biosynthesis by coincubation of joint capsule tissue is mediated by an interleukin-1-independent signalling pathway. *Trans Orthop Res Soc* 28:158, 2003.

44. Pummill PE, DeAngelis PL: Alteration of polysaccharide size distribution of a vertebrate hyaluronan synthase by mutation. *J Biol Chem* 278:19808-14, 2003.

45. Recklies AD, White C, Melching L, Roughley PJ: Differential regulation and expression of hyaluronan synthases in human articular chondrocytes, synovial cells and osteosarcoma cells. *Biochem J* 354:17-24, 2001.

46. Ropes MW, Rossmeisl EC, Bauer W: The origin and nature of normal human synovial fluid. *J Clin Invest* 19:795-9, 1940.

47. Schumacher BL, Block JA, Schmid TM, Aydelotte MB, Kuettner KE: A novel proteoglycan synthesized and secreted by chondrocytes of the superficial zone of articular cartilage. *Arch Biochem Biophys* 311:144-52, 1994.

48. Schumacher BL, Hughes CE, Kuettner KE, Caterson B, Aydelotte MB: Immunodetection and partial cDNA sequence of the proteoglycan, superficial zone protein, synthesized by cells lining synovial joints. *J Orthop Res* 17:110-20, 1999.

49. Smith MM, Ghosh P: The synthesis of hyaluronic acid by human synovial fibroblasts is influenced by the nature of the hyaluronate in the extracellular environment. *Rheumatol Int* 7:113-22, 1987.

50. Stuhlmeier KM: Prostaglandin E2: a potent activator of hyaluronan synthase 1 in type-B-synoviocytes. *Biochim Biophys Acta* 1770:121-9, 2007.

51. Stuhlmeier KM, Pollaschek C: Differential effect of transforming growth factor beta (TGF-beta) on the genes encoding hyaluronan synthases and utilization of the p38 MAPK pathway in TGF-beta-induced hyaluronan synthase 1 activation. *J Biol Chem* 279:8753-60, 2004.

52. Stuhlmeier KM, Pollaschek C: Adenovirus-mediated gene transfer of mutated IkappaB kinase and IkappaBalpha reveal NF-kappaB-dependent as well as NF-kappaB-independent pathways of HAS1 activation. *J Biol Chem* 280:42766-73, 2005.

53. Su J-L, Schumacher BL, Lindley KM, Soloveychik V, Burkhart W, Triantafillou JA, Kuettner KE, Schmid TM: Detection of superficial zone protein in human and animal body fluids by cross-species monoclonal antibodies specific to superficial zone protein. *Hybridoma* 20:149-57, 2001.

54. Thibault M, Poole AR, Buschmann MD: Cyclic compression of cartilage/bone explants in vitro leads to physical weakening, mechanical breakdown of collagen and release of matrix fragments. *J Orthop Res* 20:1265-73, 2002.

55. Visser NA, van Kampen GPJ, Dekoning MHMT, van der Korst JK: The effects of loading on the synthesis of biglycan and decorin in intact mature articular cartilage in vitro. *Connect Tissue Res* 30:241-50, 1994.

56. Wei X, Messner K: Age- and injury-dependent concentrations of transforming growth factor-beta 1 and proteoglycan fragments in rabbit knee joint fluid. *Osteoarthritis Cartilage* 6:10-8, 1998.

CHAPTER 4:

SEMI-PERMEABLE MEMBRANE RETENTION OF SYNOVIAL FLUID LUBRICANTS, HYALURONAN AND PROTEOGLYCAN 4, FOR A BIOMIMETIC BIOREACTOR

4.1 Abstract

Introduction: SF lubricants hyaluronan (HA) and proteoglycan 4 (PRG4) are secreted by synoviocytes lining the joint and chondrocytes in cartilage, and concentrated in SF due to the retaining property of the semi-permeable synovium. A bioreactor system with a membrane component that recapitulates the synovium function may be useful in generating a bioengineered fluid (BF) similar to that of native SF. The objectives were to assess (1) HA and PRG4 secretion rates by cultured synoviocytes on expanded polytetrafluoroethylene (ePTFE) membranes of pore sizes 50 nm, 90 nm, 170 nm, and 3 μm, and (2) the extent of HA and PRG4 retention by these membranes.

Methods: *Experiment 1*: Synoviocytes were cultured on tissue culture (TC) plastic or ePTFE membranes ± a cytokine combination that stimulates lubricant synthesis: IL-1β+TGF-β1+TNF-α. HA and PRG4 secretion rates were assessed by

ELISA analysis of medium. *Experiment 2*: Bioreactors were fabricated to provide a BF compartment enclosed by membranes ± adherent synoviocytes, and an external compartment of nutrient fluid (NF). A solution of HA (1 mg/ml, MW ranging from 30 kDa-4000 kDa) or PRG4 (50 μg/ml) was added to the BF compartment, and HA loss into the NF compartment after 2, 8, and 24 hr was determined. Analysis of lubricant loss kinetics was used to quantify membrane permeability.

Results: *Experiment 1*: Cytokine-regulated HA and PRG4 secretion rates on ePTFE membranes were comparable to those on TC plastic. *Experiment 2*: HA and PRG4 transport across membranes was dependent upon pore size, and HA transport was further dependent upon the presence of adherent cells and HA MW. ~92% of 30 kDa HA was lost with all membranes, while 450 kDa HA was lost to a greater extent with 90 nm, 170 nm, and 3 μm membranes than with 50 nm membranes (37-74%, vs. 12%). 4000 kDa HA was lost to a greater extent with 3 μm membranes than all others (56% vs. 3-23%). PRG4 loss was 3% for 50 nm membranes and 93% for 3 μm membranes. The associated HA permeability ranged from ~3 x 10^{-8} cm/s to ~449 x 10^{-8} cm/s, and PRG4 permeability ranged from ~4 x 10^{-8} cm/s to ~325 x 10^{-8} cm/s.

Conclusions: These results suggest that semi-permeable membranes with an adherent synoviocyte layer may be applied to a bioreactor system for bioengineering SF, both as a source of lubricants and as a method to modulate lubricant retention.

4.2   Introduction

The synovial joint is a low-friction, low-wear load-bearing system that includes articular cartilage, synovial fluid (SF), and synovium components. Articular cartilage is composed of chondrocytes within a dense extracellular matrix, and bears load and slides relative to an apposing surface with low-friction and low-wear properties. The SF acts biomechanically as a lubricant for articular cartilage, while containing a complex milieu of lubricating molecules, regulatory cytokines, and other factors. The synovium is the thin, flexible lining of the joint composed of synoviocytes, extracellular matrix components, and capillaries. A key function of the synovium is to serve as a semi-permeable membrane, allowing exchange of smaller solutes from SF into the underlying subsynovium but offering outflow resistance to retain larger solutes, such as lubricant molecules, in SF.

Lubricating molecules in SF include hyaluronan (HA) and proteoglycan 4 (PRG4). HA is a glycosaminoglycan polymer, comprised of the repeating disaccharide unit of D-glucuronic acid and D-N-acetylglucosamine that is secreted by fibroblast-like synoviocytes in synovium [61]. PRG4 (also called lubricin or superficial zone protein) is a mucinous glycoprotein with O-linked β-(1-3)-Gal-GalNAc oligosaccharides [65] encoded by the PRG4 gene [23] and secreted by both chondrocytes in the superficial layer of cartilage and synoviocytes. HA is present in normal SF at a concentration of ~1-4 mg/ml, while PRG4 is present at ~0.05-0.5 mg/ml [6, 7, 16, 36, 53]. HA in normal SF is primarily present at a high molecular weight (MW), with ~70% of total HA ≥4000 kDa and the remaining ~30% distributed at lower MWs in the range of <4000 kDa to ~100-200 kDa [32]. The MW of PRG4 is most commonly reported at ~200-300 kDa [63, 64]. The effective radius, or radius of

gyration, for high MW HA has been estimated at ~100-200 nm [14, 22], and for PRG4 may be estimated in a similar manner from its structural properties at ~15-20 nm [17, 65].

The native synovium has semi-permeable transport properties explained in part by its structure. The synovium is ~50-60 μm thick in humans, and its resident cells form a nearly continuous layer with intercellular gaps of ~1-2 μm in width [29, 37]. Within the gaps is a network of extracellular matrix components through which solutes permeate [46, 47], and the effective pore size is estimated at ~20-90 nm [21, 48]. Solutes that permeate the synovium enter the underlying subsynovium tissue and are cleared by an extensive system of lymphatics [25, 33, 34]. Steady-state HA and PRG4 concentrations are maintained in SF of normal joints due, in part, to a balance between the rate of lubricant loss by transport through the semi-permeable synovium and the rate of lubricant synthesis by chondrocytes and synoviocytes [10].

Certain biomimetic features of the synovial joint have been incorporated into various experimental systems to examine the biology and mechanobiology of synovium and cartilage. For example, to study the function of synoviocytes in organizing the synovial tissue, a three-dimensional synovial-like tissue has been generated in vitro [28]. Systems of chondrocyte and synoviocyte co-culture have been utilized to assess modulation of cartilage matrix metabolism [40, 44]. Mechanical regulation of joint tissues has been examined, at the scale of osteochondral fragments [66, 68], and also at the whole joint scale utilizing a joint bioreactor system [42]. However, an experimental system that recapitulates the function of the synovium to generate a lubricant enriched SF-like compartment has not yet been established. An appropriate lubricating environment may be particularly important in mechano-biological bioreactors where cartilaginous surfaces articulate and undergo joint-like

motion [19, 20, 42]. Incorporation of a lubricant-retaining membrane into a bioreactor system may enable the generation of a SF-like compartment, and the lubricant composition of the fluid may be largely determined by the membrane permeability (**Figure 4.1**).

Membrane-based techniques used in filtration and purification processes for separation of biological molecules [12, 52] may be useful for generating a lubricant-enriched fluid in a bioreactor by mimicking the filtration properties of the synovium. Certain membrane materials may be especially useful in this application, including expanded polytetrafluoroethylene (ePTFE). ePTFE is an inert material commonly used in vascular graft applications that can be engineered to have varying pore size, and thus varying solute permeability, and also a controlled structure over large surface areas. It is also resistant to degradation, a property that may help to provide consistent filtration during extended culture periods in a bioreactor. ePTFE membranes have been used in culture systems to assess diffusion of solutes across the material, such as heparin [41]; however, the transport of lubricant molecules across ePTFE has not yet been examined. Additionally, the ability of ePTFE to serve as a substrate for cell growth has been demonstrated [8, 69], with modification of the surface to facilitate cell attachment; however, the culture of a lubricant-secreting cell type on ePTFE has not yet been performed. Incorporation of ePTFE membranes in a bioreactor system may allow retention of lubricant molecules in a manner dependent upon membrane pore size, while the presence of an adherent layer of lubricant-secreting cells on the membranes may further contribute to lubricant retention and serve as a lubricant source.

The objective of this study was to assess (1) the rate of HA and PRG4 secretion by cultured synoviocytes on poly-l-lysine coated ePTFE membranes of a

range of pore sizes (~50 nm, ~90 nm, ~170 nm, and ~3 μm) and (2) the extent of HA and PRG4 retention by these membranes as measured by lubricant permeability and % of lubricant loss.

4.3   Materials and Methods

General Methods

Biomimetic Transport Chambers

Transport chambers were biomimetically designed, utilizing structural properties of the in vivo synovial joint as a model. The design consisted of two compartments, denoted as (1) a bioengineered fluid (BF) compartment and (2) a nutrient fluid (NF) compartment, separated by a semi-permeable membrane of surface area 1 cm^2 (**Figure 4.1**). Fluid volumes in the BF and NF compartments were 0.1 ml and 3 ml, respectively. The transport chamber housing was constructed from polysulphone material.

Semi-Permeable Membrane Selection

Poly-l-lysine coated expanded polytetrafluoroethylene (ePTFE) membranes were utilized to separate BF and NF compartments in the bioreactors. As the pore size of the in vivo semi-permeable synovium has been estimated at ~20-90 nm [51, 52], membranes of both near-equivalent pore size and of larger pore size were selected to obtain a range of experimental responses. The average pore sizes of membranes utilized were ~50 nm, ~90 nm, ~170 nm, and ~3 μm.
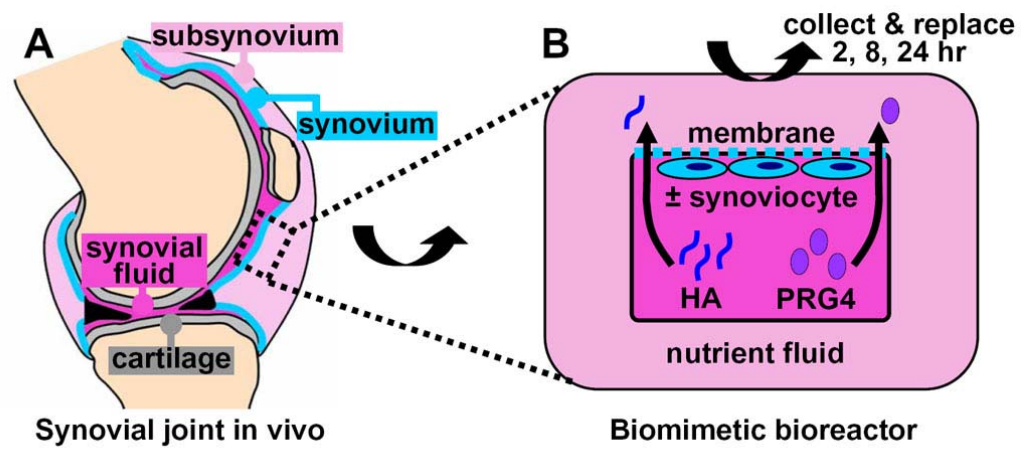
Figure 4.1: (**A**) SF lubricant retention by the synovium in the in vivo synovial joint can be (**B**) biomimetically modeled in a bioreactor where a synovial fluid compartment containing lubricants is separated from a nutrient fluid compartment void of lubricants by a semi-permeable membrane ± adhered synoviocytes.

Synoviocyte Isolation

Human synovial tissue was collected with IRB approval and informed donor consent, and studies were approved by the University of California, San Diego Human Subjects Research Protection Program. The synovial tissue was obtained from patients with osteoarthritis (OA) and rheumatoid arthritis (RA) at the time of joint replacement, as described previously [3]. The diagnosis of RA conformed to the 1987 revised American College of Rheumatology criteria [4]. Synovial tissues were minced and incubated with 1 mg/ml collagenase in serum free DMEM with additives (100 U/ml penicillin, 100 μg/ml streptomycin, 0.25 μg/ml Fungizone, 0.1 mM MEM non-essential amino acids, 10 mM HEPES, 0.4 mM L-proline, 2 mM L-glutamine) for 2 hr at 37ºC, filtered through a nylon mesh, extensively washed, and cultured in DMEM supplemented with 10% fetal bovine serum. After overnight culture, nonadherent cells were removed. Adherent cells were later trypsinized, split at a 1:3 ratio, and cultured in DMEM+10% FBS. Synoviocytes were used from passages 3 through 9 when they are a homogeneous population of fibroblast-like synoviocytes (<1% CD11b, <1% phagocytic, and <1% FcgRII positive [3]).

Experimental Design

Synoviocyte Lubricant Secretion on Membranes

Synoviocytes were applied to ePTFE membranes of pore size 50 nm, 90 nm, 170 nm, and 3 μm to assess cell proliferation and also lubricant secretion rates, in comparison to those on tissue culture (TC) plastic. Synoviocytes were cultured within the BF compartment of bioreactors in DMEM+10% FBS for 6d. Confluent cell layers were then cultured in DMEM + 0.5% FBS for 2 days and then with the addition of a

cytokine combination that stimulates HA and PRG4 synthesis: IL-1β (10 ng/ml), TGF-β1 (10 ng/ml), and TNF-α (100 ng/ml) (abbreviated as ITT) [11].

Lubricant secretion was assessed after the 3 day ITT cytokine treatment by analyzing conditioned medium for HA by an enzyme-linked binding assay using HA binding protein [1], and for human PRG4 by ELISA using mAb GW4.23 (gift from Dr. Klaus Kuettner [63]). Secretion rates were determined by normalizing total mass of secreted lubricant to culture duration and cell number on day 3. Cell numbers were determined by solubilizing cell layers with 0.5 mg/ml proteinase K (Roche, Indianapolis, IN) and analyzing the solution for DNA using PicoGreen® [38] (Molecular Probes, Eugene, OR).

Lubricant Flux Across Membranes in Transport Chambers

Synoviocytes were cultured on ePTFE membranes of pore size 50 nm, 90 nm, 170 nm, and 3 μm within the BF compartment of bioreactors in DMEM+10% FBS for 6d, and subsequently in DMEM + 0.5% FBS for 2 days. Bioreactors were also assembled utilizing ePTFE membranes with no adherent cells. A prepared HA or PRG4 lubricant solution was then added to the BF compartment of all bioreactors, and DMEM was added in the NF compartment. Bioreactors were incubated at 37ºC and 5% CO_2 with gentle mixing for durations of 2, 8, and 24 hr. At the 2 hr and 8 hr timepoints, NF was collected from the bioreactors and replenished with fresh DMEM. After the 24 hr timepoint, both the NF and BF were collected.

A 1 mg/ml solution of HA was prepared with a molecular weight (MW) distribution similar to that of normal SF where ~70% of HA is present at high MWs of ~4000 kDa and ~30% is distributed at lower MWs [32]. The solution consisted of a combination of the following MWs and concentrations of HA, all reconstituted in

DMEM: 4000 kDa (0.7 mg/ml) and 2400 kDa, 1156 kDa, 450 kDa, 262 kDa, 160 kDa, and 30 kDa (each at 0.05 mg/ml) (Associates of Cape Code, East Falmouth, MA).

A 50 μg/ml solution of PRG4 was prepared from bovine cartilage explant conditioned media from a 12 day culture under media conditions of DMEM + 0.01% BSA + 10 ng/ml TGF-β1 + 25 μg/ml to stimulate PRG4 secretion by chondrocytes [54]. Conditioned media was ultrafiltrated with a 100 kDa MWCO centrifugal filtration device, (Millipore, Billerica, MA), and treated with *Streptomyces* hyaluronidase (1 U/ml) (Seikagaku Corp., Tokyo, Japan) overnight at 37ºC to remove any HA present. The digested ultrafiltrate was subsequently subjected to a second round of ultrafiltration with a 100 kDa MWCO centrifugal filtration device to remove the *Streptomyces* hyaluronidase enzyme. PRG4 concentration in this final preparation was assessed by ELISA (described below), and reconstituted in DMEM to a concentration of 50 μg/ml, a value within physiologically observed range [53].

To assess transport of the mixture of HA MWs and also PRG4, lubricant loss from BF into NF was determined by analyzing collected BF and NF solutions from each time point for HA by an enzyme-linked binding assay using HA binding protein [1] and for bovine PRG4 by ELISA using mAb 3-A-4 (gift from Dr. Bruce Caterson [56]). The percentage of total lubricant loss at 2, 8, and 24 hr timepoints for each condition was calculated by dividing the lubricant mass collected at the respective time point by the total sum of lubricant mass collected from all time points. Data is presented as cumulative lubricant loss at each time point, as determined by addition of lubricant loss from earlier time points.

To assess HA transport as a function of MW, lubricant loss from BF into NF was determined for each MW of HA, i.e. 4000 kDa, 2400 kDa, 1156 kDa, 450 kDa,

262 kDa, 160 kDa, and 30 kDa, utilizing a gel electrophoresis technique [32]. An HA mass of 1.5 µg from NF samples collected at 2, 8, and 24 hr and from BF collected at 24 hr were applied to 1% agarose gels (Lonza, Rockland, ME), separated by horizontal electrophoresis at 100V for 110 minutes in TAE buffer (0.4 M Tris-acetate, 0.01 M EDTA, pH 8.3), and visualized after incubation with 0.1% Stainsall reagent (Sigma, St. Louis, MO). Gel images were digitized with a D80 digital camera (Nikon, Melville, NY) and then processed to determine the percent contribution of each of the 7 HA MW species. These percentage values were then multiplied by the total loss of HA mass at 2, 8, and 24 hr time points to determine the loss of mass for each MW. Finally, the percentage of total HA loss for each MW at 2, 8, and 24 hr was calculated by dividing the HA mass collected for each MW at the respective time point by the total sum of HA mass collected for each MW over all time points.

Engineering Analysis of Membrane Permeability to Lubricants

The permeability of the membranes ± adherent cells to the lubricant i, where i = HA or PRG4, during lubricant transport studies was estimated as similarly done in previous studies assessing solute diffusion across a cell-laden membrane, by obeying Fick's law [2, 26, 41, 50]. The assumption that fluid compartments were well mixed with no gradients in lubricant concentration was also applied. The expression for lubricant flux is:

$$\frac{dM_i}{dt} = AD_i \frac{\partial c_i}{\partial x} \qquad (1)$$

where dM_i/dt is the mass flux of lubricant across the membrane in units of mass per time, A is the surface area of membrane in units of length squared, D_i is the diffusivity

of the lubricant in units of length squared per time, c_i is the concentration of lubricant within the membrane, and x is the position within the membrane.

The permeability P_i is related to membrane and solute properties by:

$$P_i = \frac{D_i}{\Delta x} \tag{2}$$

which can be combined with Equation (1) to yield:

$$\frac{dM_i}{dt} = P_i A \Delta c_i \tag{3}$$

Assuming the concentration of lubricant in the NF compartment (c_i^{NF}) is $<<$ the concentration in the BF compartment (c_i^{BF}), equation (3) can be simplified as follows:

$$\Delta c_i = c_i^{BF} - c_i^{NF} \approx c_i^{BF} \tag{4}$$

$$\frac{dM_i}{dt} = P_i A c_i^{BF} \tag{5}$$

The rate of loss in M_i is balanced by the rate of change in c_i^{BF} within the volume (V^{BF}) and can also be expressed as:

$$\frac{dM_i}{dt} = -V^{BF}\left(\frac{dc_i^{BF}}{dt}\right) \tag{6}$$

Combining equations (5) and (6) results in the following first order differential equation:

$$-V^{BF}\left(\frac{dc_i^{BF}}{dt}\right) = P_i A c_i^{BF} \tag{7}$$

which can be rearranged to:

$$\frac{dc_i^{BF}}{c_i^{BF}} = -\frac{P_i A}{V^{BF}} dt \tag{8}$$

and the form of the solution to this equation is:

$$c_i^{BF}(t) = C_{i,0}^{BF} e^{-\left(\frac{P_i A}{V^{BF}}\right)t} \tag{9}$$

where $C_{i,0}^{BF}$ is a constant.

The above expression was utilized to estimate the permeability of membranes to the various lubricants, i.e. the mixture of HA MWs, HA of individual MWs, and PRG4. To do so, the mass of lubricant in BF vs. time (with time points of 0, 2, 8, and 24 hr) was first fit with an exponential curve to the data points with a fit described by an R^2 value in the range of ~0.75-0.99. Then, the exponential coefficient (coeff) from the equation of fit, along with values for A and V^{BF}, were used to calculate permeability as follows:

$$P_i = \frac{V^{BF} \cdot coeff}{A} \tag{10}$$

Statistical Analysis

Data are expressed as mean ± SEM. For lubricant secretion studies, data were log transformed to improve normality, and a 1-way ANOVA was used with Tukey post-hoc tests to determine the effect of cytokines.

For lubricant transport studies assessing % of total lubricant loss, statistical analysis was performed on cumulative data from the 24 hr time point. Since percentages form binomial rather than normal distributions, arcsine transformation was applied to normalize these data [62]. For HA (with mixture of MWs) and PRG4 transport, a 1-way ANOVA was used to determine the effect of membrane pore size on % of total lubricant loss, and a t-test was used for each membrane pore size to determine the effect an adhered cell layer. For % of HA loss as a function of MW, a 3-way ANOVA was used to determine the individual and interactive effects of membrane pore size, HA MW, and an adherent cell layer.

For permeability analysis, data were log transformed to improve normality. Statistical analysis for the mixture of HA MWs and PRG4, and also for each HA MW individually was performed as described above for lubricant transport analysis.

4.4   Results

Synoviocyte Lubricant Secretion on Membranes

Synoviocytes remained viable on ePTFE and proliferated over 6 days to a greater extent on 50 nm and 90 nm membranes than on TC plastic (~3-fold vs. ~2-

fold; p<0.05, **Figure 4.2A**). Synoviocyte secretion of HA was stimulated by the ITT cytokine combination for all substrates, including TC plastic and ePTFE of all tested pore sizes (p<0.05, **Figure 4.2B**). The average HA secretion rate induced by ITT was ~150 µg/(10^6 cell•d), a marked ~60-fold increase over basal controls. Secretion of PRG4 by synoviocytes on TC plastic and 50 nm, 90 nm, and 170 nm membranes exhibited a similar trend of ITT responsiveness (**Figure 4.2C**).

Lubricant Flux Across Membranes in Transport Chambers

The loss of HA across membranes was dependent upon pore size and the presence of adherent cells, and also the MW of HA. The average percentage of total HA loss (with the mixture of MWs) after 24 hr from BF to NF was ~10% for 50 nm membranes, ~21% for 90 nm, 36% for 170 nm, and ~66% for 3 µm membranes (**Figure 4.3A**). The percentage loss from 3 µm membranes was greater than that of all other membranes (p<0.05); additionally, the percentage loss from 170 nm membranes was greater than that of 50 nm membranes. The presence of adherent cells led to decreased HA loss after 24 hr for the small pore size membranes (16% vs. 4% for 50 nm and 26% vs. 15% for 90 nm, p<0.05).

The loss of HA across membranes was further dependent upon the MW species of HA, and there was a significant interaction with membrane pore size (p<0.05) (**Figure 4.4**). 30 kDa HA had a high percentage loss after 24 hr (~92% avg.) that was similar for all pore size membranes (**Figure 4.4G**). 160 kDa HA was lost to a greater extent from 90 nm (60%), 170 nm (70%), and 3 µm (83%) membranes than from 50 nm membranes (29%) (p<0.05) (**Figure 4.4F**). 262 kDa and 450 kDa HA similarly had the least percentage loss from 50 nm membranes compared to all others (p<0.05), but there was also a greater loss of each from 3 µm (37%, 54%) than from

90 nm membranes (13%, 16%) ($p<0.05$) (**Figure 4.4D,E**). 1156 kDa, 2400 kDa, and 4000 kDa HA were all lost into BF to a similar extent by the membranes, with a significantly greater percentage loss from 3 μm (61% avg) than 50 nm (5% avg), 90 nm (12% avg), and 170 nm (29% avg) ($p<0.05$) (**Figure 4.4A,B,C**). 1156 kDa and 2400 kDa HA were also lost to a greater extent from 170 nm membranes than from 50 nm membranes ($p<0.05$). In a similar manner to the HA transport analysis with the mixture of MWs, the presence of an adherent cell layer significantly decreased the percentage of HA loss into BF for both 50 nm and 90 nm pore size membranes ($p<0.05$).

The loss of PRG4 across membranes was dependent upon pore size, but was not affected by the presence of adhered cells. The average percentage of total PRG4 loss after 24 hr from BF to NF was ~3% for 50 nm membranes, ~28% for 90 nm, 67% for 170 nm, and ~93% for 3 μm membranes (**Figure 4.3B**). The percentage loss from each membrane was significantly different than that of all other membranes ($p<0.05$).
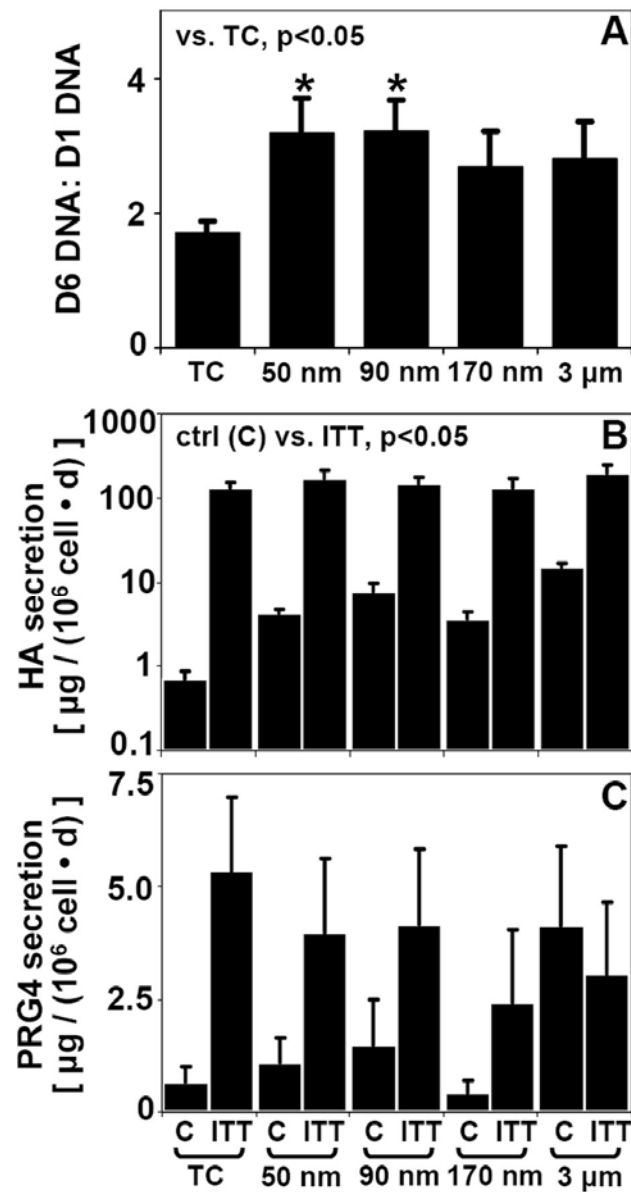
Figure 4.2: (**A**) Effects of substrate on synoviocyte proliferation over a 6 day culture period. Effects of substrate and cytokines (IL-1β+TGF-β1+TNF-α) on (**B**) HA and (**C**) PRG4 secretion rates, n=4.
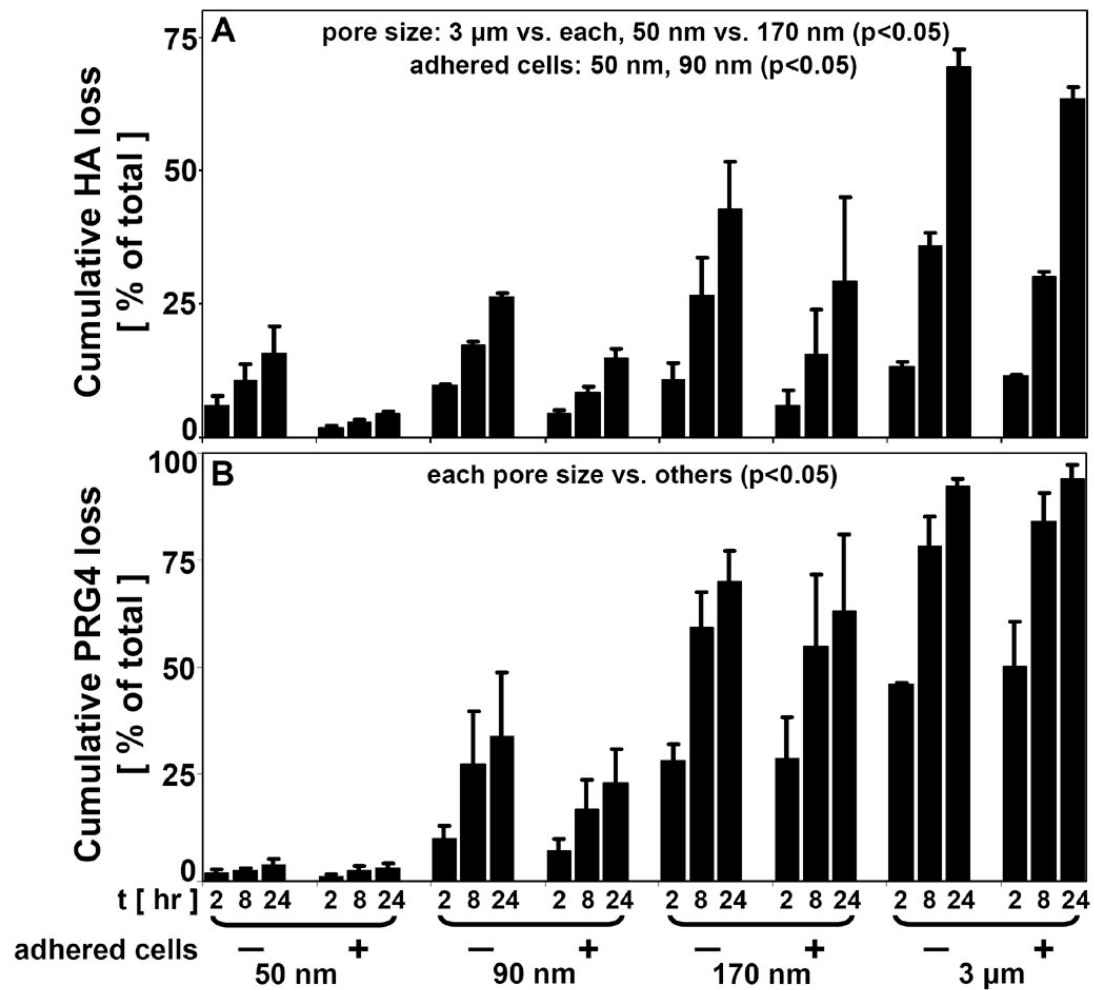
Figure 4.3: (**A**) HA loss and (**B**) PRG4 loss from the BF compartment into NF due to transport across indicated membranes ± adhered cells as a % of total, n=3-4.
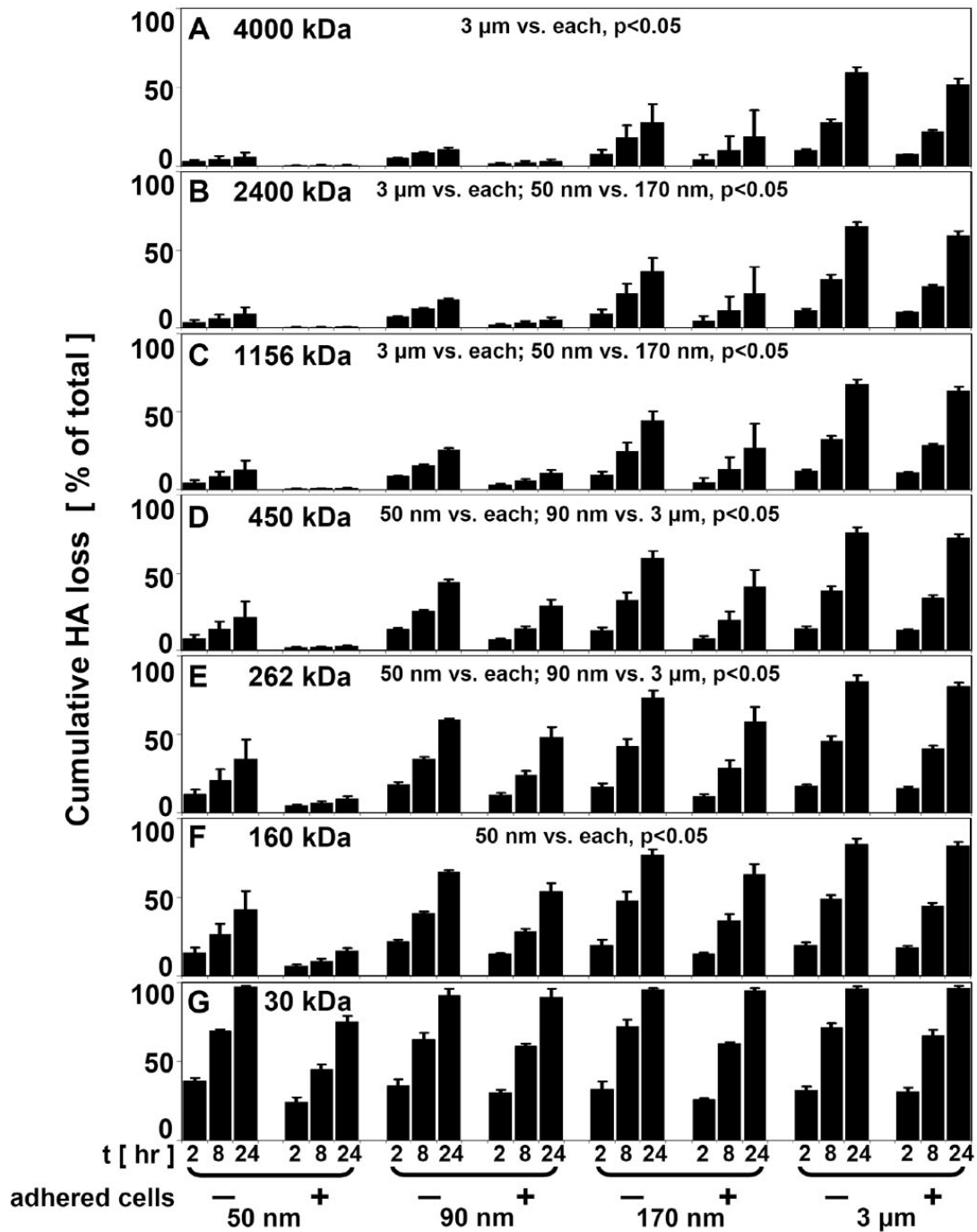
Figure 4.4: HA loss, as a function of HA MW, from the BF compartment into NF due to transport across indicated membranes ± adhered cells, (**A**) 4000 kDa, (**B**) 2400 kDa, (**C**) 1156 kDa, (**D**) 450 kDa, (**E**) 262 kDa, (**F**) 160 kDa, and (**G**) 30 kDa, n=3-4.

Permeability of Membranes to Lubricants

Reduction of the experimental data according to the engineering analysis yielded permeability values for the lubricant molecules (**Figure 4.5, 4.6, Table 4.1**). Representative curves of the mass of lubricant in BF vs. time (0, 2, 8, and 24 hr timepoints) were fit with an exponential curve (with R^2 value in the range of ~0.75-0.99) predicted by the engineering analysis to calculate permeability (**Figure 4.7**).

The permeability of membranes to HA was dependent upon pore size, the presence of adherent cells, and also the MW of HA. The average permeability for HA (with the mixture of MWs) was ~12 x 10^{-8} cm/s for 50 nm membranes, ~27 x 10^{-8} cm/s for 90 nm, ~74 x 10^{-8} cm/s for 170 nm, and ~139 x 10^{-8} cm/s for 3 μm membranes (**Figure 4.5A, Table 4.1**). The permeability of 3 μm membranes was greater than that of all other membranes (p<0.05); additionally, the permeability of 170 nm membranes was greater than that of 50 nm and 90 nm membranes (p<0.05). The presence of an adherent cell layer led to decreased permeability for the small pore size membranes (~20 x 10^{-8} vs. ~5 x 10^{-8} cm/s for 50 nm, and ~35 x 10^{-8} vs. ~19 x 10^{-8} cm/s for 90 nm, p<0.05).

The permeability of membranes to HA was further dependent upon the MW species of HA, and there was a significant interaction with membrane pore size (p<0.05) (**Figure 4.6, Table 4.1**). 30 kDa HA had a high permeability (~373 x 10^{-8} cm/s avg.) and was similar for all pore size membranes, in contrast to the permeability for all other MWs (**Figure 4.6G**). For example, the permeability for 160 kDa HA was ~4-5x lower for 50 nm membranes than for 170 nm and 3 μm membranes (45 x 10^{-8} vs. 158 x 10^{-8} and 231 x 10^{-8} cm/s, respectively) (p<0.05) (**Figure 4.6F**). Additionally, the permeability for 262 kDa, 450 kDa, and 1156 kDa HA was ~3-15x lower for 50 nm membranes compared to all other membranes (p<0.05) (**Figure 4.6C,D,E**). In a

similar manner, for HA of 2400 kDa and 4000 kDa, the permeability of 50 nm membranes (~5 x 10^{-8} cm/s avg.) was ~2-30x lower than that of all other membranes, and the permeability of 3 μm membranes (~113 x 10^{-8} cm/s avg.) was ~3-30x higher than that of all other membranes (p<0.05) (**Figure 4.6A,B**). In comparing HA of different MWs across the same pore size membrane, the permeability of 450 kDa HA was ~40x lower than that of 30 kDa HA for 50 nm membranes, but only ~2.5x lower for 3 μm membranes. The permeability of 4000 kDa HA was ~250x lower than that of 30 kDa HA for 50 nm membranes, but only ~4x lower for 3 μm membranes. In a similar manner to the other HA transport analyses, the presence of an adherent cell layer significantly affected the permeability of both 50 nm and 90 nm pore size membranes (~12x and ~2x lower permeability, respectively, p<0.05).

The permeability of membranes to PRG4 was dependent upon pore size, but was not affected by the presence of adherent cells. The average permeability for PRG4 was ~4 x 10^{-8} for 50 nm membranes, ~48 x 10^{-8} for 90 nm, ~144 x 10^{-8} for 170 nm, and ~336 x 10^{-8} for 3 μm membranes (**Figure 4.5B, Table 4.1**). The permeability of 3 μm membranes was greater than that of all other membranes, and the permeability of 170 nm membranes was greater than that of 50 nm and 90 nm membranes (p<0.05).
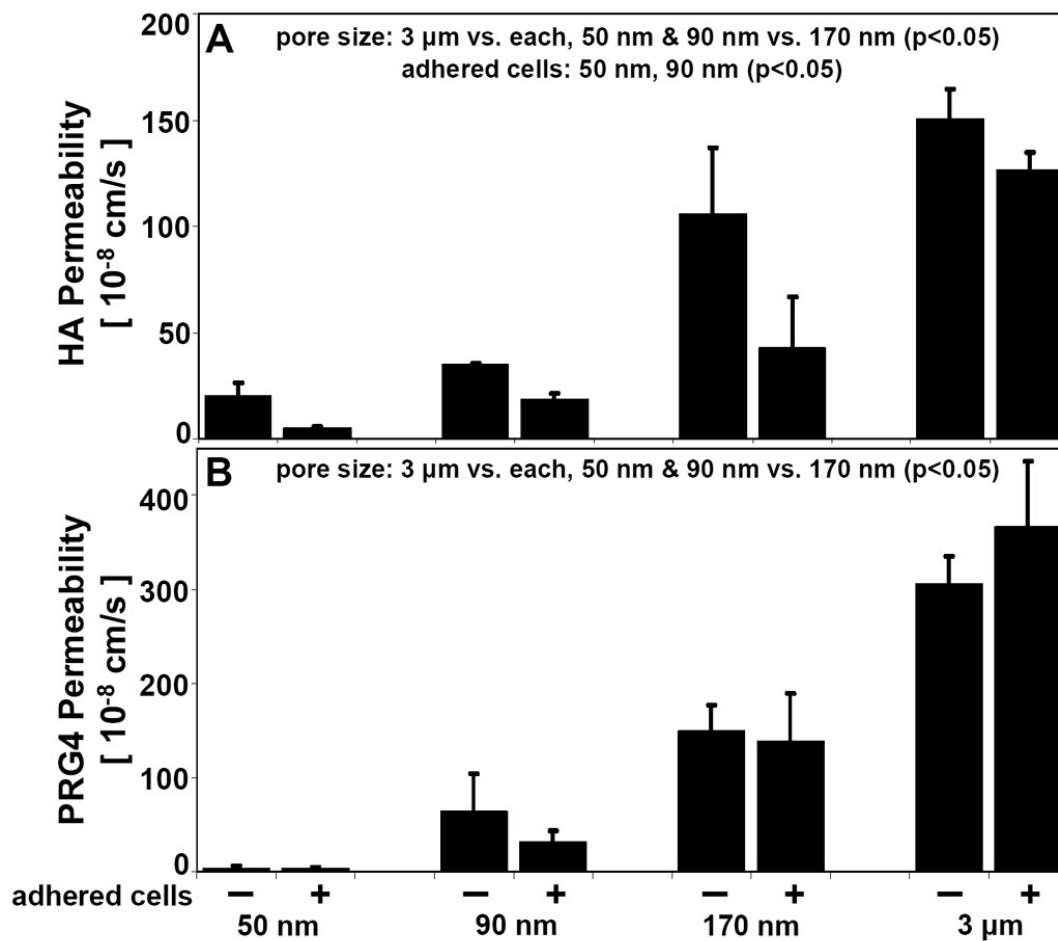
Figure 4.5: Permeability of ePTFE membranes ± adhered cells to (**A**) HA (with mixture of MWs) and (**B**) PRG4, n=3-4.
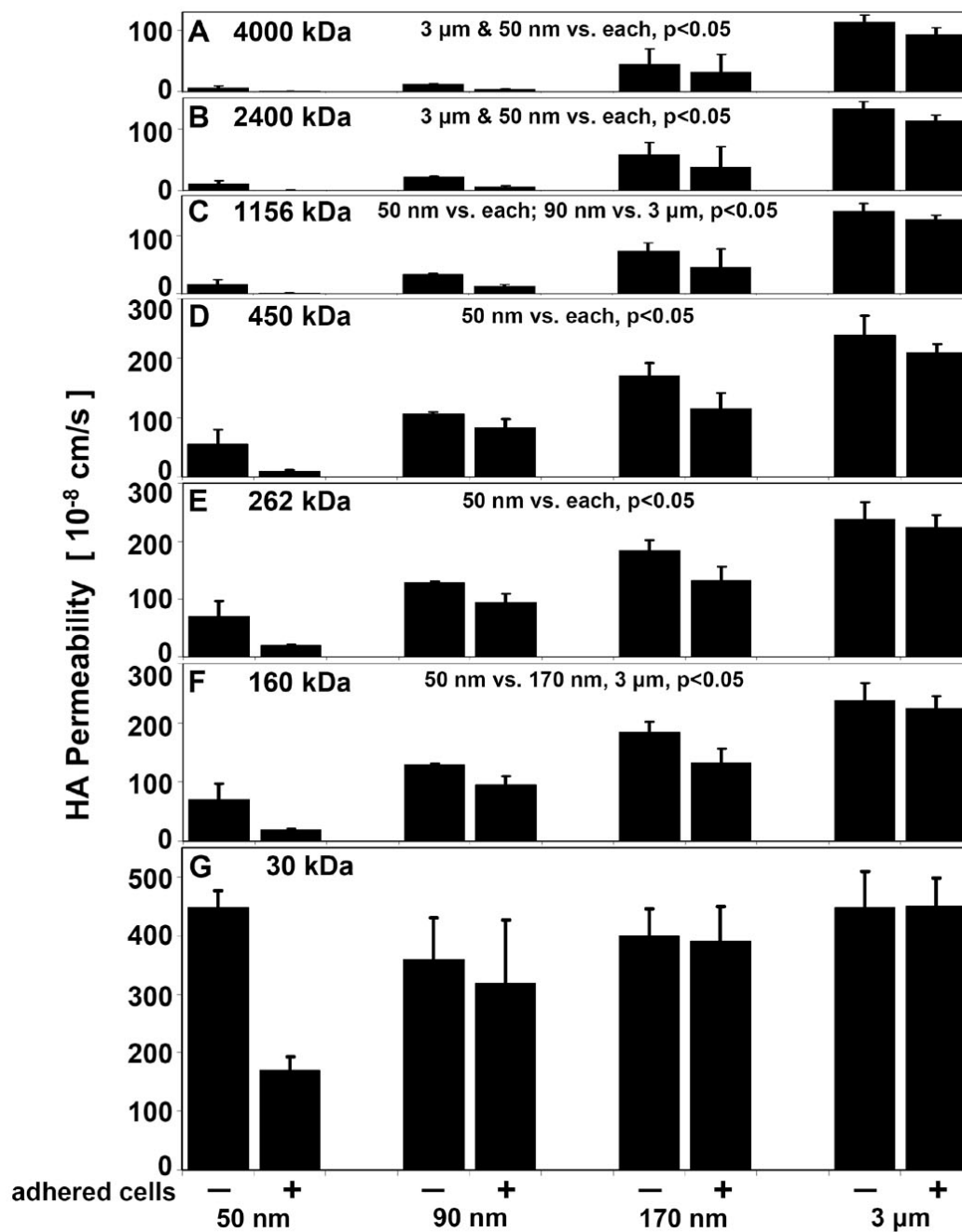
Figure 4.6: Permeability of ePTFE membranes ± adherent cells to HA, as a function of HA MW, (**A**) 4000 kDa, (**B**) 2400 kDa, (**C**) 1156 kDa, (**D**) 450 kDa, (**E**) 262 kDa, (**F**) 160 kDa, and (**G**) 30 kDa, n=3-4.

Table 4.1: Permeability of membranes ± adherent cells to (**A**) HA and (**B**) PRG4, calculated from lubricant transport studies.

A

HA MW [kDa]	Permeability [10^{-8} cm/s]							
	50 nm		90 nm		170 nm		3 μm	
	- cells	+ cells	- cells	+ cells	- cells	+ cells	- cells	+ cells
total HA	19.6 ± 6.9	4.8 ± 0.6	34.5 ± 1.1	18.5 ± 2.5	105.5 ± 31.7	42.5 ± 24.4	150.4 ± 14.2	126.5 ± 8.3
4,000	6.4 ± 3.0	0.4 ± 0.2	11.6 ± 2.0	3.1 ± 1.4	45.0 ± 24.8	31.6 ± 29.7	113.8 ± 11.2	93.1 ± 11.1
2,400	10.6 ± 5.2	0.5 ± 0.3	21.7 ± 1.9	5.9 ± 2.2	58.1 ± 19.3	38.0 ± 32.7	132.6 ± 11.5	113.4 ± 9.1
1,156	16.1 ± 8.1	0.7 ± 0.3	33.3 ± 1.7	12.7 ± 3.0	73.5 ± 14.6	45.4 ± 31.7	142.3 ± 13.6	127.6 ± 8.3
450	31.3 ± 15.4	2.3 ± 0.5	68.3 ± 3.7	41.7 ± 7.1	114.0 ± 14.8	70.7 ± 24.7	181.8 ± 19.9	163.1 ± 12.3
262	55.1 ± 23.9	9.2 ± 2.4	106.3 ± 2.7	82.4 ± 14.8	169.8 ± 22.2	114.0 ± 27.0	238.8 ± 32.5	208.7 ± 15.3
160	71.2 ± 26.1	18.8 ± 2.5	128.4 ± 2.9	94.6 ± 15.1	184.3 ± 17.4	131.7 ± 24.3	237.2 ± 30.5	224.1 ± 20.4
30	447.6 ± 28.8	170.2 ± 22.3	358.9 ± 70.7	317.5 ± 109.2	399.4 ± 46.9	389.8 ± 59.1	447.4 ± 62.7	449.6 ± 48.2

B

PRG4	Permeability [10^{-8} cm/s]							
	50 nm		90 nm		170 nm		3 μm	
	- cells	+ cells	- cells	+ cells	- cells	+ cells	- cells	+ cells
	3.9 ± 1.8	3.3 ± 1.4	63.8 ± 39.5	31.7 ± 12.4	149.4 ± 28.1	137.8 ± 51.8	305.1 ± 29.8	366.4 ± 68.9
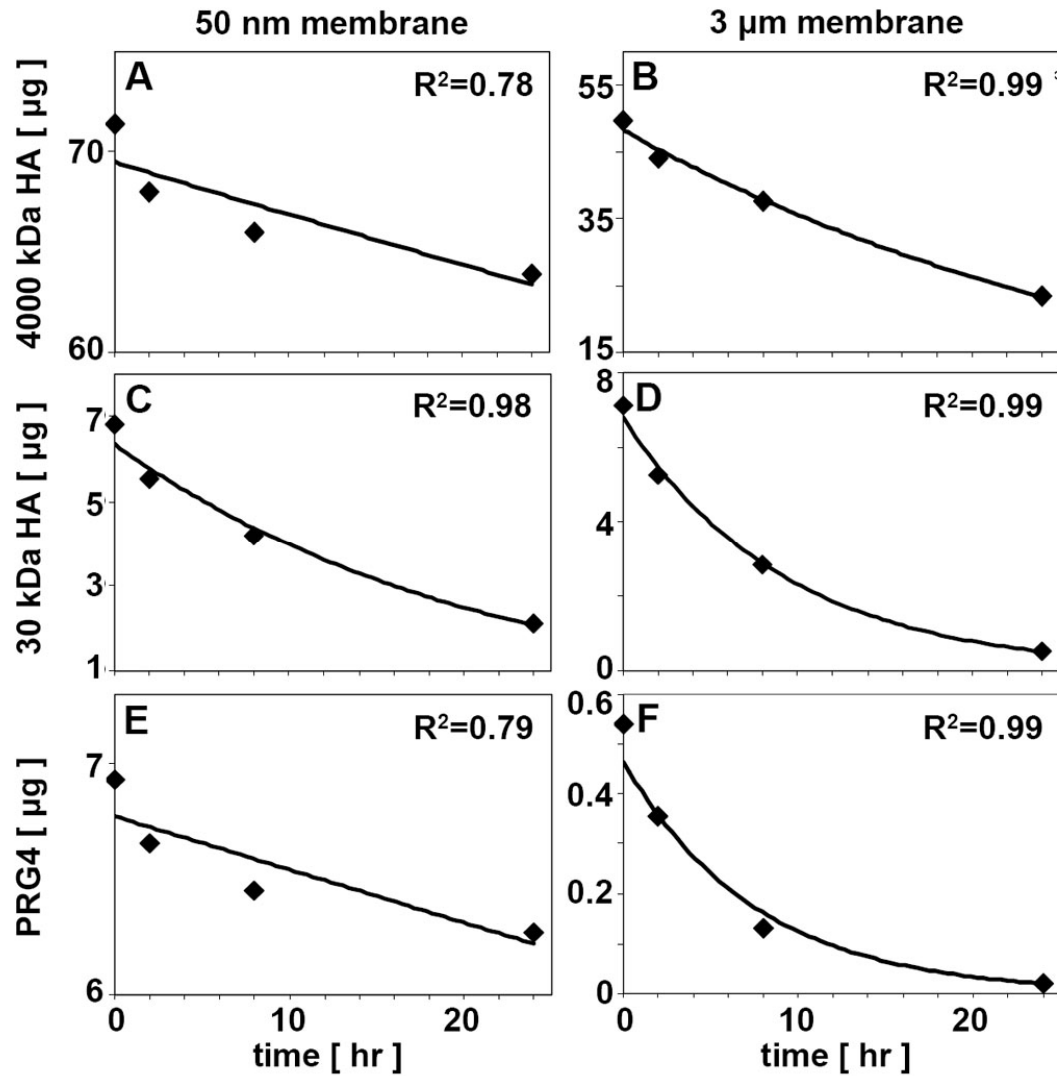
Figure 4.7: Representative curves of the mass of lubricant in BF vs. time (0, 2, 8, and 24 hr timepoints) fit with exponential curves predicted by engineering analysis utilized in permeability calculations: (**A**) 4000 kDa HA with 50 nm membranes, (**B**) 4000 kDa HA with 3 μm membranes, (**C**) 30 kDa HA with 50 nm membranes, (**D**) 30 kDa HA with 3 μm membranes, (**E**) PRG4 with 50 nm membranes, (**F**) PRG4 3 μm membranes.

4.5 Discussion

This study examined HA and PRG4 secretion rates by cultured synoviocytes on ePTFE membranes of pore sizes ~50 nm to ~3 μm, and also the extent of HA and PRG4 retention by these membranes. Synoviocyte HA and PRG4 secretion rates on membranes were comparable to those on tissue-culture plastic and stimulated by application of cytokines (**Figure 4.2**). Transport of HA and PRG4 across membranes was dependent upon pore size, with % of total lubricant loss and membrane permeability to lubricant being lowest with 50 nm membranes and highest with 3 μm membranes (**Figure 4.3, 4.5**). HA transport was further dependent upon the presence of adherent cells and HA MW, with the presence of a cell layer (for 50 nm and 90 nm membranes) and higher MWs resulting in decreased loss and permeability (**Figure 4.4, 4.6**). ~92% of low MW HA (30 kDa) was lost after 24 hr with membranes of all pore sizes, while HA of intermediate MW (450 kDa) was lost to a greater extent with 90 nm, 170 nm, and 3 μm membranes than with 50 nm membranes (37-74%, vs. 12%) (**Figure 4.4**). HA of high MW (4000 kDa) was lost to a greater extent with 3 μm membranes than all others (56% vs. 3-23%). In comparison, the % of total PRG4 loss was 3% for 50 nm membranes and 93% for 3 μm membranes (**Figure 4.3B**). The associated HA permeability ranged from ~3 x 10^{-8} cm/s to ~449 x 10^{-8} cm/s, and PRG4 permeability ranged from ~4 x 10^{-8} cm/s to ~325 x 10^{-8} cm/s (**Figure 4.5B, 4.6, Table 4.1**). These results suggest that membranes of various pore sizes may be applied to a bioreactor system to modulate the lubricant composition in a bioengineered SF. The presence of an adherent layer of synoviocytes on the membranes may not only serve to further modulate lubricant retention, but could also serve as a lubricant source.

Although a large percentage of total lubricants diffused across the membranes in certain conditions in this study, the assumption that the lubricant concentration in NF was negligible in comparison to BF remained valid due to the large volume of NF in relation to BF (30x greater). It should also be noted that endogenous HA and PRG4 secretion by adherent synoviocytes on the membranes likely had negligible contribution to the BF lubricant concentration, as transport studies were performed in basal media conditions in which lubricant secretion by synoviocytes is predicted to be very low, i.e. ~0.1-1% of exogenously applied mass during the duration of the study.

The ability to culture synoviocytes on material substrates, rather than on standard tissue culture plastic, with maintenance of a desired phenotype is consistent with and extends previous studies [28, 39, 43, 67]. Synoviocytes attached to ePTFE membranes within hours, proliferated to confluency within ~1 week, and maintained secretion of both HA and PRG4 in a cytokine-regulated manner. A thin, flexible lubricant-secreting sheet could be incorporated into various types of synovial joint bioreactors to enclose cartilage surfaces and form a SF compartment, including bioreactor systems of simple geometry and also complex whole joint-scale systems where cartilage surfaces are large and contoured in an anatomical configuration.

The findings in this study showing the importance of MW in HA transport provide an in vitro analog to previous work examining in vivo transport of HA across the synovium. Studies that infused HA of varying MW into the knee joint cavity of rabbits demonstrated that with HA of lower MW (~140 kDa, ~500 kDa) there was less retention by the synovium and accumulation in the cavity than with HA of higher MW (~2200 kDa) [14, 48]. Similar observations were made with studies on intraarticular infusion of fluorescein-labeled HA into the knee joint cavity of dogs, where HA of

2300 kDa MW scarcely penetrated the synovial lining, but 840 kDa HA penetrated readily [5].

As PRG4 loss across membranes in this study was affected by pore size in a relatively similar manner to that of HA, the transport of PRG4 of varying MW may also be differentially transported. The commonly reported MW of PRG4 present in normal SF is ~345 kDa, although it has also been shown that PRG4 may exist not only in larger multimeric forms [45] but also in smaller MW forms [64]. The relative abundance of the different MWs of PRG4 in SF and their contribution to PRG4 transport remains to be established, but it is likely that increases in the effective MW of PRG4 would decrease the relative rate of PRG4 loss from SF.

The different molecular structures of HA and PRG4 may account for some of the differences in transport patterns observed in this study between PRG4 (~350 kDa) and HA of a similar MW (450 kDa). The % of total PRG4 loss with 50 nm membranes was limited compared to that of 450 kDa HA (3% vs. 12% (avg.)), while the % loss with 170 nm and 3 μm pore sizes was greater for PRG4 (67% vs. 50% and 93% vs. 74% (avg.)). Comparison of the permeability values calculated in this study between PRG4 and 450 kDa HA also reveals similar distinctions. The large mucin-like domain present in the PRG4 structure and potential differences in the secondary structures of these lubricants could contribute to their distinct transport properties.

The efflux of solutes from SF in vivo is a function of both diffusion-driven and convection-driven solute flux across the synovium, and although many studies have assessed the latter [14, 48, 49, 57, 59, 60], some comparisons may still be drawn between the permeability parameters obtained in this in vitro study and the available literature. Numerical values for synovium permeability to HA or PRG4 remain to be measured experimentally, but the reported free diffusion coefficients are 0.98×10^{-7}

cm^2/s and 1.11 x 10^{-7} cm^2/s, respectively [48, 65]. The permeability values obtained here for 50 nm pore size membranes, a pore size within the reported range of synovium pore size, were on the order of ~1-5 x 10^{-8} cm/s for PRG4 and HA of physiological MW. An estimation of the restricted diffusion coefficient through the membrane, calculated using these permeability values and a membrane thickness of ~0.02 cm, is ~1 x 10^{-9} cm^2/s to 2 x 10^{-10} cm^2/s, a value expectedly orders of magnitude lower than the free diffusion coefficients. Reports of synovium permeability to albumin, a low MW solute that is transported very readily across the synovium, have been published and are expectedly greater than that of HA and PRG4 found here (~6 x 10^{-5} cm/s vs. ~1-5 x 10^{-8} cm/s) [21]. Taken together, some of the permeability values reported in this study for HA and PRG4 obtained with ePTFE membranes, particularly those of 50 nm pore size, could be within the range of native synovium lubricant permeability.

As in vivo alterations in the synovium structure may occur in disease or injury and affect the rate of lubricant loss from SF, a range of membrane pore sizes were utilized in this study to potentially parallel various in vivo conditions. For example, the observed HA half-life in SF is decreased in arthritic joints compared to normal joints (~12 hours vs. ~24 hours) [15, 18, 31, 51], while the concentrations of certain SF cytokines that may contribute to degradation of synovium extracellular matrix are often increased [9, 27, 30, 35, 70]. Digestion of synovium matrix components increases hydraulic permeability of the tissue, with degradation by *Streptomyces* hyaluronidase, chymopapain, and chondroitinase ABC increasing hydraulic permeability by ~5x, 4x, and 2x, respectively, over untreated synovium [13, 57, 58]. In the present study, the permeability of the larger pore size membranes (90 nm, 170 nm, 3 μm) to total HA and PRG4 were ~2-12x and ~10-90x greater, respectively, than

that of smallest pore size membrane (50 nm). If the 50 nm pore size membrane mimics certain transport properties of the normal synovium, then membranes of pore sizes 90 nm to 3 μm may mimic properties of injured or diseased synovium with varying degrees of increased permeability.

The bioreactor system developed here could be utilized to gain a better understanding of whether interactions of lubricant molecules affect their transport properties. HA and PRG4 have been reported to synergistically interact in lowering friction at cartilage-cartilage interfaces and also latex-glass interfaces by postulated mechanisms involving molecular interactions of the lubricant [24, 55]. Such interactions in SF could increase the effective MW of HA and PRG4 and limit the rate of lubricant transport across the synovium. HA and albumin have also been demonstrated to synergistically interact in decreasing fluid flow rates across the synovium by proposed molecular associations affecting osmotic pressure or viscosity [60]. Physical interactions of lubricants with surrounding joint tissues may also occur, including the synovium, and could effectively slow transport. Various biological solutions may be applied to the bioreactor system developed here to study the effects of these different types of interactions on lubricant transport properties.

The results of this study demonstrate (1) the ability of human synoviocytes to adhere and proliferate on semi-permeable membranes and to be regulated in their lubricant secretion rates by applied chemical factors, and (2) the ability of these membranes, with or without an adherent cell layer, to retain lubricant molecules in a manner dependent upon membrane pore size and lubricant MW. Such membranes may be applied to a synovial joint bioreactor system as a method to modulate lubricant retention and thus lubricant composition in a bioengineered SF. An adherent layer of synoviocytes on the membranes may not only serve to further modulate lubricant

retention, but could also serve as a lubricant source. The ability to bioengineer SF with modulated lubricant composition may have application in tissue engineering whole joints for biological joint replacement, by providing an appropriate lubricating environment to articulating cartilage surfaces during applied mechanical stimulation in bioreactors. A bioreactor for generating bioengineered SF may also have applications in developing lubricant supplements to be delivered to deficient SF, and in identifying molecules involved in lubricant regulation.

4.6   Acknowledgments

4.7   References

1. Afify A, Lynne LC, Howell L: Correlation of cytologic examination with ELISA assays for hyaluronan and soluble CD44v6 levels in evaluation of effusions. *Diagn Cytopathol* 35:105-10, 2007.

2. Albelda SM, Sampson PM, Haselton FR, McNiff JM, Mueller SN, Williams SK, Fishman AP, Levine EM: Permeability characteristics of cultured endothelial cell monolayers. *J Appl Physiol* 64:308-22, 1988.

3. Alvaro-Gracia JM, Zvaifler NJ, Firestein GS: Cytokines in chronic inflammatory arthritis. V. Mutual antagonism between interferon-gamma and tumor necrosis factor-alpha on HLA-DR expression, proliferation, collagenase production, and granulocyte macrophage colony-stimulating factor production by rheumatoid arthritis synoviocytes. *J Clin Invest* 86:1790-8, 1990.

4. Arnett FC, Edworthy SM, Bloch DA, McShane DJ, Fries JF, Cooper NS, Healey LA, Kaplan SR, Liang MH, Luthra HS: The American Rheumatism Association 1987 revised criteria for the classification of rheumatoid arthritis. *Arthritis Rheum* 31:315-24, 1988.

5. Asari A, Miyauchi S, Matsuzaka S, Ito T, Kominami E, Uchiyama Y: Molecular weight-dependent effects of hyaluronate on the arthritic synovium. *Arch Histol Cytol* 61:125-35, 1998.

6. Balazs EA: The physical properties of synovial fluid and the special role of hyaluronic acid. In: *Disorders of the knee,* ed. by AJ Helfet, Lippincott Co., Philadelphia, 1974, 63-75.

7. Balazs EA, Watson D, Duff IF, Roseman S: Hyaluronic acid in synovial fluid. I. Molecular parameters of hyaluronic acid in normal and arthritis human fluids. *Arthritis Rheum* 10:357-76, 1967.

8. Bellon JM, Bujan J, Honduvilla NG, Hernando A, Navlet J: Endothelial cell seeding of polytetrafluoroethylene vascular prostheses coated with a fibroblastic matrix. *Ann Vasc Surg* 7:549-55, 1993.

9. Bertone AL, Palmer JL, Jones J: Synovial fluid cytokines and eicosanoids as markers of joint disease in horses. *Vet Surg* 30:528-38, 2001.

10. Blewis ME, Nugent-Derfus GE, Schmidt TA, Schumacher BL, Sah RL: A model of synovial fluid lubricant composition in normal and injured joints. *Eur Cell Mater* 13:26-39, 2007.

11. Blewis ME, Orwoll BE, Lao BJ, Schumacher BL, Bugbee WD, Firestein GS, Sah RL: Interactive cytokine regulation of synoviocyte hyaluronan and proteoglycan 4 secretion rates. *Trans Orthop Res Soc* 33:374, 2008.

12. Charcosset C: Membrane processes in biotechnology: an overview. *Biotechnol Adv* 24:482-92, 2006.

13. Coleman PJ, Scott D, Abiona A, Ashhurst DE, Mason RM, Levick JR: Effect of depletion of interstitial hyaluronan on hydraulic conductance in rabbit knee synovium. *J Physiol* 509 (Pt 3):695-710, 1998.

14. Coleman PJ, Scott D, Mason RM, Levick JR: Role of hyaluronan chain length in buffering interstitial flow across synovium in rabbits. *J Physiol* 526 Pt 2:425-34, 2000.

15. Coleman PJ, Scott D, Ray J, Mason RM, Levick JR: Hyaluronan secretion into the synovial cavity of rabbit knees and comparison with albumin turnover. *J Physiol* 503 (Pt 3):645-56, 1997.

16. Dahl LB, Dahl IM, Engstrom-Laurent A, Granath K: Concentration and molecular weight of sodium hyaluronate in synovial fluid from patients with rheumatoid arthritis and other arthropathies. *Ann Rheum Dis* 44:817-22, 1985.

17. Flory PJ. Principles of Polymer Chemistry. Ithaca, NY, USA: Cornell University Press; 1971.

18. Fraser JR, Kimpton WG, Pierscionek BK, Cahill RN: The kinetics of hyaluronan in normal and acutely inflamed synovial joints: observations with experimental arthritis in sheep. *Semin Arthritis Rheum* 22:9-17, 1993.

19. Grad S, Gogolewski S, Alini M, Wimmer MA: Effects of simple and complex motion patterns on gene expression of chondrocytes seeded in 3D scaffolds. *Tissue Eng* 12:3171-9, 2006.

20. Grad S, Lee CR, Gorna K, Gogolewski S, Wimmer MA, Alini M: Surface motion upregulates superficial zone protein and hyaluronan production in chondrocyte-seeded three-dimensional scaffolds. *Tissue Eng* 11:249-56, 2005.

21. Granger HJ, Taylor AE: Permeability of connective tissue linings isolated from implanted capsules; implications for interstitial pressure measurements. *Circ Res* 36:222-8, 1975.

22. Gribbon P, Heng BC, Hardingham TE: The molecular basis of the solution properties of hyaluronan investigated by confocal fluorescence recovery after photobleaching. *Biophys J* 77:2210-6, 1999.

23. Ikegawa S, Sano M, Koshizuka Y, Nakamura Y: Isolation, characterization and mapping of the mouse and human PRG4 (proteoglycan 4) genes. *Cytogenet Cell Genet* 90:291-7, 2000.

24. Jay GD, Lane BP, Sokoloff L: Characterization of a bovine synovial fluid lubricating factor III. The interaction with hyaluronic acid. *Connect Tissue Res* 28:245-55, 1992.

25. Jensen LT, Henriksen JH, Olesen HP, Risteli J, Lorenzen I: Lymphatic clearance of synovial fluid in conscious pigs: the aminoterminal propeptide of type III procollagen. *Eur J Clin Invest* 23:778-84, 1993.

26. Jo H, Dull RO, Hollis TM, Tarbell JM: Endothelial albumin permeability is shear dependent, time dependent, and reversible. *Am J Physiol* 260:H1992-6, 1991.

27. Joosten LA, Netea MG, Kim SH, Yoon DY, Oppers-Walgreen B, Radstake TR, Barrera P, van de Loo FA, Dinarello CA, van den Berg WB: IL-32, a proinflammatory cytokine in rheumatoid arthritis. *Proc Natl Acad Sci USA* 103:3298-303, 2006.

28. Kiener HP, Lee DM, Agarwal SK, Brenner MB: Cadherin-11 induces rheumatoid arthritis fibroblast-like synoviocytes to form lining layers in vitro. *Am J Pathol* 168:1486-99, 2006.

29. Knight AD, Levick JR: Morphometry of the ultrastructure of the blood-joint barrier in the rabbit knee. *Q J Exp Physiol* 69:271-88, 1984.

30. Kotake S, Udagawa N, Takahashi N, Matsuzaki K, Itoh K, Ishiyama S, Saito S, Inoue K, Kamatani N, Gillespie MT, Martin TJ, Suda T: IL-17 in synovial fluids from patients with rheumatoid arthritis is a potent stimulator of osteoclastogenesis. *J Clin Invest* 103:1345-52, 1999.

31. Laurent UB, Fraser JR, Engstrom-Laurent A, Reed RK, Dahl LB, Laurent TC: Catabolism of hyaluronan in the knee joint of the rabbit. *Matrix* 12:130-6, 1992.

32. Lee HG, Cowman MK: An agarose gel electrophoretic method for analysis of hyaluronan molecular weight distribution. *Anal Biochem* 219:278-87, 1994.

33. Levick JR: Absorption of artificial effusions from synovial joints: an experimental study in rabbits. *Clin Sci (Lond)* 59:41-8, 1980.

34. Levick JR: Contributions of the lymphatic and microvascular systems to fluid absorption from the synovial cavity of the rabbit knee. *J Physiol* 306:445-61, 1980.

35. Marks PH, Donaldson ML: Inflammatory cytokine profiles associated with chondral damage in the anterior cruciate ligament-deficient knee. *Arthroscopy* 21:1342-7, 2005.

36. Mazzucco D, Scott R, Spector M: Composition of joint fluid in patients undergoing total knee replacement and revision arthroplasty: correlation with flow properties. *Biomaterials* 25:4433-45, 2004.

37. McDonald JN, Levick JR: Morphology of surface synoviocytes in situ at normal and raised joint pressure, studied by scanning electron microscopy. *Ann Rheum Dis* 47:232-40, 1988.

38. McGowan KB, Kurtis MS, Lottman LM, Watson D, Sah RL: Biochemical quantification of DNA in human articular and septal cartilage using PicoGreen and Hoechst 33258. *Osteoarthritis Cartilage* 10:580-7, 2002.

39. Momberger TS, Levick JR, Mason RM: Hyaluronan secretion by synoviocytes is mechanosensitive. *Matrix Biol* 24:510-9, 2005.

40. Nixon AJ, Haupt JL, Frisbie DD, Morisset SS, McIlwraith CW, Robbins PD, Evans CH, Ghivizzani S: Gene-mediated restoration of cartilage matrix by combination insulin-like growth factor-I/interleukin-1 receptor antagonist therapy. *Gene Ther* 12:177-86, 2005.

41. Noh I, Choi YJ, Son Y, Kim CH, Hong SH, Hong CM, Shin IS, Park SN, Park BY: Diffusion of bioactive molecules through the walls of the medial tissue-engineered hybrid ePTFE grafts for applications in designs of vascular tissue regeneration. *J Biomed Mater Res A* 79:943-53, 2006.

42. Nugent-Derfus GE, Takara T, O'Neill J K, Cahill SB, Gortz S, Pong T, Inoue H, Aneloski NM, Wang WW, Vega KI, Klein TJ, Hsieh-Bonassera ND, Bae WC, Burke JD, Bugbee WD, Sah RL: Continuous passive motion applied to whole joints stimulates chondrocyte biosynthesis of PRG4. *Osteoarthritis Cartilage* 15:566-74, 2007.

43. Ozturk AM, Yam A, Chin SI, Heong TS, Helvacioglu F, Tan A: Synovial cell culture and tissue engineering of a tendon synovial cell biomembrane. *J Biomed Mater Res A* 84:1120-6, 2008.

44. Patwari P, Norris SA, Kumar S, Lark MW, Grodzinsky AJ: Inhibition of bovine cartilage biosynthesis by coincubation of joint capsule tissue is mediated by an interleukin-1-independent signalling pathway. *Trans Orthop Res Soc* 28:158, 2003.

45. Plaas A, Chekerov I, Zheng Y, Schmidt T, Sah R, Carter J, Sandy J: Disulfide-bonded multimers of lubricin (LGP-1, PRG4) glycovariants in cartilage, synovium and synovial fluid. *Trans Orthop Res Soc* 52:1422, 2006.

46. Price FM, Levick JR, Mason RM: Glycosaminoglycan concentration in synovium and other tissues of rabbit knee in relation to synovial hydraulic resistance. *J Physiol (Lond)* 495:803-20, 1996.

47. Price FM, Mason RM, Levick JR: Radial organization of interstitial exchange pathway and influence of collagen in synovium. *Biophys J* 69:1429-39, 1995.

48. Sabaratnam S, Arunan V, Coleman PJ, Mason RM, Levick JR: Size selectivity of hyaluronan molecular sieving by extracellular matrix in rabbit synovial joints. *J Physiol* 567:569-81, 2005.

49. Sabaratnam S, Mason RM, Levick JR: Filtration rate dependence of hyaluronan reflection by joint-to-lymph barrier: evidence for concentration polarisation. *J Physiol* 557:909-22, 2004.

50. Sahagun G, Moore SA, Hart MN: Permeability of neutral vs. anionic dextrans in cultured brain microvascular endothelium. *Am J Physiol* 259:H162-6, 1990.

51. Sakamoto T, Mizono, S, Miyazaki, K, Yamaguchi, T, Toyoshima, H, Namiki, O.: Biological fate of sodium hyaluronate (SPH): Studies on the distribution, metabolism, and excretion of ^{14}C-SPH in rabbits after intra-articular administration. *Pharmacometrics* 28:375-87, 1984.

52. Saxena A, Tripathi BP, Kumar M, Shahi VK: Membrane-based techniques for the separation and purification of proteins: An overview. *Adv Colloid Interface Sci*, 2008.

53. Schmid T, Lindley K, Su J, Soloveychik V, Block J, Kuettner K, Schumacher B: Superficial zone protein (SZP) is an abundant glycoprotein in human synovial fluid and serum. *Trans Orthop Res Soc* 26:82, 2001.

54. Schmidt TA, Gastelum NS, Han EH, Nugent-Derfus GE, Schumacher BL, Sah RL: Differential regulation of proteoglycan 4 metabolism in cartilage by IL-1α, IGF-I, and TGF-β1. *Osteoarthritis Cartilage* 16:90-7, 2008.

55. Schmidt TA, Gastelum NS, Nguyen QT, Schumacher BL, Sah RL: Boundary lubrication of articular cartilage: role of synovial fluid constituents. *Arthritis Rheum* 56:882-91, 2007.

56. Schumacher BL, Block JA, Schmid TM, Aydelotte MB, Kuettner KE: A novel proteoglycan synthesized and secreted by chondrocytes of the superficial zone of articular cartilage. *Arch Biochem Biophys* 311:144-52, 1994.

57. Scott D, Coleman PJ, Abiona A, Ashhurst DE, Mason RM, Levick JR: Effect of depletion of glycosaminoglycans and non-collagenous proteins on interstitial hydraulic permeability in rabbit synovium. *J Physiol* 511 (Pt 2):629-43, 1998.

58. Scott D, Coleman PJ, Mason RM, Levick JR: Glycosaminoglycan depletion greatly raises the hydraulic permeability of rabbit joint synovial lining. *Exp Physiol* 82:603-6, 1997.

59. Scott D, Coleman PJ, Mason RM, Levick JR: Concentration dependence of interstitial flow buffering by hyaluronan in synovial joints. *Microvasc Res* 59:345-53, 2000.

60. Scott D, Coleman PJ, Mason RM, Levick JR: Interaction of intraarticular hyaluronan and albumin in the attenuation of fluid drainage from joints. *Arthritis Rheum* 43:1175-82, 2000.

61. Smith MM, Ghosh P: The synthesis of hyaluronic acid by human synovial fibroblasts is influenced by the nature of the hyaluronate in the extracellular environment. *Rheumatol Int* 7:113-22, 1987.

62. Sokal RR, Rohlf FJ. Biometry. 3rd ed. New York: WH Freeman and Co.; 1995.

63. Su J-L, Schumacher BL, Lindley KM, Soloveychik V, Burkhart W, Triantafillou JA, Kuettner KE, Schmid TM: Detection of superficial zone protein in human and animal body fluids by cross-species monoclonal antibodies specific to superficial zone protein. *Hybridoma* 20:149-57, 2001.

64. Swann DA, Silver FH, Slayter HS, Stafford W, Shore E: The molecular structure and lubricating activity of lubricin isolated from bovine and human synovial fluids. *Biochem J* 225:195-201, 1985.

65. Swann DA, Slayter HS, Silver FH: The molecular structure of lubricating glycoprotein-I, the boundary lubricant for articular cartilage. *J Biol Chem* 256:5921-5, 1981.

66. Thibault M, Poole AR, Buschmann MD: Cyclic compression of cartilage/bone explants in vitro leads to physical weakening, mechanical breakdown of collagen and release of matrix fragments. *J Orthop Res* 20:1265-73, 2002.

67. Vickers SM, Johnson LL, Zou LQ, Yannas IV, Gibson LJ, Spector M: Expression of alpha-Smooth Muscle Actin by and Contraction of Cells Derived from Synovium. *Tissue Eng* 10:1214-23, 2004.

68. Visser NA, van Kampen GPJ, Dekoning MHMT, van der Korst JK: The effects of loading on the synthesis of biglycan and decorin in intact mature articular cartilage in vitro. *Connect Tissue Res* 30:241-50, 1994.

69. Walluscheck KP, Steinhoff G, Kelm S, Haverich A: Improved endothelial cell attachment on ePTFE vascular grafts pretreated with synthetic RGD-containing peptides. *Eur J Vasc Endovasc Surg* 12:321-30, 1996.

70. Wei X, Messner K: Age- and injury-dependent concentrations of transforming growth factor-beta 1 and proteoglycan fragments in rabbit knee joint fluid. *Osteoarthritis Cartilage* 6:10-8, 1998.

CHAPTER 5:

BIOMIMETIC BIOENGINEERING OF SYNOVIAL FLUID: A BIOREACTOR FOR GENERATING FUNCTIONAL LUBRICANT SOLUTIONS

5.1   Abstract

Introduction: The synovial fluid (SF) lubricants, hyaluronan (HA) and proteoglycan 4 (PRG4), are secreted by synoviocytes lining the joint and chondrocytes in cartilage, and concentrated in SF due to the retaining property of the semi-permeable synovium. We hypothesized that a biomimetic bioreactor, recapitulating these biophysical features, is capable of producing a bioengineered fluid (BF) with lubricant composition and function similar to that of native SF. The objectives of this study were, using such a bioreactor, to (1) assess the lubricant composition and friction-reducing function of BF, and (2) compare measured lubricant concentrations in BF with those predicted by a model incorporating lubricant transport and mass balance principles.

Methods: Bioreactors were fabricated to provide (1) a BF compartment enclosed by 50 nm or 3 μm pore size membranes with adherent synoviocytes and

containing bovine articular cartilage explants, and (2) an external compartment of nutrient fluid (NF). The bioreactors were maintained for 12d with NF medium being changed every 3d and supplemented with IL-1β + TGF-β1 (IT) or IL-1β + TGF-β1 + TNF-α (ITT), cytokine mixtures that stimulate lubricant synthesis. Samples were analyzed for HA and PRG4 concentration and MW by ELISA, Western blot, and gel electrophoresis. Additionally, BF and normal bovine SF were analyzed for friction-lowering function with a cartilage-on-cartilage friction test. The bioreactor system was also modeled to predict transient and steady-state lubricant concentration in BF using principles of mass balance and transport, as well as experimentally-determined parameters of lubricant secretion rates and membrane permeability.

Results: HA and PRG4 concentrations were 10x-50,000x higher in BF than in NF, and 10x-30x higher with 50 nm membranes than with 3 μm membranes. BF with 50 nm membranes achieved HA and PRG4 concentrations similar to that of native SF, ~600 μg/ml and ~400 μg/ml, respectively. The HA MW distributions in BF with both pore size membranes and in NF with 3 μm membranes were largely distributed at high MWs (~4000 kDa) and resembled that of native SF, while the distribution in NF with 50 nm membranes was predominantly of low MW (~30 kDa). PRG4 structure in BF was of the same high MW for all conditions and equivalent to that of native SF. The lubricating function of BF with 50 nm membranes was greater than that with 3 μm membranes (μ= ~0.037 vs. ~0.097), and approached that of native SF (μ=0.023). Model predictions of lubricant concentrations were similar to those observed experimentally, and the predicted kinetics were distinct for the different pore size membranes and MW forms of HA.

Conclusions: This is the first report of a bioreactor system capable of generating fluid with lubricant composition and friction-lowering function similar to

that of native SF. The ability to bioengineer a lubricious fluid in a biomimetic bioreactor system may have applications in tissue engineering of articular cartilage using mechanical stimuli, in generating viscosupplements, and in identifying lubricant-regulating molecules.

5.2   Introduction

The synovial fluid (SF) of joints contains a number of molecules that mediate its lubricating biomechanical function on articular cartilage and other biological functions, including lubricants, regulatory cytokines and growth factors, nutrients, and waste products. The lubricating molecule hyaluronan (HA) in SF is secreted predominantly by fibroblast-like synoviocytes (abbreviated in this paper as "synoviocytes") in synovium [27, 52], while the lubricating molecule proteoglycan 4 (PRG4) is secreted by synoviocytes as well as chondrocytes in the superficial layer of articular cartilage [28, 47, 48].

In addition to serving as a source of lubricant molecules, the synovium acts as a semi-permeable membrane. It allows the exchange of small solutes between SF and the underlying subsynovium while also offering outflow resistance to high molecular weight macromolecules, such as HA and PRG4 lubricants. The balance between the rate of synthesis of lubricants, resulting from secretion by chondrocytes and synoviocytes, and loss of lubricants by transport across the semi-permeable synovium and/or by degradation in SF, dictate the lubricant composition and, likely, the lubricant function of SF [12, 33].

Tissue engineering of articular cartilage and synovial joints for the treatment of arthritis may benefit from a lubricious fluid recapitulating that of normal SF. An appropriate lubricating environment may facilitate maintenance of the low-friction, low-wear properties of articulating cartilage surfaces undergoing joint-like motion in bioreactors [38]. A bioreactor system that encloses lubricant secreting cell types within a lubricant-retaining membrane may have the capability to generate a bioengineered fluid similar in composition and lubricating function to native SF

(**Figure 5.1**). The ability to bioengineer such a fluid may have additional applications in developing arthritis therapies targeted at restoration of failed joint lubrication, such as viscosupplements and molecules that regulate lubricant secretion. A SF bioreactor system might also further our understanding of joint physiology and pathophysiology by allowing assessment of the relationship between various chemical and mechanical regulatory stimuli and resulting composition and function of bioengineered SF.

Certain membrane materials, including expanded polytetrafluoroethylene (ePTFE), may be especially useful in mimicking the function of the synovium in a SF bioreactor system. ePTFE is an inert material that can be engineered to have specific pore sizes and, thus, varying solute permeability. It also has a controlled structure over large surface areas and is resistant to degradation, properties that may help to provide consistent filtration during extended periods of bioreactor usage. Such ePTFE membranes have been used in culture systems to assess diffusion of solutes across the material [37] and also to provide a substrate for cell attachment and growth, especially with ePTFE surface-modification [9, 56]. Our preliminary studies have demonstrated the ability of human synoviocytes to maintain their lubricant-secreting phenotype when cultured on ePTFE membranes and the ability of these membranes to retain lubricant molecules in a pore-size dependent manner [11]. Incorporation of this material in a bioreactor system to enclose lubricant secreting cell types may allow the generation of a bioengineered SF with membrane-modulated lubricant composition and, potentially, function.

The objectives of this study were, using a biomimetic bioreactor system, to (1) assess the lubricant composition and friction-reducing function of bioengineered fluid (BF), and (2) compare measured lubricant concentrations in BF with those predicted by a model incorporating lubricant transport and mass balance principles.
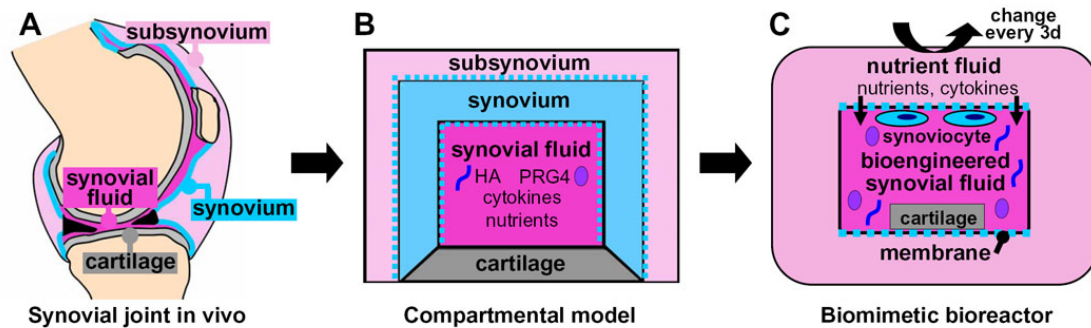
Figure 5.1: (**A**) The in vivo synovial joint can be (**B**) theoretically and (**C**) experimentally modeled as a system of communicating components which include lubricant-secreting cell types, a SF compartment, and a lubricant-retaining semi-permeable membrane.

5.3   Bioengineering Analysis & Design of Synovial Fluid Bioreactor

Overview

The bioreactor was designed to have a Bioengineered Fluid (BF) compartment that is separated via a semi-permeable membrane from an adjacent Nutrient Fluid (NF) compartment. As described in a model for native synovial joints [12], lubricants are secreted into the BF by synoviocytes adherent on the membrane and by chondrocytes in articular cartilage explants located within the BF. Some molecules are lost from the BF by flux through the membrane into the NF; however, the membrane offers a degree of outflow resistance sufficient to retain a pool of lubricants in the BF. With perturbations in BF, transient changes in the BF compartment are predicted to occur (see below) until the system reaches a steady-state lubricant.

Lubricant Secretion Rates

The lubricant composition in BF is predicted to depend, in part, upon the rate of lubricant secretion by chondrocytes and synoviocytes, and also the transport properties of the secreted lubricant. In vitro, lubricant secretion rates and transport-determining structure can be regulated by applied cytokines, including IL-1β + TGF-β1 (abbreviated IT) and IL-1β + TGF-β1 + TNF-α (abbreviated ITT). IT and ITT stimulate synoviocytes to markedly increase the rate of HA secretion, with an effect that is ~7-fold that of the additive effects of individual cytokines and ~100-fold higher than basal secretion rates [13]. IT and ITT also regulate the structure of the secreted HA, with a resultant molecular weight (MW) distribution resembling that of native SF (manuscript submitted for publication). IT and ITT also stimulate PRG4 secretion by

chondrocytes (~8-fold) and by synoviocytes (~80-fold) over basal secretion rates, with the IT tending to have a greater stimulatory effect than ITT [13].

Transport of Lubricants

The lubricant composition in BF is also predicted to depend, in part, upon the rate of lubricant loss across the semi-permeable membrane component. Such lubricant transport is a function of membrane permeability to lubricants, membrane area, and concentration gradient of lubricant between the BF and NF compartments. The membrane permeability of the bioreactor can be altered by using membranes with different pore sizes. Our previous studies indicated that ePTFE membranes of pore sizes 50 nm, 90 nm, 170 nm, and 3 μm offered a spectrum of permeability to HA and PRG4 [11]. The 50 nm pore size membranes were ~25-100x less permeable to HA of high MW (2400 kDa to 4000 kDa) than 3 μm pore size membranes, and were ~100x less permeable to PRG4. The rate of loss of lubricant from SF can also be affected by the rate of its degradation, but is not modeled here.

Geometrical Parameters

The geometry of the bioreactor system, including fluid volumes and tissue and membrane areas, affects the dynamics and steady-state concentrations of lubricant in the BF and NF. The native synovial joint in vivo was used as a design guide for selecting volume and area parameters of the bioreactor system. In the adult human knee joint, the total cartilage surface area is ~120 cm^2 [19, 20] and the thickness is ~2-5 mm [20]. The synovium surface area is ~277 cm^2 [19], the thickness is ~50 μm [40], and the estimated pore size is ~20-90 nm [15, 16, 26, 51]. The SF volume enclosed by

these tissue surfaces is ~1-2 ml [42]. A key design guide is the ratio of SF volume to synovium surface area, approximately 2 cm^3/200 cm^2, or ~0.01 cm.

Predicted Lubricant Concentrations (Transient & Steady-State)

Principles of mass transport have been used to mathematically model transient and steady-state lubricant concentration in SF of native joints [12] and were also applied to the present bioreactor system. With such an application of the model, the mass of lubricant i in BF (i = HA or PRG4), where mass is equal to the concentration of i in BF (c_i^{BF}) multiplied by the fluid volume in BF (V^{BF}), is increased by lubricant secretion rates by cartilage (r_i^{AC}) and synoviocytes (r_i^{SYN}) scaled to tissue areas (A^{AC}, A^{SYN}) and is decreased by flux due to diffusion of lubricant across the semi-permeable membrane (J_i^{MEM}):

$$\frac{\partial[V^{BF}c_i^{BF}(t)]}{\partial t} = r_i^{SYN}A^{SYN} + r_i^{AC}A^{AC} - J_i^{MEM} \tag{1}$$

Such diffusive flux is dependent upon membrane permeability to lubricant (p_i^{MEM}) and membrane area (A^{MEM}), and the concentration gradient of lubricant between BF and NF compartments (c_i^{BF} - c_i^{NF}):

$$J_i^{MEM}(t) = p_i^{MEM}[c_i^{BF}(t) - c_i^{NF}(t)]A^{MEM} \tag{2}$$

In this model, c_i^{NF} is assumed $\ll c_i^{BF}$ due to the comparably larger fluid volume of NF (i.e., 30x V^{BF}) and due to the frequent replenishment of fluid in the NF compartment. Thus, in the bioreactor system, the expression for transient changes in c_i^{BF} is:

$$\frac{\partial [V^{BF} c_i^{BF}(t)]}{\partial t} = r_i^{SYN} A^{SYN} + r_i^{AC} A^{AC} - p_i^{MEM} c_i^{BF}(t) A^{MEM} \tag{3}$$

which at steady-state simplifies to the following expression for c_i^{BF}:

$$c_i^{BF}(t = \infty) = \frac{r_i^{SYN} A^{SYN} + r_i^{AC} A^{AC}}{p_i^{MEM} A^{MEM}} \tag{4}$$

An important parameter associated with this analysis is the time constant τ_i, describing the kinetics of lubricant concentration in BF. As previously described, it represents the time over which lubricant i reaches 63% of the steady state concentration starting from a zero concentration [12].

$$\tau_i = \frac{V^{BF}}{p_i^{MEM} A^{MEM}} \tag{5}$$

The form of τ_i indicates that increases in p_i^{MEM} and A^{MEM} result in decreases in τ_i, while increases in V^{BF} cause increases in τ_i.

5.4   Materials and Methods

Bioreactor System

Bioreactors were fabricated to create two compartments: (1) a bioengineered fluid (BF) compartment and (2) a nutrient fluid (NF) compartment. The housing of the bioreactor was constructed from polysulphone. The BF and NF compartments were separated by two plane-parallel semi-permeable membranes each with a surface area of 1 cm^2 and separated by a distance of 1 mm (**Figure 5.1**). The BF compartment had a fluid volume of 0.1 ml, while the NF compartment had a volume of 3 ml.

Inert poly-l-lysine coated expanded polytetrafluoroethylene (ePTFE) membranes with average pore sizes of either ~50 nm or ~3 μm (W.L. Gore & Associates, Inc.) were utilized in the bioreactor in order to achieve varying degrees of lubricant retention. The 50 nm pore size is in the range of estimates of pore size of the synovium in vivo, and our previous studies demonstrated that the small ~50 nm pore size membranes retained HA and PRG4 lubricant molecules much more effectively than membranes of 3 μm pore size [11].

Human synoviocytes from four donors were prepared for use in bioreactors. Human synovial tissue was collected with Institutional Review Board (IRB) approval and informed donor consent, and studies were approved by the University of California, San Diego Human Subjects Research Protection Program. The synovial tissue was obtained from patients with osteoarthritis (OA) and rheumatoid arthritis (RA) at the time of joint replacement, as described previously [2]. The diagnosis of RA conformed to the 1987 revised American College of Rheumatology criteria [4]. Synovial tissues were minced and incubated with 1 mg/ml collagenase in serum free DMEM with additives (100 U/ml penicillin, 100 μg/ml streptomycin, 0.25 μg/ml Fungizone, 0.1 mM MEM non-essential amino acids, 10 mM HEPES, 0.4 mM L-proline, 2 mM L-glutamine) for 2 hr at 37ºC, filtered through a nylon mesh, extensively washed, and cultured in DMEM supplemented with 10% fetal bovine serum. After overnight culture, nonadherent cells were removed. Adherent cells were later trypsinized, split at a 1:3 ratio, and cultured in DMEM+10% FBS. Synoviocytes were used from passages 3 through 9 when they are a homogeneous population of fibroblast-like synoviocytes (<1% CD11b, <1% phagocytic, and <1% FcgRII positive [2]).

Bovine cartilage explants were harvested from the patellofemoral groove of four immature (1-3 week old) bovine stifle joints. Cartilage disks of 4 mm diameter and ~300-400 μm thickness containing the superficial zone with intact articular surface were obtained using a dermal biopsy punch and scalpel.

Experimental Design

Synoviocytes were seeded at 10,000 cells/cm^2 on a 50 nm pore size membrane applied to one end of the BF compartment of each bioreactor, and were cultured in DMEM+10% FBS for 6 days. Confluent cell layers were then incubated in DMEM + 0.5% FBS for 2 days to establish basal conditions prior to the addition of bovine cartilage explants (1 disk per bioreactor) and the application of either a 50 nm pore size or 3 μm pore size membrane on the other end of the BF compartment (**Figure 5.1**). Media, initially used to fill the BF compartment and also added to the NF compartment initially and with media changes, consisted of basal medium supplemented with either IL-1β + TGF-β1 (IT) or IL-1β + TGF-β1 + TNF-α (ITT) using concentrations of 10 ng/ml for IL-1β and TGF-β1, and 100 ng/ml for TNF-α. These cytokine combinations stimulate HA and PRG4 secretion over basal media conditions [13], as noted above. Bioreactors were incubated at 37ºC in a humidified 5% CO_2 environment with nutation for 12 days. Every 3 days, spent NF (either IT or ITT) was saved at -20ºC and fresh NF was provided. At the end of the culture period, BF was collected and weighed to determine volume, and both BF and NF were frozen at -70ºC. Subsequent analyses were performed on BF collected at day 12 and portions of NF pooled from all time point collections (days 3, 6, 9, and 12).

Analysis of Composition & Function of BF, NF, and SF

BF and NF were analyzed for concentration of HA by an enzyme-linked binding assay using HA binding protein [1].

The MW distribution of HA in BF and NF was assessed with an agarose gel electrophoresis technique [32], with several modifications. BF and NF samples, normal human SF (obtained from the normal knee, as assessed by X-ray, of subjects with intra-articular fractures in the contralateral knee, with IRB approval and informed consent), and HA standards in the MW range 30-4000 kDa (Associates of Cape Cod Inc., East Falmouth, MA) were first treated with proteinase K (0.5 mg/ml) overnight at 37ºC. The proteinase K was then subsequently inhibited by addition of 4-(2-Aminoethyl)-benzenesulfonyl fluoride (AEBSF) (1 mg/ml) (Roche, Indianapolis, IN), and a portion of each sample was treated with *Streptomyces* hyaluronidase (10 U/ml) (Seikagaku Corp., Tokyo, Japan) overnight at 37ºC. Samples with an HA mass of 700 ng were applied to 1% agarose gels (Lonza, Rockland, ME), separated by horizontal electrophoresis at 100V for 110 minutes in TAE buffer (0.4 M Tris-acetate, 0.01 M EDTA, pH 8.3), and visualized after incubation with 0.1% Stainsall reagent (Sigma, St. Louis, MO). Gel images were digitized with a D80 digital camera (Nikon, Melville, NY) and also processed to quantify HA distribution by subtracting the intensities of hyaluronidase-treated samples from those of non-hyaluronidase-treated samples and integrating the differential intensities within the MW ranges of <1000 kDa, 1000-3000 kDa, and >3000 kDa in order to determine the percentage of total HA in these regions.

Samples were also analyzed for PRG4. NF was analyzed for PRG4 concentration by ELISA using mAb 3-A-4 to detect bovine PRG4 (gift from Dr. Bruce Caterson [47]) or mAb GW4.23 to detect human PRG4 (gift from Dr. Klaus Kuettner [53]. BF and normal bovine SF were analyzed for PRG4 concentration by Western

blot with quantitative comparison to a band of similar MW of a known amount of PRG4 (Western blot methods described in detail below).

The structure of PRG4 in BF and in normal bovine SF was also assessed by Western blot. NF was not analyzed for PRG4 structure due to a very low PRG4 content. BF samples (2, 6, or 12 μl), normal bovine SF (0.25 μl), and PRG4 protein standards (0.1 μg, 0.2 μg) were treated with 10 U/ml *Streptomyces* hyaluronidase (Seikagaku Corp., Tokyo, Japan) overnight at 37ºC. Samples were then applied to precast 3-8% acrylamide Tris-acetate gels, and separated by electrophoresis at 150V for 1 hr in Tris-acetate SDS running buffer (50 mM Tricine, 50 mM Tris base, 0.1% SDS, pH 8.24), blotted onto PVDF membranes (Amersham, Piscataway, NJ) at 30V for 1 hr in transfer buffer (25 mM Bicine, 25 mM Bis-Tris, 1 mM EDTA, pH 7.20. The membranes were then blocked for 1 hr in 5% normal goat serum in PBS + 0.1% Tween 20 (pH 7.4), reacted with mAb 3-A-4 to bovine PRG4 [48] or mAb GW4.23 to human PRG4 (or non-specific mouse IgG as a control (Pierce, Rockford, IL)) at 0.5 μg/ml in 1% BSA in PBS + 0.1% Tween 20 for 1 hr, and then a goat anti-mouse secondary antibody conjugated to horse radish peroxidase. Immunoreactivity was detected by ECL-Plus chemiluminescence (Amersham Biosciences, Piscataway, NJ) and recorded with a Storm Imager (GMI, Ramsey, Minnesota). Signal intensities for each PRG4-immunoreactive band in BF and SF, and also in the PRG4 protein standards, were quantified with ImageQuant software (Molecular Dynamics, Fairfield, CT) and utilized to calculate PRG4 concentration in unknown samples.

Analysis of Lubricant Function

BF and normal bovine SF samples were also analyzed for friction-lowering function with boundary-mode friction tests performed on articulating adult bovine

cartilage as described previously [46]. Test lubricant solutions (~0.6 ml each) consisted of the following (each with proteinase inhibitors, PI): (1) PBS (as a negative control), (2,3) 10% BF from 50 nm pore size, for IT and ITT conditions, (4,5) 100% BF from 50 nm pore size, for IT and ITT conditions, (6,7) 10% BF from 3 μm pore size, for IT and ITT conditions, (8,9) 100% BF from 3 μm pore size, for IT and ITT conditions, and (10) normal bovine SF. Friction testing was performed using articular cartilage substrate from n=4 animals in an annulus-on-disk configuration at an offset compression of 18%, to yield boundary-mode friction coefficients, calculated from the measured torque and peak and equilibrium axial load.

Theoretical Predictions of Lubricant Concentration

Theoretical predictions of transient and steady-state lubricant concentrations in BF were performed as outlined in the Bioengineering Analysis section. Additionally, the relationship between day 12 measured lubricant concentrations and day 12 predicted lubricant concentrations were assessed. Theoretical predictions were made utilizing membrane permeability and lubricant secretion rate parameter values listed in **Table 5.1**. Permeability parameters were obtained from our previous studies assessing lubricant transport across 50 nm and 3 μm pore size ePTFE membranes for HA of a range of molecular weights (MWs) and for PRG4 (**Table 5.1A**). Lubricant secretion rate parameters (as a function of MW for HA) were obtained from lubricant composition analyses of the current study in both IT and ITT cytokine conditions and in both 50 nm and 3 μm membrane conditions (**Table 5.1A**). Additional parameters used in the model analysis were the volume of bioengineered fluid (0.09 ml), the area of cartilage (0.13 cm^2), the area of synoviocytes (1 cm^2), and the area of each membrane (1 cm^2) (**Table 5.1B**).

Statistical Analysis

Data are expressed as mean ± SEM. For HA and PRG4 concentration data, a 1-way ANOVA was used with Tukey post-hoc tests to compare all samples of either BF or NF. For analysis of HA MW, a 1-way ANOVA and Tukey post-hoc test was used to assess differences among all BF and NF samples in the MW ranges of <1,000 kDa, 1,000-3,000 kDa, and >3,000 kDa. For analysis of BF and SF lubricating function, a 3-way ANOVA was used to determine the effect of cytokine treatment (IT, ITT), membrane pore size (50 nm, 3 μm), and dilution (10%, 100%) of BF fluid tested. A 1-way ANOVA with Tukey post-hoc test was also used to assess differences in lubricaint function among all samples. Univariate and multivariate regression was used to analyze the relationships between friction-lowering ability of BF & SF and the lubricant concentrations. Univariate regression was also used to analyze the relationship between measured lubricant concentrations and those predicted by theory, and t-tests were utilized to assess differences between these.

Table 5.1: (**A**) Membrane permeability and lubricant secretion rate parameters. (**B**) Geometric parameters utilized in the mathematical model. AC = articular cartilage, SYN = synoviocytes.

A

Lubricant		Secretion Rates [10^{-6} μg/(cm^{2}s)]				Permeability [10^{-8} cm/s]	
		50 nm IT	50 nm ITT	3 μm IT	3 μm ITT	50 nm	3 μm
4000 kDa HA		21.6	16.9	23.9	22.8	6.8	114.2
2400 kDa HA		13.5	9.6	14.2	9.1	11.2	133.5
1156 kDa HA		14.0	8.9	12.5	7.9	16.8	143.0
450 kDa HA		8.19	5.5	10.1	7.4	33.6	184.1
262 kDa HA		4.3	2.9	5.2	3.6	64.3	248.2
160 kDa HA		4.0	3.7	4.7	3.2	90.0	256.0
30 kDa HA		2.5	3.3	2.4	2.0	618.2	617.7
PRG4	AC	352.8	226.5	14.3	10.5	7.2	308.3
	SYN	0.3	<0.01	0.1	<0.01		

B

Parameter	Value
V^{BF}	0.09 ml
A^{AC}	0.13 cm^2
A^{SYN}	1.0 cm^2
A^{MEM}	1.0 cm^2

5.5   Results

HA Concentration & Structure in Bioengineered, Nutrient, & Native Synovial Fluid

The HA concentrations in BF were greater than those in NF, and higher in bioreactors with 50 nm membranes than with 3 μm membranes (**Figure 5.2A,B**). The HA concentration in BF with 50 nm membranes was ~11-fold higher than that with 3 μm membranes (~572 μg/ml vs. ~53 μg/ml, p<0.05), and comparable to that of bovine SF (~600 μg/ml). Lubricant concentrations in NF were 10-100x lower than those in BF (p<0.05). In contrast to BF, the HA concentration in NF with 50 nm membranes was 13-fold lower than that in NF with 3 μm membranes (~0.4 μg/ml vs. ~5 μg/ml, p<0.05). The different cytokine combinations applied (IT, ITT) had no statistically significant effect on HA concentration in BF or NF, although there was a trend of higher HA concentration in BF with 50 nm membranes and IT treatment compared to ITT treatment (659 μg/ml vs. 484 μg/ml, p=0.16).

The HA MW distribution in NF, but not BF, was dependent upon membrane pore size for most MW ranges. In agarose gels, HA at high MWs (of ~4000 kDa) was evident in BF samples from bioreactors both with 50 nm and 3 μm membranes, as well as for NF samples with 3 μm membranes. In contrast, HA at low MWs (of ~30 kDa) was evident in NF samples from bioreactors with 50 nm but not 3 μm membranes (**Figure 5.2C,D**). Quantitatively, the distribution of HA in BF samples for MW ranges of >3000 kDa, 1000-3000 kDa, and 1000 kDa was ~31%, ~34%, and ~35%, respectively, with 50 nm membranes, and ~39%, ~23%, and ~28%, respectively, with 3 μm membranes (**Figure 5.2E,F**). The concentrations of HA in each of these MW ranges in BF samples was markedly higher with 50 nm membranes than with 3 μm

membranes due to the overall higher HA concentration with the smaller pore membrane ($p < 0.05$). However, the distribution amongst different size HA among BF samples were not significantly different, with the exception of the 50 nm vs. 3 μm membranes from the ITT cytokine condition in the > 3000 kDa range (32% vs. 54%, $p < 0.05$). Analogously, the concentrations of HA in each of these MW ranges in NF samples was markedly lower with 50 nm membranes than with 3 μm membranes due to the overall lower HA concentration with the smaller pore membrane ($p < 0.05$). However, in contrast to BF samples, NF samples exhibited MW distributions of HA that were markedly affected by membrane pore size for all MW ranges ($p < 0.05$). In NF samples with 50 nm membranes, HA was primarily distributed in the <1000 kDa range (~84 %), whereas in NF samples with 3 μm membranes, HA distribution extended to the higher MWs and resembled that of BF. The type of cytokine stimulus (IT, ITT) did not affect the HA MW distribution in either BF or NF ($p = 0.37-0.99$).

PRG4 Concentration & Structure in Bioengineered, Nutrient, & Native Synovial Fluid

The PRG4 concentrations were predominantly (>99%) of bovine origin (i.e., from bovine articular cartilage chondrocytes rather than human synoviocytes), higher in BF than in NF, and higher with 50 nm membranes than with 3 μm membranes (**Figure 5.3A,B**). The concentration of PRG4 in BF with 50 nm membranes was 33-fold higher than that with 3 μm membranes (~380 μg/ml vs. ~11 μg/ml; $p < 0.05$) and also comparable to that of bovine SF (~450 μg/ml). The PRG4 concentrations in NF were 500-50,000-fold lower than those in corresponding BF ($p < 0.05$). In NF, the PRG4 concentration with 50 nm membranes was 7-fold lower than that with 3 μm membranes (~0.006 μg/ml vs. ~0.04 μg/ml, $p < 0.05$). The type of cytokine stimulus

(IT, ITT) did not affect the PRG4 concentration in BF or NF, although there was a trend of higher PRG4 concentration in BF with 50 nm membranes and IT treatment compared to ITT treatment (461 µg/ml vs. 294 µg/ml, p=0.12).

The PRG4 in BF with both 50 nm and 3 µm membranes, and from both IT and ITT cytokine combinations, had a high MW structure that appeared similar to that present in normal bovine SF (**Figure 5.3C**, shows bovine PRG4).
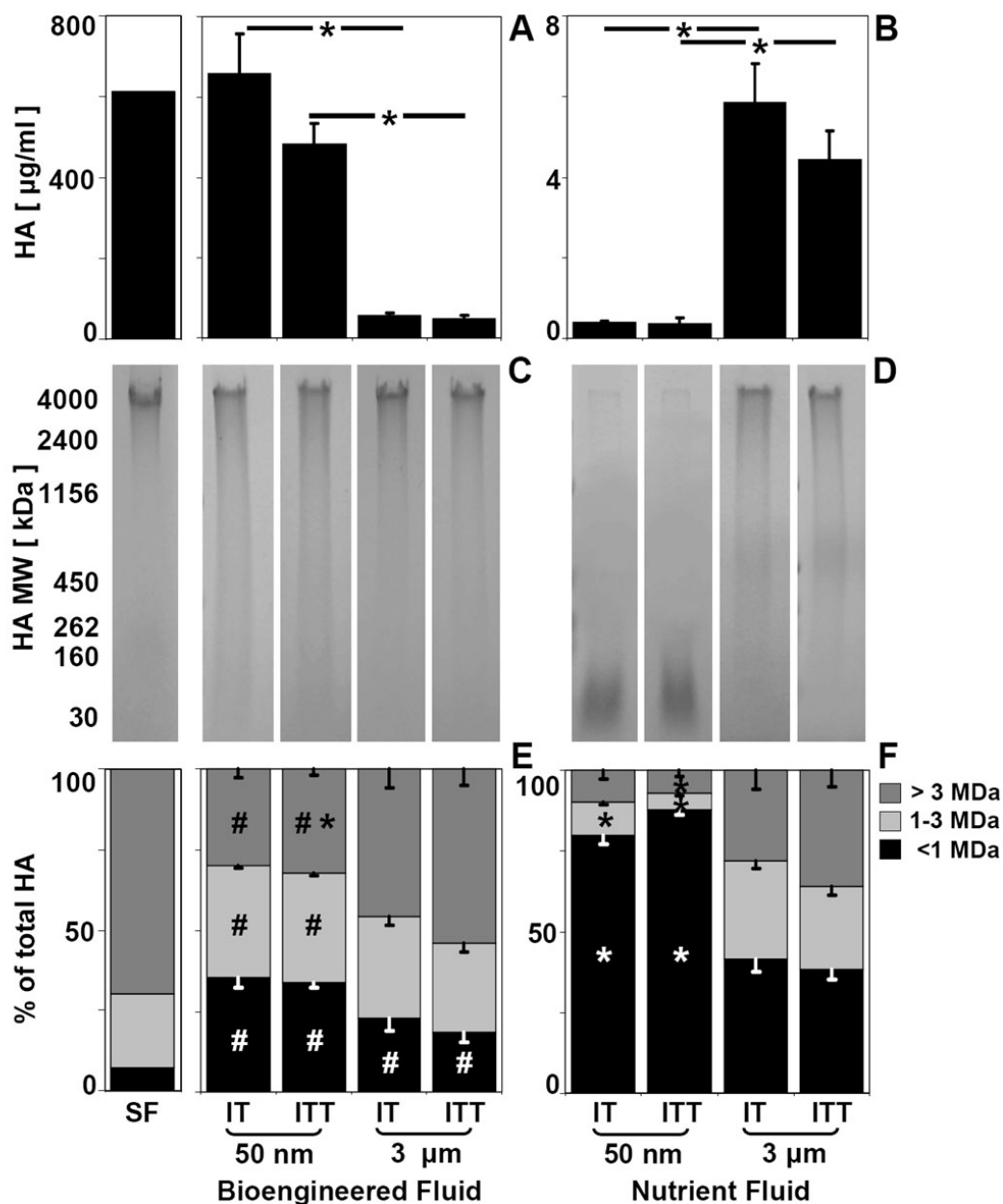
Figure 5.2: HA concentration and size distribution in native bovine synovial fluid (SF) and bioengineered fluid (**A, C**, **E**), and in nutrient fluid (**B**, **D**, **F**). (**A,B**) HA concentration, (**C,D**) Assessment of MW distribution of HA by agarose gel electrophoresis, (**E,F**) Quantitative analysis of HA MW distribution as a % of total HA in the MW ranges of >3 MDa, 1-3 MDa, and <1 MDa. Cytokine stimulus conditions were IL-1β + TGF-β1 (IT) and IL-1β + TGF-β1 + TNF-α (ITT), and membranes had pore sizes of 50 nm or 3 μm, n=4-5. * = 50 nm vs. 3 μ, # = BF vs. NF for same pore size.
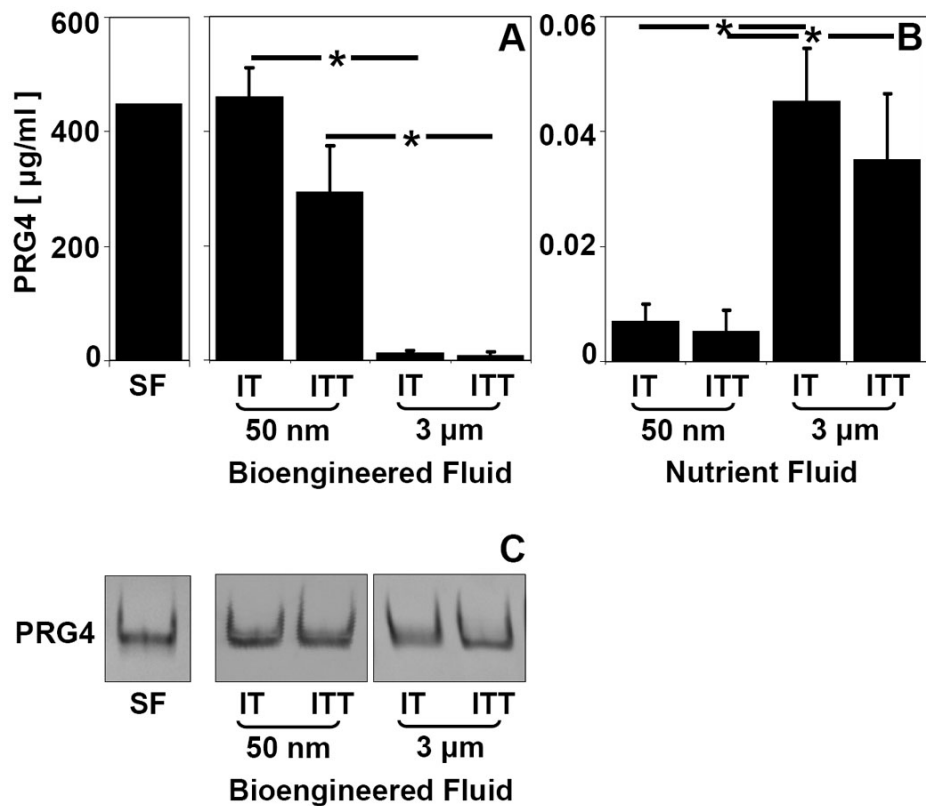
Figure 5.3: Characterization of PRG4 concentration in native bovine synovial fluid (SF) and bioengineered fluid (BF) (**A,C**), and in nutrient fluid (NF) (**B**). PRG4 concentration in BF and NF is determined as the sum of PRG4 of both bovine and human origins for IT and ITT stimulus groups (defined in legend to **Figure 5.2**), and that in SF is that of bovine origin. (**C**) Western blot of BF from IT and ITT stimulus groups for 50 nm and 3 μm pore size membranes. Data are for n=4-5.

Friction-Reducing Lubricating Function of Bioengineered Fluid (BF) and native SF

The lubricating function of BF in a cartilage-on-cartilage friction test was dependent upon membrane pore size and percent strength of fluid tested, but not on the selected cytokine combinations (**Figure 5.4**). BF with 50 nm membranes was a markedly better lubricant than that of BF with 3 μm membranes (μ= ~0.037 vs. ~0.097, p<0.05). Additionally, the lubricating function of 100% strength fluids was markedly better than that of 10% strength fluids (p<0.05). Both 10% and 100% strength BF with 50 nm membranes had greater lubricating ability than that of PBS (μ=0.20), as did 100% strength BF with 3 μm membranes (each, p<0.05). However, only 100% BF with 50 nm membranes approached that of native SF (μ= ~0.037 vs. ~0.023, p=0.08-0.29).

Correlation Between Fluid Lubricant Composition and Lubricating Function

For BF and SF samples, friction coefficient was correlated negatively with the concentrations of HA and PRG4. Univariate regression analysis demonstrated significant relationships between friction coefficient and each lubricant with R^2 values of 0.70-0.71 (**Figure 5.5A,B**, each, p<0.05). Multivariate regression analysis revealed the independent effects of both HA and PRG4 lubricants on friction coefficient with an even stronger overall correlation with R^2 values of 0.81-0.83 (**Figure 5.5C,D**, each, p<0.05). A plot of the residuals from the multivariate regression showed relatively little variation (R^2=0.28), indicating that HA and PRG4 accounted for most of the observed variation in lubricating function of fluid samples (**Figure 5.5E**).
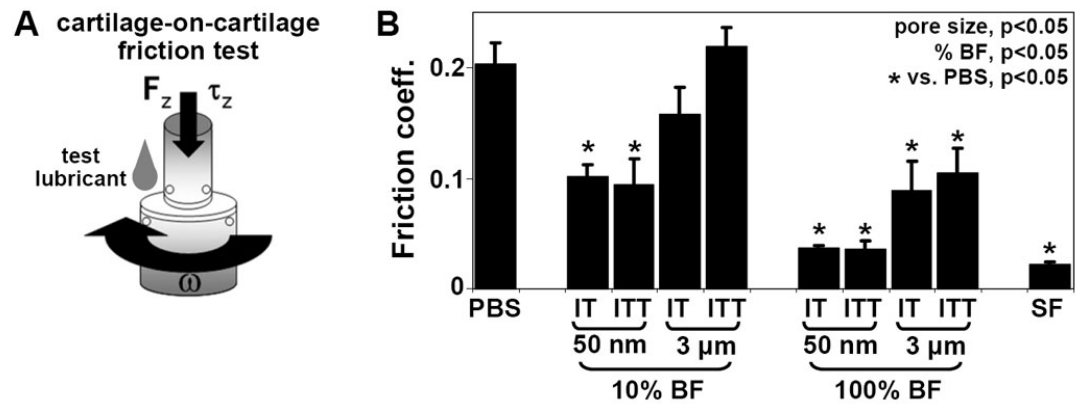
Figure 5.4: Characterization of friction coefficients of fluid samples. (**A**) Schematic of cartilage-on-cartilage friction test utilized to assess boundary-mode friction coefficient. (**B**) Effect of PBS (negative control), bovine synovial fluid (SF) (positive control), and bioengineered fluid (BF) (both 100% strength and 10% strength) from IT and ITT stimulus groups for 50 nm and 3 μm pore size membranes on friction coefficient, n=4-16.
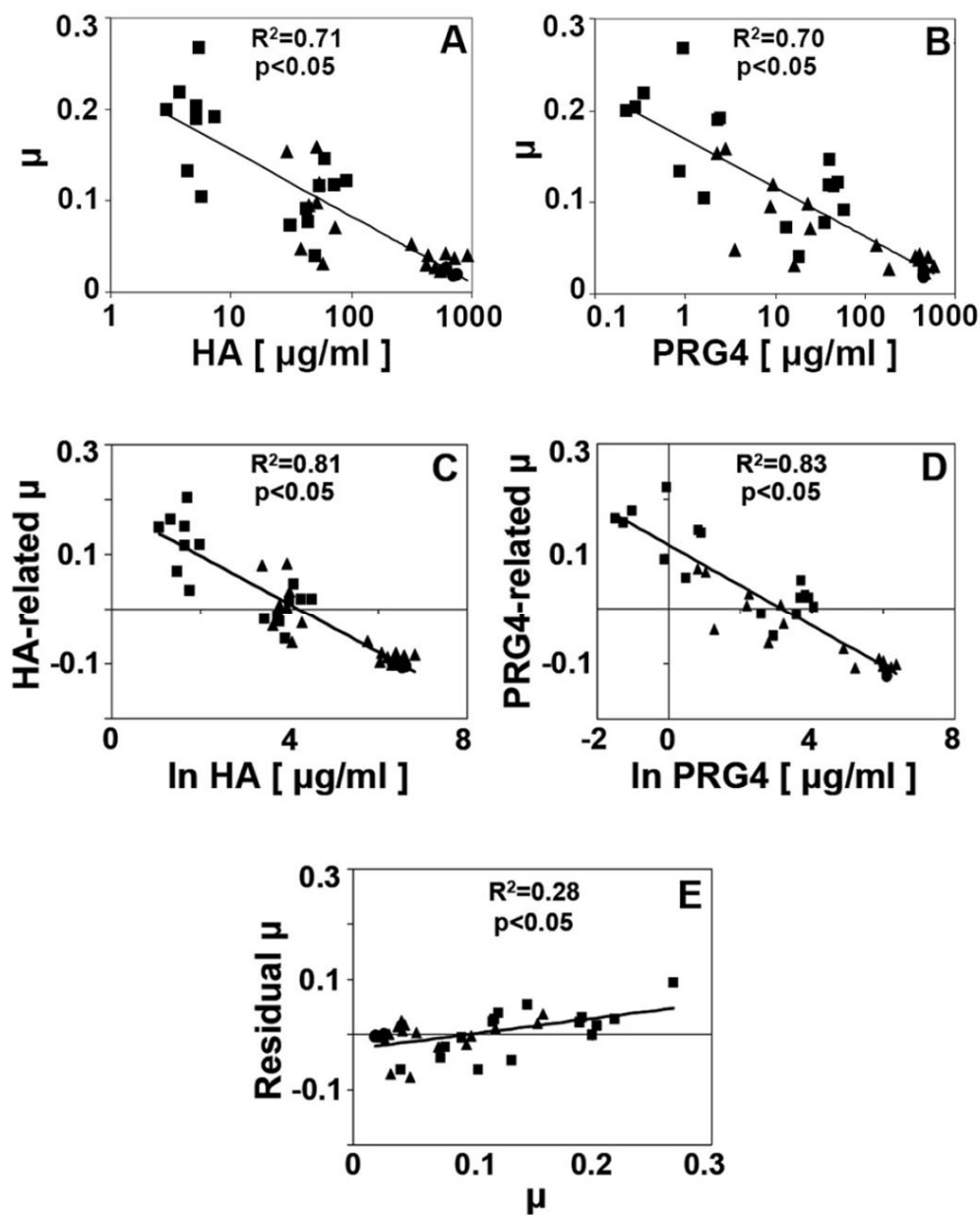
Figure 5.5: Correlations between lubricant composition and lubricating function of BF and SF. Linear regression analysis between friction coefficient (μ) and (**A**) HA or (**B**) PRG4 concentration. Multivariate regression analysis between (**C**) HA-related μ and HA concentration or (**D**) PRG4-related μ and PRG4 concentration, with residuals shown in (**E**). n=4-16, ■ = 10% BF data, ▲ = 100% BF data, ● = SF data.

Predicted Lubricant Concentrations

Theoretical analysis of HA and PRG4 concentrations in BF predicted trends (**Figure 5.6**) similar to those observed experimentally, and there was a strong correlation between predicted and measured lubricant concentrations (R^2 values between 0.82-0.85, **Figure 5.7**). After 12 days, the predicted total HA concentrations (sum of the predicted concentrations in each MW form of HA) were 366 μg/ml and 268 μg/ml with 50 nm membranes of IT and ITT conditions, respectively, while experimentally observed values were 659 μg/ml and 484 μg/ml, showing similar trends but higher magnitudes (**Figure 5.7A**, $p<0.05$). With 3 μm membranes, the predicted concentrations for IT and ITT conditions were lower at 50 μg/ml and 39 μg/ml, respectively, and similar to experimentally observed values of 57 μg/ml and 49 μg/ml ($p=0.22-0.26$). The predicted PRG4 concentrations in BF were 361 μg/ml and 231 μg/ml with 50 nm membranes of IT and ITT conditions, respectively, and experimental measurements were similar at 461 μg/ml and 294 μg/ml, respectively (**Figure 5.7C**, $p=0.15-0.48$). Predicted PRG4 concentrations in BF were markedly lower with 3 μm membranes, at 0.6 and 0.4 μg/ml, respectively, and trends were consistent with experimental observations at 14 μg/ml and 9.5 μg/ml ($p=0.06-0.14$).

The contributions of HA of different MWs to the total HA concentration varied (**Figure 5.6C-F, Figure 5.7B**) likely as a function of the distinct secretion rates (**Table 5.1A**, calculated from data in **Figure 5.2C-F**) and membrane permeabilities. For the condition of 50 nm membranes and IT cytokine stimulation, predicted vs. measured day 12 HA concentrations were 219 μg/ml vs. 172 μg/ml for 4000 kDa HA, 137 μg/ml vs. 87 μg/ml for 2400 kDa HA, 143 μg/ml vs. 71 μg/ml for 1156 kDa HA, 77 μg/ml vs. 24 μg/ml for 450 kDa HA, 41 μg/ml vs. 7 μg/ml for 262 kDa HA, 35 μg/ml vs. 5 μg/ml for 160 kDa HA, and 8 μg/ml vs. 0.4 μg/ml for 30 kDa HA (**Figure**

5.6C, **Figure 5.7B**). For the condition of 3 μm membranes and IT stimulation, similar results of decreasing concentration with decreasing MW were predicted and observed, although with lower magnitudes due to higher membrane permeability. Predicted vs. measured HA concentrations were 28.9 μg/ml vs. 20.9 μg/ml for 4000 kDa HA, 11.0 μg/ml vs. 10.7 μg/ml for 2400 kDa HA, 9.0 μg/ml vs. 8.7 μg/ml for 1156 kDa HA, 4.0 μg/ml vs. 5.5 μg/ml for 450 kDa HA, 2.1 μg/ml vs. 2.1 μg/ml for 262 kDa HA, 1.5 μg/ml vs. 1.8 μg/ml for 160 kDa HA, and 0.7 μg/ml vs. 0.4 μg/ml for 30 kDa HA (**Figure 5.6E**, **Figure 5.7B**). For the ITT cytokine conditions, the predicted trends paralleled those for the IT cytokine conditions (**Figure 5.6D,F**, **Figure 5.7B**).

The predicted time constants associated with kinetics of HA and PRG4 buildup were dependent upon variations in membrane permeability, reflecting both membrane properties and lubricant structure (**Figure 5.6G**). For HA of 4000 kDa, the time constant τ was predicted to be 15.2 days with 50 nm membranes and 0.91 days with 3 μm membranes. For an intermediate MW of 450 kDa, both τ's were predicted to be markedly lower, at 3.1 days and 0.57 days with 50 nm and 3 μm membranes, respectively. Low MW HA of 30 kDa was predicted to have even lower τ's of 0.17 days that were similar for the membranes with different pore sizes. With 50 nm and 3 μm pore size membranes, the predicted τ's for HA overall were 11.1 days and 0.75 days, respectively, and those for PRG4 were 14.5 days and 0.34 days, respectively. The model thus suggested that steady-state concentrations were not yet achieved in the bioreactor system for total HA and PRG4 in 50 nm conditions. Steady-state concentrations in these conditions were predicted to be 556 μg/ml and 412 μg/ml for HA with 50 nm membranes of IT and ITT conditions, respectively, and 649 μg/ml and 409 μg/ml for PRG4 with 50 nm membranes of IT and ITT conditions, respectively (**Figure 5.6A,B**).
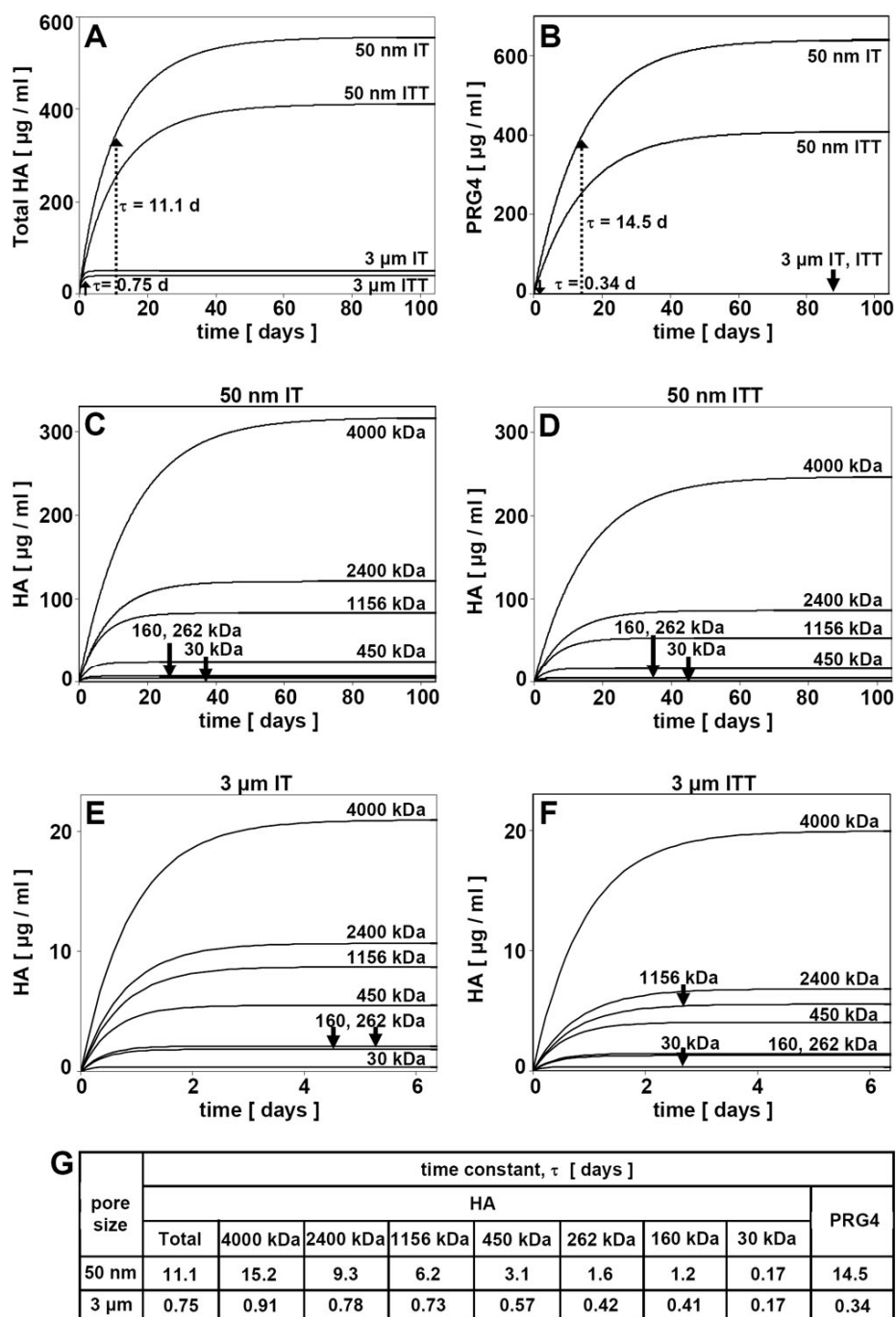
Figure 5.6: Theoretical predictions of BF lubricant concentrations in bioreactor. Predicted transient and steady-state lubricant concentrations in BF for (**A**) total HA (sum of all MW's) and (**B**) PRG4. Predicted HA concentration as a function of MW in the different conditions are shown in **C-F**: (**C**) 50 nm IT, (**D**) 50 nm ITT (**E**) 3 μm IT, and (F) 3 μm ITT. Associated time constants, τ, to reach steady-state values (~63% of rise) are shown in (**G**).
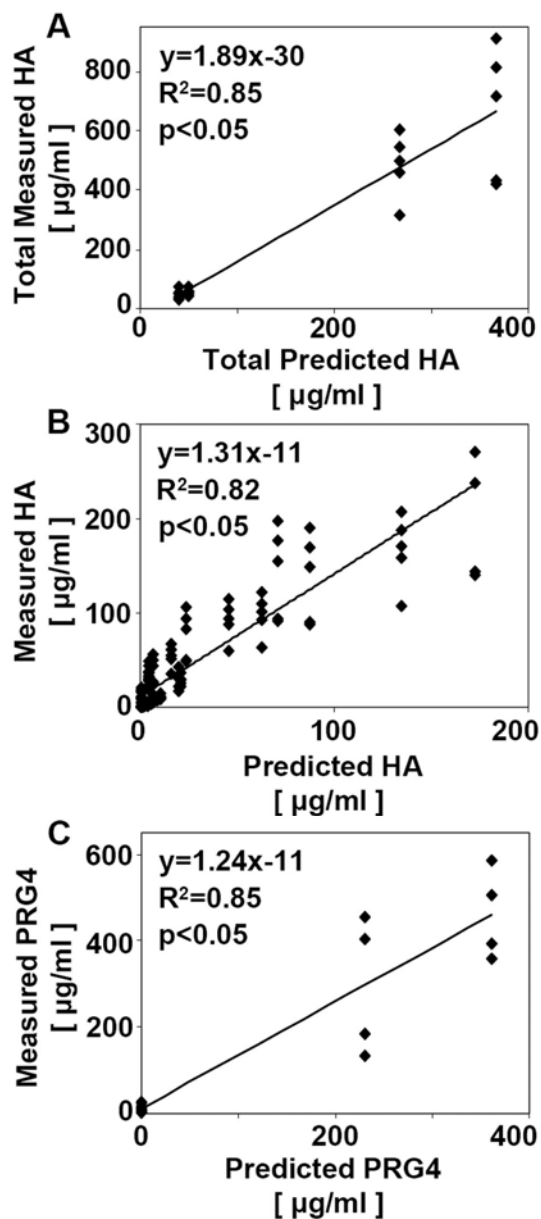
Figure 5.7: Correlations between measured lubricant concentrations and predicted lubricant concentrations after a duration of 12 days, for both IT and ITT cytokine groups and 50 nm and 3 μm membranes. (**A**) total HA (sum of all MW's), (**B**) HA for each individual MW, and (**C**) PRG4.

5.6   Discussion

In this study, a biomimetic bioreactor system was developed and capable of generating fluid with lubricant composition and friction-lowering function similar to that of native SF. HA and PRG4 concentrations in BF were 10x-50,000x higher than those in NF, 10x-30x higher with 50 nm membranes than with 3 μm membranes, and did not differ significantly between IT and ITT cytokine groups (**Figure 5.2AB, 5.3AB**). BF with 50 nm membranes achieved HA and PRG4 concentrations similar to that of native bovine SF, ~600 μg/ml and ~400 μg/ml, respectively. The distributions of HA in BF with both pore size membranes and in NF with 3 μm membranes included a heavy contribution of high MWs (~4000 kDa) and resembled that of native SF, while the distribution of HA in NF with 50 nm membranes was predominantly of low MW (~30 kDa) (**Figure 5.2C**). PRG4 structure in BF was of the same high MW form for all conditions and similar to that of native bovine SF (**Figure 5.3C**). The lubricating function of BF with 50 nm membranes was better than that with 3 μm membranes (μ= ~0.037 vs. ~0.097), and approached that of native SF (μ=0.023), without a marked difference between IT and ITT cytokine stimulus groups (**Figure 5.4**). Friction coefficients were correlated negatively with HA and PRG4 concentrations (**Figure 5.5**), with increasing lubricant concentrations correlated to lower friction coefficients, consistent with the dose-dependence of BF function (**Figure 5.4**). Model predictions of HA and PRG4 concentrations in BF were consistent with those observed experimentally, with distinct kinetics for the membranes of different pore sizes and for the HA of different MW forms. The ability to bioengineer a fluid with lubricant qualities similar to native SF may have

applications in tissue engineering of articular cartilage using mechanical stimuli, in generating viscosupplements, and in identifying lubricant-regulating molecules.

The design of this study allowed interpretation of the relative contributions of cartilage explants vs. synoviocytes to the total PRG4 and HA lubricant pool in BF. The use of cartilage explants from bovine species and synoviocytes from human species allowed the specific detection of bovine vs. human PRG4. Under the culture conditions of the study, PRG4 present in both BF and NF was predominantly of bovine (i.e. cartilage and chondrocyte) origin. As synoviocytes are considered the primary source of HA in synovial joints and their HA secretion rate greatly exceeds that of chondrocytes, particularly with cytokine stimulation [41], it is likely that HA in BF and NF was predominantly of synoviocyte origin. The interactive effects of the chondrocytes and synoviocytes as a result of co-culture were not assessed, but could have affected the results and could differ from the additive effects of these cells independently. In addition, only one duration of incubation was chosen for lubricant analysis, and, based on theory, the duration approached that at which steady-state concentrations were predicted. Further, the effects of cytokine stimuli were limited to two combinations, found in previous studies to markedly stimulate HA synthesis. Thus, a number of areas of future investigation are possible using the bioreactor system described here.

The findings in this study of 50 nm pore size membranes acting as a molecular sieve to allow HA of only very low MW to be transported is analogous to findings of previous studies of the transport of HA of different MWs across the native synovium. There, infusion of HA of different MWs into the synovial joint cavity of rabbits demonstrated that HA of relatively low MW (~140 kDa, ~500 kDa) was reflected less by the synovium and accumulated more readily in the synovial cavity than did HA of

higher MW (~2200 kDa) [16, 43]. Similar patterns of transport were observed in studies with intraarticular infusion of fluorescein-labeled HA in dog knee joints, where HA of 2300 kDa MW barely penetrated the synovial lining, but 840 kDa HA penetrated more readily [5]. Thus, the 50nm pore size membrane used in the present study provides transport properties resembling those of the native synovium under normal conditions.

However, since the structure and ultrafiltration function of synovium may occur in disease or injury and affect the composition of the SF, membranes with other pore sizes, especially larger ones, could be utilized in the current bioreactor system to mimic different conditions occurring *in vivo*. For example, the half-life of HA in SF decreases in arthritic or inflamed joints (~12 hr vs. ~24 hr) [17, 24, 31, 44], as do the SF concentrations of HA and PRG4 [3, 6-8, 18, 21, 22, 54]. At the same time, the SF concentrations of certain cytokines that may contribute to degradation of the synovium extracellular matrix are often increased [10, 29, 30, 34, 57], and such degradation can increase the permeability of the tissue [14, 49, 50]. Membrane permeability and SF lubricant concentration and kinetics were associated in the present study, as 3 μm pore size membranes with a relatively high permeability to lubricants were predicted to have relatively low steady-state lubricant concentrations, and a relatively small time constant, compared to the 50 nm pore size membranes. Thus, modulation of membrane pore size in the bioreactor system can allow modulation of lubricant dynamics and equilibration in order to mimic various aspects of *in vivo* physiology and disease.

The correlation between lubricant concentration and lubricating function of BF found in this study is consistent with other studies identifying the lubricating functions of solutions containing HA and PRG4. The boundary lubrication functions of native

SF and also purified preparations of HA and PRG4 showed concentration-dependent effects for reducing friction [45, 46]. Likewise, SF from injured or diseased joints with decreased lubricant concentrations have a diminished boundary lubrication function [3, 22, 54].

Model predictions suggest distinct kinetics due to membranes with different pore sizes and permeabilities, for the different lubricant molecules and the varying MW forms of HA. The predicted time constants associated with lubricant build-up with the 3 μm membrane suggest that concentrations were near steady-state levels after the 12 day culture period for all lubricant molecules, including PRG4 and HA of all MWs. However, with the 50 nm pore size membrane, predictions suggest that HA of higher MW (4000 kDa, 2400 kDa) and also PRG4 may have attained only ~50-80% of steady-state concentrations, while HA of lower MW reached equilibrium. Thus for the smaller pore size membrane, the concentration of HA and PRG4 may continue to increase slowly for several weeks beyond the 12 day duration of incubation used in the present study.

The strong correlation between experimentally measured lubricant concentrations and theoretical predictions suggests that the bioreactor system is operating within well-described principles of mass balance and transport under potent biological regulation, and demonstrates the utility of applying the mathematical model and quantitative analyses to the bioreactor system to acquire information that may not be readily determined through experiments. For example, continuous sampling of fluid in the bioreactor would be complicated by the small volume available, while theoretical predictions can provide useful estimates of the time course of lubricant buildup. Mathematical modeling may allow future experimental designs to be condensed by making theoretical predictions of the culture duration required to

achieve a desired lubricant concentration in the fluid, and also by predicting the effects of various chemical factors and membrane pore sizes on lubricant concentration in BF. Differences between certain experimentally observed and theoretically predicted results could be scrutinized in terms of biological and physical mechanisms not yet incorporated in the theoretical model. Features that could be modeled are physicochemical interactions of lubricants, and the dependence of membrane permeability on lubricant concentration.

A bioreactor system capable of generating a bioengineered fluid with lubricant composition and function similar to that of native SF may have application in developing and improving biological and biomechanical treatments of the synovial joint. Intra-articular HA injections are commonly performed clinically and have been purported to affect the biology of the joint in order to restore the viscosity and protective functions of the synovial fluid [35, 55]. Injection of a PRG4 protein construct has been shown in a rat model of induced OA to be therapeutically effective in inhibiting cartilage degeneration [23]. Anti-cytokine pharmaceutical agents are also administered as arthritis therapies to reduce pain and inflammation [25, 36]. A bioengineered lubricous fluid may have application as a viscosupplement, while a bioreactor system for creating such a fluid may enable analysis of the effects of pharmaceutical therapies on lubricant regulation and identification of molecules that regulate lubricant secretion by cells in the joint.

Biomimetic synovial joint bioreactor systems may also be useful for developing therapies that use or provide the sustained restoration or enhancement of joint lubrication. Delivery of lubricant-secreting cells themselves into deficient joints, whether at the tissue or whole joint scale, may be a method for sustaining lubricant molecules in SF. For example, introduction of a synoviocyte- or chondrocyte-laden

material generated in bioreactors may be introduced to the joint as a therapy on the tissue scale; experimental developments in this area includes a tissue engineered synoviocyte-laden membrane for lubricating tendon repair sites and preventing adhesions to surrounding tissues [39]. Tissue engineering of whole joints for biological arthroplasty is an emerging research area that may also benefit from the results of the present study. In tissue engineering whole joints for such applications, a lubricating environment may be critical to the appropriate mechanical stimulation of cartilage surfaces undergoing joint-like motion in bioreactors [38].

Thus, the results of this study demonstrate the ability to bioengineer a lubricious fluid in a biomimetic bioreactor system with concentration and function that is modulated by the pore-size-based retention of lubricants by semi-permeable membranes. The ability to bioengineer such a fluid in a system where experimental parameters that affect lubricant secretion and retention can be controlled may have applications in understanding lubricant regulation in health, injury, and disease, and in developing improved arthritis therapies targeted at restoration of failed joint lubrication.

5.7   Acknowledgments

5.8 References

1. Afify A, Lynne LC, Howell L: Correlation of cytologic examination with ELISA assays for hyaluronan and soluble CD44v6 levels in evaluation of effusions. *Diagn Cytopathol* 35:105-10, 2007.

2. Alvaro-Gracia JM, Zvaifler NJ, Firestein GS: Cytokines in chronic inflammatory arthritis. V. Mutual antagonism between interferon-gamma and tumor necrosis factor-alpha on HLA-DR expression, proliferation, collagenase production, and granulocyte macrophage colony-stimulating factor production by rheumatoid arthritis synoviocytes. *J Clin Invest* 86:1790-8, 1990.

3. Antonacci JM, Schmidt TA, Serventi LA, Shu YL, Gastelum NS, Schumacher BL, McIlwraith CW, Sah RL: Effects of joint injury on synovial fluid and boundary lubrication of cartilage. *Trans Orthop Res Soc* 32:156, 2007.

4. Arnett FC, Edworthy SM, Bloch DA, McShane DJ, Fries JF, Cooper NS, Healey LA, Kaplan SR, Liang MH, Luthra HS: The American Rheumatism Association 1987 revised criteria for the classification of rheumatoid arthritis. *Arthritis Rheum* 31:315-24, 1988.

5. Asari A, Miyauchi S, Matsuzaka S, Ito T, Kominami E, Uchiyama Y: Molecular weight-dependent effects of hyaluronate on the arthritic synovium. *Arch Histol Cytol* 61:125-35, 1998.

6. Balazs EA: The physical properties of synovial fluid and the special role of hyaluronic acid. In: *Disorders of the knee,* ed. by AJ Helfet, Lippincott Co., Philadelphia, 1974, 63-75.

7. Balazs EA, Watson D, Duff IF, Roseman S: Hyaluronic acid in synovial fluid. I. Molecular parameters of hyaluronic acid in normal and arthritis human fluids. *Arthritis Rheum* 10:357-76, 1967.

8. Belcher C, Yaqub R, Fawthrop F, Bayliss M, Doherty M: Synovial fluid chondroitin and keratan sulphate epitopes, glycosaminoglycans, and hyaluronan in arthritic and normal knees. *Ann Rheum Dis* 56:299-307, 1997.

9. Bellon JM, Bujan J, Honduvilla NG, Hernando A, Navlet J: Endothelial cell seeding of polytetrafluoroethylene vascular prostheses coated with a fibroblastic matrix. *Ann Vasc Surg* 7:549-55, 1993.

10. Bertone AL, Palmer JL, Jones J: Synovial fluid cytokines and eicosanoids as markers of joint disease in horses. *Vet Surg* 30:528-38, 2001.

11. Blewis ME, Jadin KD, Lao BJ, McCarty WJ, Antonacci JM, Bugbee WD, Firestein GS, Sah RL: Bioengineering of lubricious synovial fluid in a biomimetic bioreactor. *TERMIS,* Submitted, 2008.

12. Blewis ME, Nugent-Derfus GE, Schmidt TA, Schumacher BL, Sah RL: A model of synovial fluid lubricant composition in normal and injured joints. *Eur Cell Mater* 13:26-39, 2007.

13. Blewis ME, Orwoll BE, Lao BJ, Schumacher BL, Bugbee WD, Firestein GS, Sah RL: Interactive cytokine regulation of synoviocyte hyaluronan and proteoglycan 4 secretion rates. *Trans Orthop Res Soc* 33:374, 2008.

14. Coleman PJ, Scott D, Abiona A, Ashhurst DE, Mason RM, Levick JR: Effect of depletion of interstitial hyaluronan on hydraulic conductance in rabbit knee synovium. *J Physiol* 509 (Pt 3):695-710, 1998.

15. Coleman PJ, Scott D, Mason RM, Levick JR: Characterization of the effect of high molecular weight hyaluronan on trans-synovial flow in rabbit knees. *J Physiol* 514 (Pt 1):265-82, 1999.

16. Coleman PJ, Scott D, Mason RM, Levick JR: Role of hyaluronan chain length in buffering interstitial flow across synovium in rabbits. *J Physiol* 526 Pt 2:425-34, 2000.

17. Coleman PJ, Scott D, Ray J, Mason RM, Levick JR: Hyaluronan secretion into the synovial cavity of rabbit knees and comparison with albumin turnover. *J Physiol* 503 (Pt 3):645-56, 1997.

18. Dahl LB, Dahl IM, Engstrom-Laurent A, Granath K: Concentration and molecular weight of sodium hyaluronate in synovial fluid from patients with rheumatoid arthritis and other arthropathies. *Ann Rheum Dis* 44:817-22, 1985.

19. Davies DV: Synovial membrane and synovial fluid of joints. *Lancet* 248:815-22, 1946.

20. Eckstein F, Winzheimer M, Hohe J, Englmeier KH, Reiser M: Interindividual variability and correlation among morphological parameters of knee joint cartilage plates: analysis with three-dimensional MR imaging. *Osteoarthritis Cartilage* 9:101-11, 2001.

21. Elsaid KA, Fleming BC, Oksendahl HL, Machan JT, Fadale PD, Hulstyn MJ, Shalvoy R, Jay GD: Decreased lubricin concentrations and markers of joint inflammation in the synovial fluid of patients with anterior cruciate ligament injury. *Arthritis Rheum* 58:1707-15, 2008.

22. Elsaid KA, Jay GD, Warman ML, Rhee DK, Chichester CO: Association of articular cartilage degradation and loss of boundary-lubricating ability of synovial fluid following injury and inflammatory arthritis. *Arthritis Rheum* 52:1746-55, 2005.

23. Flannery CR, Zollner R, Corcoran C, Jones AR, Root A, Rivera-Bermudez M, Blanchet T, Bendele AM, Morris EA, Glasson SS: Lubricin Supplementation Prevents Osteoarthritis Progression in a Rat Surgical Model. *Trans ORS* 54:266, 2008.

24. Fraser JR, Kimpton WG, Pierscionek BK, Cahill RN: The kinetics of hyaluronan in normal and acutely inflamed synovial joints: observations with experimental arthritis in sheep. *Semin Arthritis Rheum* 22:9-17, 1993.

25. Furst DE: Anakinra: review of recombinant human interleukin-I receptor antagonist in the treatment of rheumatoid arthritis. *Clin Ther* 26:1960-75, 2004.

26. Granger HJ, Taylor AE: Permeability of connective tissue linings isolated from implanted capsules; implications for interstitial pressure measurements. *Circ Res* 36:222-8, 1975.

27. Haubeck H-D, Kock R, Fischer D-C, van de Leur E, Hoffmeister K, Greiling H: Transforming growth factor ß1, a major stimulator of hyaluronan synthesis in human synovial lining cells. *Arthritis Rheum* 38:669-77, 1995.

28. Jay GD, Britt DE, Cha D-J: Lubricin is a product of megakaryocyte stimulating factor gene expression by human synovial fibroblasts. *J Rheumatol* 27:594-600, 2000.

29. Joosten LA, Netea MG, Kim SH, Yoon DY, Oppers-Walgreen B, Radstake TR, Barrera P, van de Loo FA, Dinarello CA, van den Berg WB: IL-32, a proinflammatory cytokine in rheumatoid arthritis. *Proc Natl Acad Sci USA* 103:3298-303, 2006.

30. Kotake S, Udagawa N, Takahashi N, Matsuzaki K, Itoh K, Ishiyama S, Saito S, Inoue K, Kamatani N, Gillespie MT, Martin TJ, Suda T: IL-17 in synovial fluids from patients with rheumatoid arthritis is a potent stimulator of osteoclastogenesis. *J Clin Invest* 103:1345-52, 1999.

31. Laurent UB, Fraser JR, Engstrom-Laurent A, Reed RK, Dahl LB, Laurent TC: Catabolism of hyaluronan in the knee joint of the rabbit. *Matrix* 12:130-6, 1992.

32. Lee HG, Cowman MK: An agarose gel electrophoretic method for analysis of hyaluronan molecular weight distribution. *Anal Biochem* 219:278-87, 1994.

33. Levick JR: A method for estimating macromolecular reflection by human synovium, using measurements of intra-articular half-lives. *Ann Rheum Dis* 57:339-44, 1998.

34. Marks PH, Donaldson ML: Inflammatory cytokine profiles associated with chondral damage in the anterior cruciate ligament-deficient knee. *Arthroscopy* 21:1342-7, 2005.

35. Moreland LW: Intra-articular hyaluronan (hyaluronic acid) and hylans for the treatment of osteoarthritis: mechanisms of action. *Arthritis Res Ther* 5:54-67, 2003.

36. Moreland LW: Drugs that block tumour necrosis factor: experience in patients with rheumatoid arthritis. *Pharmacoeconomics* 22:39-53, 2004.

37. Noh I, Choi YJ, Son Y, Kim CH, Hong SH, Hong CM, Shin IS, Park SN, Park BY: Diffusion of bioactive molecules through the walls of the medial tissue-engineered hybrid ePTFE grafts for applications in designs of vascular tissue regeneration. *J Biomed Mater Res A* 79:943-53, 2006.

38. Nugent-Derfus GE, Takara T, O'Neill J K, Cahill SB, Gortz S, Pong T, Inoue H, Aneloski NM, Wang WW, Vega KI, Klein TJ, Hsieh-Bonassera ND, Bae WC, Burke JD, Bugbee WD, Sah RL: Continuous passive motion applied to whole joints stimulates chondrocyte biosynthesis of PRG4. *Osteoarthritis Cartilage* 15:566-74, 2007.

39. Ozturk AM, Yam A, Chin SI, Heong TS, Helvacioglu F, Tan A: Synovial cell culture and tissue engineering of a tendon synovial cell biomembrane. *J Biomed Mater Res A* 84:1120-6, 2008.

40. Price FM, Mason RM, Levick JR: Radial organization of interstitial exchange pathway and influence of collagen in synovium. *Biophys J* 69:1429-39, 1995.

41. Recklies AD, White C, Melching L, Roughley PJ: Differential regulation and expression of hyaluronan synthases in human articular chondrocytes, synovial cells and osteosarcoma cells. *Biochem J* 354:17-24, 2001.

42. Ropes MW, Rossmeisl EC, Bauer W: The origin and nature of normal human synovial fluid. *J Clin Invest* 19:795-9, 1940.

43. Sabaratnam S, Arunan V, Coleman PJ, Mason RM, Levick JR: Size selectivity of hyaluronan molecular sieving by extracellular matrix in rabbit synovial joints. *J Physiol* 567:569-81, 2005.

44. Sakamoto T, Mizono, S, Miyazaki, K, Yamaguchi, T, Toyoshima, H, Namiki, O.: Biological fate of sodium hyaluronate (SPH): Studies on the distribution, metabolism, and excretion of ^{14}C-SPH in rabbits after intra-articular administration. *Pharmacometrics* 28:375-87, 1984.

45. Schmidt TA, Gastelum NS, Nguyen QT, Schumacher BL, Sah RL: Boundary lubrication of articular cartilage: role of synovial fluid constituents. *Arthritis Rheum* 56:882-91, 2007.

46. Schmidt TA, Sah RL: Effect of synovial fluid on boundary lubrication of articular cartilage. *Osteoarthritis Cartilage* 15:35-47, 2007.

47. Schumacher BL, Block JA, Schmid TM, Aydelotte MB, Kuettner KE: A novel proteoglycan synthesized and secreted by chondrocytes of the superficial zone of articular cartilage. *Arch Biochem Biophys* 311:144-52, 1994.

48. Schumacher BL, Hughes CE, Kuettner KE, Caterson B, Aydelotte MB: Immunodetection and partial cDNA sequence of the proteoglycan, superficial zone protein, synthesized by cells lining synovial joints. *J Orthop Res* 17:110-20, 1999.

49. Scott D, Coleman PJ, Abiona A, Ashhurst DE, Mason RM, Levick JR: Effect of depletion of glycosaminoglycans and non-collagenous proteins on interstitial hydraulic permeability in rabbit synovium. *J Physiol* 511 (Pt 2):629-43, 1998.

50. Scott D, Coleman PJ, Mason RM, Levick JR: Glycosaminoglycan depletion greatly raises the hydraulic permeability of rabbit joint synovial lining. *Exp Physiol* 82:603-6, 1997.

51. Scott D, Coleman PJ, Mason RM, Levick JR: Action of polysaccharides of similar average mass but differing molecular volume and charge on fluid drainage through synovial interstitium in rabbit knees. *J Physiol* 528:609-18, 2000.

52. Smith MM, Ghosh P: The synthesis of hyaluronic acid by human synovial fibroblasts is influenced by the nature of the hyaluronate in the extracellular environment. *Rheumatol Int* 7:113-22, 1987.

53. Su J-L, Schumacher BL, Lindley KM, Soloveychik V, Burkhart W, Triantafillou JA, Kuettner KE, Schmid TM: Detection of superficial zone

protein in human and animal body fluids by cross-species monoclonal antibodies specific to superficial zone protein. *Hybridoma* 20:149-57, 2001.

54. Teeple E, Elsaid KA, Fleming BC, Jay GD, Aslani K, Crisco JJ, Mechrefe AP: Coefficients of friction, lubricin, and cartilage damage in the anterior cruciate ligament-deficient guinea pig knee. *J Orthop Res*, 2007.

55. Tehranzadeh J, Booya F, Root J: Cartilage metabolism in osteoarthritis and the influence of viscosupplementation and steroid: a review. *Acta Radiol* 46:288-96, 2005.

56. Walluscheck KP, Steinhoff G, Kelm S, Haverich A: Improved endothelial cell attachment on ePTFE vascular grafts pretreated with synthetic RGD-containing peptides. *Eur J Vasc Endovasc Surg* 12:321-30, 1996.

57. Wei X, Messner K: Age- and injury-dependent concentrations of transforming growth factor-beta 1 and proteoglycan fragments in rabbit knee joint fluid. *Osteoarthritis Cartilage* 6:10-8, 1998.

CHAPTER 6:

CONCLUSIONS

6.1   Summary of Findings

This dissertation has incorporated biophysical features of the synovial joint into a theoretical model of the SF compartment, and has recapitulated these features in a biomimetic bioreactor system to produce a bioengineered fluid with lubricant composition and function similar to that of native SF. A mathematical model was developed to describe the dynamics of HA and PRG4 concentration in native SF of joints that were normal, injured, or treated, and also in bioengineered SF in bioreactors. Synoviocyte HA and PRG4 secretion rates and structures were experimentally assessed in response to cytokines, applied individually or in combination. The extent of retention of HA (of various MWs) and PRG4 by semi-permeable membranes was also assessed for membranes of a range of pore sizes. Finally, a biomimetic bioreactor system, incorporating cytokine-stimulated lubricant secretion by synoviocytes and chondrocytes and also membrane pore size-modulated lubricant retention, was developed and used to generate a bioengineered fluid with lubricant composition and function similar to that of native SF.

Mathematical modeling of SF lubricant dynamics in native joints (Chapter 2) predicted steady-state lubricant concentrations that were dependent on several key

parameters, including lubricant secretion rates, area of the cartilage and synovium tissues, and synovium permeability to lubricant molecules. The predicted lubricant concentrations were consistent with those observed physiologically. Altered cytokine concentrations in SF that may occur in injury and disease were predicted to alter steady-state lubricant concentrations by regulating chondrocyte and synoviocyte lubricant secretion rates. Analysis of the kinetics of HA and PRG4, starting from either a zero SF lubricant concentration or with a bolus increase in concentration after therapeutic injection, predicted that PRG4 and HA achieve steady-state concentrations on distinct time scales (on the order of hours for PRG4, and days for HA).

Application of cytokines, individually and in combination, to cultured synoviocytes (Chapter 3) resulted in a wide range of lubricant secretion rates and structures. HA secretion rates were markedly increased by IL-1β, while PRG4 secretion rates were markedly increased by TGF-β1. Certain combinations of cytokines synergistically increased HA secretion rates up to 7-fold over the predicted additive effects of individual cytokines. In contrast, PRG4 secretion rates were stimulated to a lesser extent by combinations of cytokines compared to treatment with TGF-β1 alone. Secreted HA was primarily of low MW (<1 MDa) under control conditions and after stimulation by individual cytokines, but was distributed in higher MW ranges to more closely resemble the MW distribution in normal human SF after stimulation with certain combinations of cytokines. Under the cytokine conditions examined, the MW of secreted PRG4 was not affected, and equivalent to the high MW form in human SF.

The retention of HA and PRG4 by semi-permeable expanded polytetrafluoroethylene (ePTFE) membranes (Chapter 4) was dependent upon pore size, with % of total lubricant loss and membrane permeability increasing with

increasing pore size. HA retention was further dependent upon the presence of adherent cells and HA MW. Low MW HA was lost equally from membranes of all pore sizes, while HA of intermediate MW and high MW was lost to a greater extent by larger pore size membranes. The presence of an adherent synoviocyte layer decreased loss of HA only in the smallest pore size membranes. The associated permeability values were reflective of these trends in lubricant loss. This study also demonstrated that cytokine-regulated synoviocyte HA and PRG4 secretion rates on ePTFE membranes were comparable to those of synoviocytes on tissue-culture plastic.

Studies representing an integration of results of Chapters 2-4 demonstrated the ability of a biomimetic bioreactor system to bioengineer a lubricious fluid with composition and function that is modulated by the pore-size-based retention of lubricants by semi-permeable membranes (Chapter 5). HA and PRG4 concentrations in bioengineered fluid (BF) with small pore size membranes (50 nm) were ~600 μg/ml and ~400 μg/ml, respectively, which were similar to concentrations in native SF and ~10-30-fold greater than concentrations with larger pore size membranes (3 μm). For both pore size membranes, HA and PRG4 concentrations in BF were orders of magnitude greater than that of nutrient fluid (NF) present on the opposite side of the semi-permeable membrane. Additionally, the MW of HA retained in BF by the 50 nm membrane was higher than the MW of HA lost into NF. The lubricant concentration in BF was strongly correlated to its lubricating ability, with BF from 50 nm membranes having a friction-lowering function that was greater than that of 3 μm membranes, and approached that of native SF. Application of the theoretical model developed in Chapter 2 provided predictions of HA and PRG4 concentrations in BF that were similar to those observed experimentally, with the predicted kinetics being distinct for the different pore size membranes and MW forms of HA.

In summary, biomimetic theoretical and experimental models of the synovial joint were developed, and the results obtained using these models have contributed to an understanding of key factors that dictate SF lubricant concentration, and ultimately function namely (1) cytokine-regulated lubricant secretion rates and (2) pore-size modulated lubricant retention by semi-permeable membranes.

6.2   Discussion

Major contributions of the current work include: (1) development of a mathematical model for describing dynamic and steady-state concentrations of lubricant molecules in native and bioengineered joints and also SF bioreactors of different geometry and with different chemical environments; (2) demonstration of the ability to modulate HA and PRG4 lubricant secretion rates and structure over a range of magnitudes by application of individual and combinations of cytokines present in SF; (3) demonstration of the ability to modulate retention of these lubricant molecules in a fluid volume by altering the pore size of a semi-permeable membrane; and (4) development of a novel bioreactor system with biomimetic features of the synovial joint for generating a bioengineered SF in which the lubricant composition and function can be modulated by altering membrane pore size and the cytokine regulatory environment. Clinical implications of this work include (1) the potential utility of a lubricious bioengineered fluid as a viscosupplement to help restore deficient SF, and (2) the utility of a SF bioreactor system in examining the effects of different arthritis-related pharmaceuticals on composition and function of bioengineered SF.

The theoretical model developed in this study included several assumptions that allowed for a straightforward analysis that could be expanded upon. For example,

the model could be extended by including additional environmental factors, such as mechanical stimuli, and allowing a number of parameters to change with the environment and time, such as synovium permeability. Some parameters in the model are also described in bulk and spatially averaged terms rather than on multiple scale levels. Additionally, physical and chemical interactions of lubricants with their environment were not considered in the model, and may affect the free concentration of lubricants in SF.

The synergistic effects of cytokines applied in combination on synoviocyte HA secretion would likely lead to dramatic increases in the total HA content in SF, with effects on concentration that are dependent on fluid volume. For example, in injured or diseased joints, the HA concentration is often decreased, but the SF volume is more substantially increased, resulting in a net increase in total lubricant content [2-5, 15, 20]. Synergistic effects were most common in cytokine combinations including TNF-α, supporting the observation that TNF-α inhibitors used in the treatment of arthritis have demonstrated higher success than other cytokine inhibitors likely due to TNF-α's potent interaction with a number of SF cytokines [6, 11]. The observed cytokine regulation of HA MW secreted by synoviocytes may also affect the total HA content in SF, as an altered structure would likely affect the rate that HA permeates the synovium and is lost from SF. Such regulation of HA MW may involve a combination of synthesis, stabilization, or degradation processes and may have marked effects on the lubricating function of SF. Further studies are needed to elucidate the mechanisms by which cytokines regulate lubricant secretion rates and structure.

Varying degrees of SF lubricant retention have been observed in vivo, perhaps due to the observations made here that retention is dependent on membrane pore size and lubricant MW. For example, decreases in the concentration and half-life of HA

have been reported in arthritic joints compared to normal joints [3, 4, 9, 10, 14, 17, 22]. This may be related to a decreased retention by the synovium due to alterations in tissue structure, as studies have demonstrated that digestion of selected matrix components of the synovium results in increased permeability [7, 25]. It could also be related to changes in the synovium cellularity, as it was shown here that an adherent cell layer played a role in lubricant retention. Decreases in HA concentration and half-life may also be related to decreased HA MW. In vivo studies that infused HA of different MWs into the synovial joint cavity of rabbit models demonstrated that with HA of lower MW (~140 kDa, ~500 kDa) there was less reflection by the synovium and accumulation in the cavity than with HA of higher MW (~2200 kDa) [8, 21].

The ability to modulate the composition and function of bioengineered SF through cytokine-regulation of lubricant secretion and membrane pore-size-regulated lubricant retention may allow fluid properties to be precisely controlled. Engineered lubricant solutions have been developed for intra-articular injection into injured or diseased joints in which SF may be deficient, such as formulations of HA with various concentrations and MW used clinically [18, 27], and more recently, a PRG4 protein construct being used in animal models [13]. However, a biomimetically bioengineered SF with both HA and PRG4 components is a novel development and may have similar applications in viscosupplementation. The correlation between composition and function of bioengineered SF and the dose-dependent effects on reducing friction found here are consistent with other studies examining the lubricating function of SF and purified preparations of HA and PRG4 [23, 24]. SF from injured or diseased joints has similarly shown a relationship between composition and function, as fluid with decreased lubricant concentration has a decreased lubricating ability [1, 12, 26].

The findings of this work have implications for the development of improved arthritis therapies specifically targeted at restoration of failed joint lubrication. For example, a bioengineered lubricous fluid that includes both HA and PRG4 lubricant components may have application as a novel viscosupplement. A bioreactor system for creating such a fluid may enable analysis of the effects of different arthritis-related pharmaceuticals on lubricant regulation. Introduction of a synoviocyte-laden material generated in bioreactors may be introduced to the joint as a method for sustainable long-term delivery of lubricant molecules into deficient SF, as would the implantation of whole tissue engineered joints for complete biological arthroplasty. An appropriate lubricating environment may be critical during the growth and development of such tissue engineered joints in bioreactors [19], to maintain the low-friction, low-wear properties of articulating cartilage surfaces with imposed mechanical stimulation and joint-like motion.

Taken together, the results of this dissertation work have contributed to an understanding of the relationships between alterations in SF lubricant concentration, SF cytokine concentration, and synovium permeability to lubricants, and associated implications of these changes on the function of SF. The findings reported here are consistent with the overall hypothesis that recapitulation of the biophysical features of the synovial joint in a biomimetic bioreactor system would allow the generation of a bioengineered SF, and that the lubricant composition and function of this fluid is highly dependent upon the rate of synthesis and the rate of loss of lubricants. Cytokine-regulated lubricant secretion rates and lubricant retention by the semi-permeable synovium are likely key regulators of in vivo SF lubricant composition and function.

6.3   Future Work

The current work can be expanded in the future in a number of ways, from extension of the mathematical model to include additional features of the in vivo synovial joint, to investigation of additional lubricant-regulating cytokines and additional semi-permeable membrane materials, to analysis of the effects of arthritis-related pharmaceuticals on bioengineered SF composition and function, and ultimately to the scaling the biomimetic features of current tissue-scale bioreactor to the whole joint level.

Although the mathematical model incorporated many biophysical features of the synovial joint and allowed the chemical environment to alter lubricant secretion rate parameters, it could be extended by including additional environmental factors, such as mechanical stimuli, and by allowing a number of parameters to change with the environment and time, such as synovium permeability and SF volume. Extension of the model in these directions, along with additional analysis of SF lubricant dynamics in various physiological and pathophysiological conditions, would further contribute to an understanding of in vivo lubricant regulation.

Given the marked regulatory effects of individual and combinations of cytokines on synoviocyte lubricant secretion, it would be interesting to investigate the effects of additional SF cytokines and the signaling mechanisms behind cytokine regulation. Those utilized in the current work, IL-1β, IL-17, IL-32, TGF-β1, and TNF-α, are primarily secreted by macrophage and T cells present in the synovial joint, but synoviocytes themselves secrete a number of cytokines, such as IL-6 and IL-8, that are often present at elevated levels in disease and injury and implicated in arthritis pathogenesis. In addition to investigating other cytokines, analysis of the mechanisms behind cytokine regulation of lubricant secretion could also be studied, through the

use of specific inhibitors and siRNA of associated intracellular signaling molecules of these cytokines, such as various MAP kinases, NF-κB, Smads, etc. As SF contains a complex milieu of chemical factors, continued examination of the effects of cytokines on lubricant secretion and the mechanisms of action will contribute to the knowledge of potential in vivo regulation and development of therapies targeted at regulating lubricant secretion.

While the ability of semi-permeable membranes to retain individual lubricant molecules was assessed in the current studies, it would be interesting to study retention with HA and PRG4 applied in combination, either by mixing purified preparations, or through the use of native SF. Such a study may reveal additive and/or synergistic interactions between the molecules that affect retention by the membranes. Considering the potential for HA and PRG4 to physically interact [16], a decreased loss across membranes may be observed compared to the loss with purified lubricant solutions. Additionally, other types of membranes could be investigated for their ability to retain lubricant molecules, including bioactive materials. Although they may have changing properties over extended culture durations due to degradation and remodeling processes, biological materials may offer more promise with therapeutic potential due to their ability to eventually be resorbed with remodeling in vivo.

As generation of bioengineered fluid in the bioreactor system was performed in just a few different cytokine environments, other individual and combinations of cytokines could also be examined to likely demonstrate the dependence of composition and function of fluid on these chemical factors. To investigate the dynamics of lubricant concentration, fluid could be analyzed at various time points through the use of multiple bioreactors or a method for continuous sampling of fluid, and the observations compared to those theoretically predicted. Additionally, analysis

of the effects of arthritis-related pharmaceuticals on composition and function of bioengineered SF could be performed to provide insight into their effects on in vivo SF lubricant regulation. As the action of these commonly prescribed therapeutics are targeted at inhibition of the activity of certain cytokines, it is likely that they would affect lubricant secretion rates by cells in the joint, and ultimately lubricant concentration.

Finally, the novel biomimetic bioreactor system developed here represents a step toward the ultimate goal of tissue engineering an implantable biological joint replacement to take the place of traditional metal and plastic artificial joints. By applying the biomimetic feature of a lubricant-retaining membrane with adherent synoviocytes to an existing joint-scale bioreactor developed in our laboratory [19] for culturing whole joints with applied joint-like motion, a lubricous bioengineered fluid may be generated to achieve and maintain low-friction, low-wear properties of tissue engineered joints.

6.4   References

1. Antonacci JM, Schmidt TA, Serventi LA, Shu YL, Gastelum NS, Schumacher BL, McIlwraith CW, Sah RL: Effects of joint injury on synovial fluid and boundary lubrication of cartilage. Trans Orthop Res Soc 32:156, 2007.

2. Asari A, Miyauchi S, Sekiguchi T, Machida A, Kuriyama S, Miyazaki K, Namiki O: Hyaluronan, cartilage destruction and hydrarthrosis in traumatic arthritis. Osteoarthritis Cartilage 2:79-89, 1994.

3. Balazs EA: The physical properties of synovial fluid and the special role of hyaluronic acid. In: Disorders of the knee, ed. by AJ Helfet, Lippincott Co., Philadelphia, 1974, 63-75.

4. Balazs EA, Watson D, Duff IF, Roseman S: Hyaluronic acid in synovial fluid. I. Molecular parameters of hyaluronic acid in normal and arthritis human fluids. Arthritis Rheum 10:357-76, 1967.

5. Belcher C, Yaqub R, Fawthrop F, Bayliss M, Doherty M: Synovial fluid chondroitin and keratan sulphate epitopes, glycosaminoglycans, and hyaluronan in arthritic and normal knees. Ann Rheum Dis 56:299-307, 1997.

6. Christodoulou C, Choy EH: Joint inflammation and cytokine inhibition in rheumatoid arthritis. Clin Exp Med 6:13-9, 2006.

7. Coleman PJ, Scott D, Abiona A, Ashhurst DE, Mason RM, Levick JR: Effect of depletion of interstitial hyaluronan on hydraulic conductance in rabbit knee synovium. J Physiol 509 (Pt 3):695-710, 1998.

8. Coleman PJ, Scott D, Mason RM, Levick JR: Role of hyaluronan chain length in buffering interstitial flow across synovium in rabbits. J Physiol 526 Pt 2:425-34, 2000.

9. Coleman PJ, Scott D, Ray J, Mason RM, Levick JR: Hyaluronan secretion into the synovial cavity of rabbit knees and comparison with albumin turnover. J Physiol 503 (Pt 3):645-56, 1997.

10. Dahl LB, Dahl IM, Engstrom-Laurent A, Granath K: Concentration and molecular weight of sodium hyaluronate in synovial fluid from patients with rheumatoid arthritis and other arthropathies. Ann Rheum Dis 44:817-22, 1985.

11. Edwards CJ: Immunological therapies for rheumatoid arthritis. Br Med Bull 73-74:71-82, 2005.

12. Elsaid KA, Jay GD, Warman ML, Rhee DK, Chichester CO: Association of articular cartilage degradation and loss of boundary-lubricating ability of synovial fluid following injury and inflammatory arthritis. Arthritis Rheum 52:1746-55, 2005.

13. Flannery CR, Zollner R, Corcoran C, Jones AR, Root A, Rivera-Bermudez M, Blanchet T, Bendele AM, Morris EA, Glasson SS: Lubricin Supplementation Prevents Osteoarthritis Progression in a Rat Surgical Model. Trans ORS 54:266, 2008.

14. Fraser JR, Kimpton WG, Pierscionek BK, Cahill RN: The kinetics of hyaluronan in normal and acutely inflamed synovial joints: observations with experimental arthritis in sheep. Semin Arthritis Rheum 22:9-17, 1993.

15. Jawed S, Gaffney K, Blake DR: Intra-articular pressure profile of the knee joint in a spectrum of inflammatory arthropathies. Ann Rheum Dis 56:686-9, 1997.

16. Jay GD, Lane BP, Sokoloff L: Characterization of a bovine synovial fluid lubricating factor III. The interaction with hyaluronic acid. Connect Tissue Res 28:245-55, 1992.

17. Laurent UB, Fraser JR, Engstrom-Laurent A, Reed RK, Dahl LB, Laurent TC: Catabolism of hyaluronan in the knee joint of the rabbit. Matrix 12:130-6, 1992.

18. Moreland LW: Intra-articular hyaluronan (hyaluronic acid) and hylans for the treatment of osteoarthritis: mechanisms of action. Arthritis Res Ther 5:54-67, 2003.

19. Nugent-Derfus GE, Takara T, O'Neill J K, Cahill SB, Gortz S, Pong T, Inoue H, Aneloski NM, Wang WW, Vega KI, Klein TJ, Hsieh-Bonassera ND, Bae WC, Burke JD, Bugbee WD, Sah RL: Continuous passive motion applied to whole joints stimulates chondrocyte biosynthesis of PRG4. Osteoarthritis Cartilage 15:566-74, 2007.

20. Ropes MW, Rossmeisl EC, Bauer W: The origin and nature of normal human synovial fluid. J Clin Invest 19:795-9, 1940.

21. Sabaratnam S, Arunan V, Coleman PJ, Mason RM, Levick JR: Size selectivity of hyaluronan molecular sieving by extracellular matrix in rabbit synovial joints. J Physiol 567:569-81, 2005.

22. Sakamoto T, Mizono, S, Miyazaki, K, Yamaguchi, T, Toyoshima, H, Namiki, O.: Biological fate of sodium hyaluronate (SPH): Studies on the distribution,

metabolism, and excretion of 14C-SPH in rabbits after intra-articular administration. Pharmacometrics 28:375-87, 1984.

23. Schmidt TA, Gastelum NS, Nguyen QT, Schumacher BL, Sah RL: Boundary lubrication of articular cartilage: role of synovial fluid constituents. Arthritis Rheum 56:882-91, 2007.

24. Schmidt TA, Sah RL: Effect of synovial fluid on boundary lubrication of articular cartilage. Osteoarthritis Cartilage 15:35-47, 2007.

25. Scott D, Coleman PJ, Mason RM, Levick JR: Glycosaminoglycan depletion greatly raises the hydraulic permeability of rabbit joint synovial lining. Exp Physiol 82:603-6, 1997.

26. Teeple E, Elsaid KA, Fleming BC, Jay GD, Aslani K, Crisco JJ, Mechrefe AP: Coefficients of friction, lubricin, and cartilage damage in the anterior cruciate ligament-deficient guinea pig knee. J Orthop Res, 2007.

27. Tehranzadeh J, Booya F, Root J: Cartilage metabolism in osteoarthritis and the influence of viscosupplementation and steroid: a review. Acta Radiol 46:288-96, 2005.

APPENDIX A:

MICROENVIRONMENT REGULATION OF PRG4 PHENOTYPE OF CHONDROCYTES

A.1 Abstract

Articular cartilage is a heterogeneous tissue with superficial (**S**), middle (**M**), and deep (**D**) zones. Chondrocytes in the **S** zone secrete the lubricating PRG4 protein, while chondrocytes from the **M** and **D** zones are more specialized in producing large amounts of the glycosaminoglycan (GAG) component of the extracellular matrix. Soluble and insoluble chemicals and mechanical stimuli regulate cartilage development, growth, and homeostasis; however, the mechanisms of regulation responsible for the distinct PRG4-positive and negative phenotypes of chondrocytes are unknown. The objective of this study was to determine if interaction between **S** and **M** chondrocytes regulates chondrocyte phenotype, as determined by co-culture in monolayer at different ratios of **S:M** (100:0, 75:25, 50:50, 25:75, 0:100) and at different densities (240,000, 120,000, 60,000, and 30,000 cells/cm^2), and by measurement of PRG4 secretion and expression, and GAG accumulation. Co-culture of **S** and **M** cells resulted in significant upregulation in PRG4 secretion and the percentage of cells expressing PRG4, with simultaneous downregulation of GAG accumulation. Tracking **M** cells with PKH67 dye in co-culture revealed that they

maintained a PRG4-negative phenotype, and proliferated less than **S** cells. Taken together, these results indicate that the upregulated PRG4 expression in co-culture is a result of preferential proliferation of PRG4-expressing **S** cells. This finding may have practical implications for generating a large number of phenotypically normal **S** cells, which can be limited in source, for tissue engineering applications.

A.2 Introduction

Articular cartilage is the low-friction, wear-resistant, load-bearing tissue at the ends of long bones in skeletal joints [34]. The tissue is typically classified into 3 zones, superficial (**S**), middle (**M**), and deep (**D**), resulting from depth-associated variation in cell and extracellular matrix properties [16]. In the superficial zone of mature articular cartilage (0-10% depth from articular surface), cell density is relatively high and cells are arranged in clusters parallel to the surface. Cell density is lower in the middle zone (10-40%), and there, cells appear more rounded and randomly dispersed. In the deep zone (40-100%), cells are present at an even lower density and have a columnar organization [14]. Chondrocytes in the **S** zone secrete superficial zone protein [33], a glycoprotein encoded by the *Prg4* gene [15] and postulated to be a lubricant adsorbed to the articular surface in synovial joints that is important in maintaining the health of the cartilage and joint [17]. Chondrocytes from the **M** and **D** zones of articular cartilage secrete very little PRG4, but produce the glycosaminoglycan (GAG) component of the extracellular matrix at a relatively high rate [1]. The zonal structure of articular cartilage and the associated zone-specific expression by chondrocytes of molecules with specific functions are features of articular cartilage that are regulated through unknown mechanisms.

Microenvironmental factors, broadly classified as soluble or insoluble chemicals, and mechanical stimuli, regulate cartilage development, growth, and homeostasis, and may be responsible for the distinct PRG4-positive and negative phenotypes. Soluble chemical signals may arise externally and enter from the articular surface [24] and, for small molecules, through the subchondral bone [10]. They may also arise internally, by autocrine or paracrine secretion from chondrocytes, and from

binding sites that form storage depots in the extracellular matrix [9, 28, 35]. These soluble signals can form gradients due to diffusive transport, binding in the matrix, or uptake by cells within the tissue [5, 23]. Cell density can greatly affect the local concentration of secreted soluble factors and, thus, chemical signaling. Other microenvironmental factors include insoluble chemical signals, such as extracellular matrix that is engaged by cell surface receptors [4, 21], and mechanical stimuli such as compressive and shear stress [11, 12, 38].

Autocrine or paracrine secretion of chemical signals by cells, at various densities in the different zones of articular cartilage, may be responsible for the different cell phenotypes in the native tissue. However, it is difficult to observe the regulatory effects of these signals in cartilage tissue without the interference of other microenvironmental factors. Short-term monolayer co-culture systems can be used to study interactions between **S** and **M** subpopulations with minimal mechanical stimuli and extracellular matrix, and little variation in external nutrients. If autocrine or paracrine chemical signals do regulate chondrocyte PRG4 phenotype, then the local concentration of these secreted regulators would be expected to be modulated by the proportion of **S** and **M** cells, and by cell density.

Thus, the objective of this study was to determine if culturing **S** and **M** chondrocytes in monolayer in different ratios of **S:M** (100:0, 75:25, 50:50, 25:75, 0:100) and at different densities (240,000, 120,000, 60,000, and 30,000 cells/cm^2) regulates chondrocyte phenotype, as measured by PRG4 secretion and expression, and GAG accumulation. The two highest densities were chosen to be analogous to the cell density in a one cell diameter-thick section of the superficial and middle zones of bovine calf cartilage, respectively, while the two lowest densities were chosen to allow lower local concentrations of soluble signal.

A.3   Methods and Materials

Chondrocyte Isolation and Culture

Chondrocytes from the **S** and **M** layers of bovine articular cartilage were obtained, seeded in varying proportions and at varying cell densities, and incubated for 10 days. Briefly, 9 mm diameter osteochondral cores were harvested from the patellofemoral groove of a total of four 1-3 week old bovine animals under sterile conditions using the Osteochondral Autograft Transfer System (Arthrex, Naples, FL). Cores were then sectioned with a microtome (Microm, Waldorf, Germany) in 0.2 mm slices to obtain superficial (**S**, <0.2 mm depth) and middle (**M**, 0.6-1.2 mm) layers (**Figure A.1A**), from which **S** and **M** chondrocyte subpopulations were isolated by sequential digestion with pronase and collagenase [27].
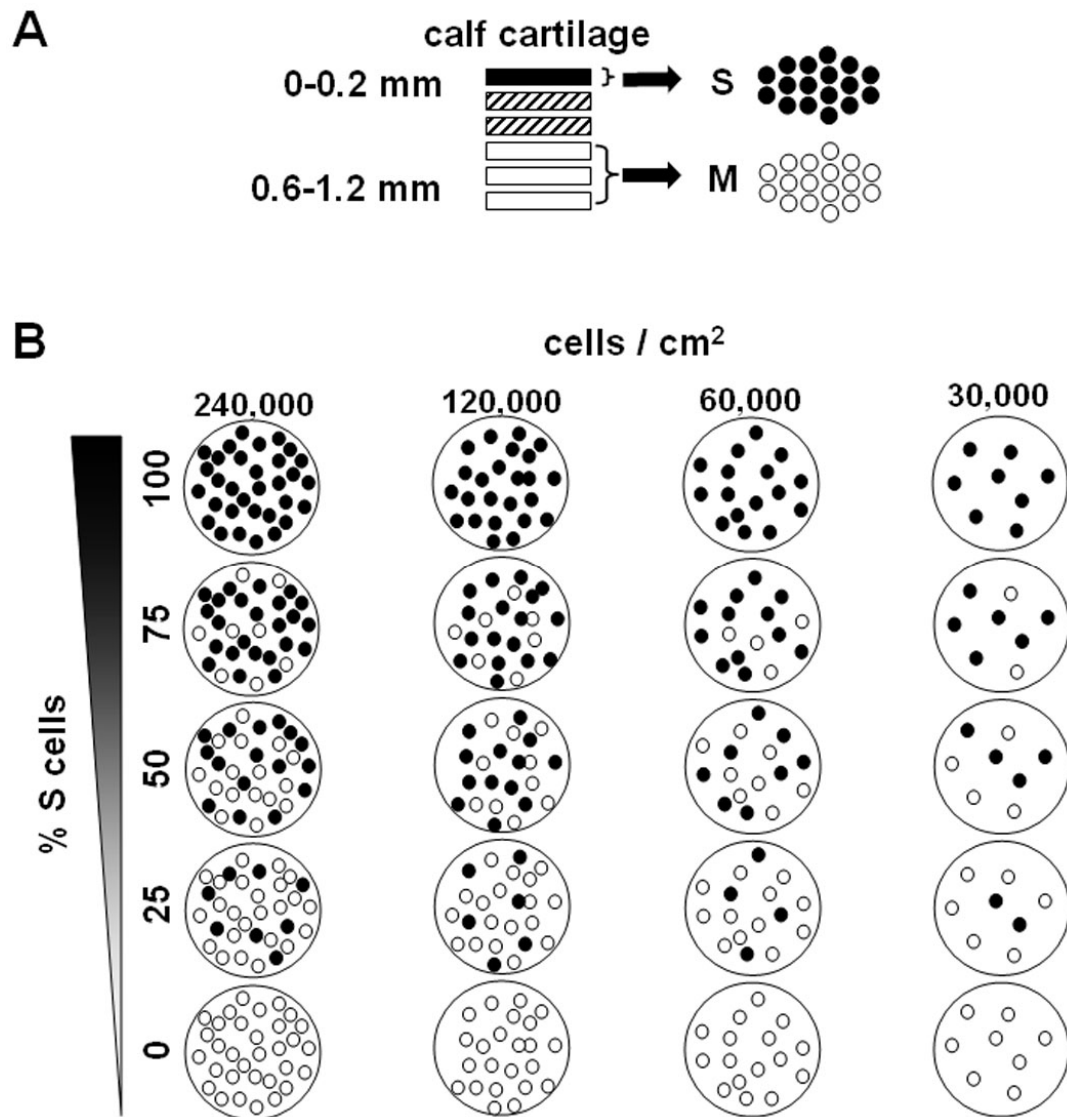
Figure A.1: Schematic of (**A**) cell isolation and (**B**) experimental conditions. (**A**) Superficial cell populations (**S**) were obtained from the top 0.2 mm of bovine calf articular cartilage, and middle cell populations (**M**) from a tissue depth of 0.6-1.2 mm. (**B**) Cells were cultured in **S:M** ratios of 0:100, 25:75, 50:50, 75:25, and 100:0, and at total cell densities of 240,000, 120,000, 60,000, and 30,000 cells/cm^2.

In one set of experiments, chondrocytes were washed and resuspended in DMEM with additives (25 μg/ml ascorbic acid, 100 U/ml penicillin, 100 μg/ml streptomycin, 0.25 μg/ml Fungizone, 0.1 mM MEM non-essential amino acids, 10 mM HEPES, 0.4 mM L-proline, 2 mM L-glutamine) supplemented with 10% fetal bovine serum. Isolated chondrocytes were plated at densities of 240,000 cells/cm^2, 120,000 cells/cm^2, 60,000 cells/cm^2, and 30,000 cells/cm^2 in **S:M** ratios of 100:0, 75:25, 50:50, 25:75, and 0:100 (**Figure A.1B**). The cells were incubated at 37°C in an atmosphere of 5% CO_2 for 10 days. Medium was changed on days 1, 4, 7, and 10 (1 ml/(10^6 initial cells•day)), collected, and frozen until further analysis.

In a separate experiment, **M** cells were labeled with 4 μM PKH67 cell tracking dye (Sigma, St. Louis, MO) to track and identify this subpopulation of cells. Immediately after chondrocyte isolation, **M** cells were incubated with 4 μM PKH67 for 5 min, then incubated with heat-inactivated serum for 1 min, and finally rinsed 3 times in complete medium, according to the manufacturer's protocol. Then, both **S** and **M** cells were cultured in **S:M** ratios of 100:0, 25:75, and 0:100 at a density of 60,000 cells/cm^2. Immunolocalization for PRG4 was performed on day 10 to measure **M** cell PRG4 expression, as described below.

Biochemical Analysis

Cell layers were harvested, solubilized with proteinase K, and analyzed for DNA using PicoGreen® (Molecular Probes, Eugene, OR) [25], or Hoechst 33258 [18] for PKH67 labeled cultures, on days 1 and 10 to determine proliferation. This solubilized cell layer and portions of media from days 1, 4, 7, and 10 were also analyzed for GAG accumulation and secretion using a dimethylmethylene blue (DMMB) assay [7].

PRG4 Analysis

PRG4 secretion and expression by cultured chondrocytes were quantified by enzyme-linked immunosorbent assay (ELISA) of spent media, and by flow cytometry and immunocytochemistry analysis of cell layers, respectively. ELISA for PRG4 was performed on portions of media from days 1, 4, 7, and 10 using the monoclonal antibody (mAb) 3-A-4, as described previously [20, 32]. Flow cytometry analysis was used to assess the percentage of cells expressing PRG4 on day 10, as previously described [19], after 16 h treatment with 0.1 µM monensin in medium to prevent secretion of PRG4 from the Golgi apparatus, and with an additional step of 1 hr 0.025% collagenase P incubation after the pronase treatment to obtain single cell suspensions. Immunocytochemistry analysis was performed on day 10 after cell cultures were treated for 16 h with 0.1 µM monensin and fixed in 100% methanol. Cells were probed for PRG4 using the Vectastain ABC Elite Kit (Vector, Burlingame, CA), employing mAb 3-A-4 or mouse IgG as a negative control. Cells were counterstained with Methyl Green for 5 min at room temperature. Positive reactivity with PRG4 was documented by photomicroscopy using brightfield illumination. Positive cells were identified manually and counted using NIH Image J software, and the percentage of PRG4 positive cells identified by immunocytochemistry and flow cytometry were correlated. Alternately, for cultures in which **M** cells were labeled with PKH67, PRG4 immunolocalization was performed using mAb 3-A-4 and R-phycoerythrin-conjugated secondary antibody at a concentration of 3 µg/ml (Molecular Probes, Eugene, OR). Cell nuclei were counterstained with Hoechst 33258, and fluorescent microscopy was used to document both the presence of PKH67 and positive reactivity with PRG4.

Statistical Analysis

Data are expressed as mean ± SEM. Two factor ANOVAs ($\alpha=0.05$) were used to determine the effects of two factors, percentage of **S** cells initially seeded and initial cell density, on a number of variables: 1) overall proliferation (d10/d1 DNA), 2) GAG accumulation and secretion, and 3) PRG4 secretion and expression. Planned comparisons were then conducted to determine if, for each density, these same variables at co-culture conditions of 25, 50, and 75% **S** cells were linearly intermediate to the data from 0 and 100% **S** cells. For each cell density, data were normalized to their maximum value before comparison. Planned comparisons were also performed to determine if PRG4 expression levels of 0 and 100% **S** cells after culture duration were significantly altered from day 1 values. Linear regression analysis was performed to confirm correlation between PRG4 expression levels by flow cytometry and immunocytochemistry methods. Statistical analysis was implemented with Systat 10.2 (Systat Software, Richmond, CA) and Excel (Microsoft, Redmond, WA).

A.4   Results

Cell Proliferation

The fold increase in DNA, or degree of proliferation from day 1 to day 10 during culture, was affected by the initial cell plating density ($p<0.01$, **Figure A.2A**) and by the percentage of **S** cells within each density ($p<0.001$). Proliferation decreased slightly from 3.51 ± 0.31 fold at 240,000 cells/cm^2, to 2.90 ± 0.25 fold at 30,000 cells/cm^2, and also decreased slightly as the percentage of **S** cells increased, from 3.54 ± 0.39 fold at 0% **S** to 2.66 ± 0.20 fold at 100% **S**.
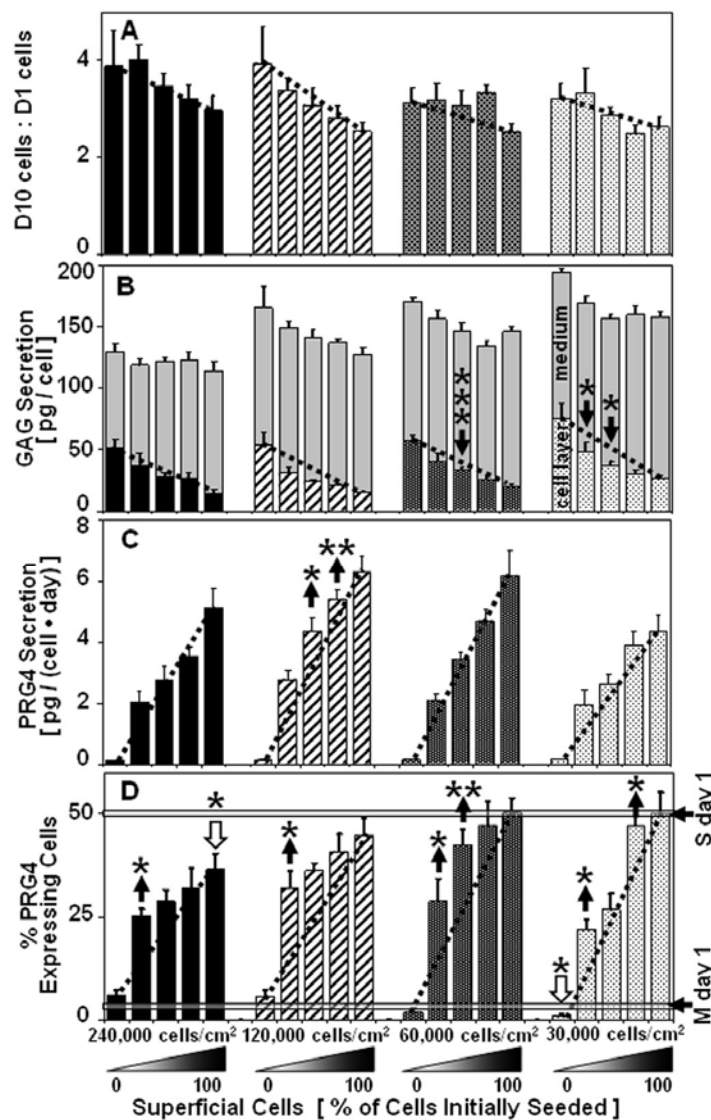
Figure A.2: The effect of co-culture on (**A**) cell proliferation as measured by the ratio of DNA content of cell layers on day 10 to day 1, (**B**) GAG accumulation and secretion over 10 days in culture, (**C**) PRG4 secretion into media over days 7-10 of culture, and (**D**) PRG4 expression on day 10. For each density (240,000, 120,000, 60,000, and 30,000 cells/cm^2), gradients represent the % **S** cells initially seeded (0, 25, 50, 75, and 100% **S**). Dotted lines linearly relate 25, 50, and 75% **S** co-culture conditions to 0 and 100% **S** populations. In (**B**), the lower bars represent GAG accumulation in the cell layer, while the upper bars represent the GAG secreted into the media over 10 days. In (**D**), horizontal gray bars represent PRG4 expression of **S** and **M** populations isolated on day 1, while stars near unfilled down-arrows indicate significant downregulation in expression of pure **S** and **M** cell populations from these day 1 values. For all graphs, stars near up-arrows indicate significant upregulation from linearly intermediate values, while stars near down-arrows indicate significant downregulation (*p<0.05, **p<0.01, ***p<0.001) (n=4).

GAG Synthesis

Both GAG accumulation in the cell layer and GAG secreted into the medium were significantly affected by cell density (p<0.001, **Figure A.2B**), whereas only GAG accumulation in the cell layer was affected by the percentage of **S** cells (p<0.001). Total accumulated plus secreted GAG increased from 121 ± 10 pg/cell at 240,000 cells/cm^2 to 167 ± 7 pg/cell at 30,000 cells/cm^2, while GAG accumulation decreased with higher percentage of **S** cells, from 59 ± 7 pg/cell at 0% **S** to 19 ± 2 pg/cell at 100% **S**. Linear interpolation between the 0% **S** data points and the 100% **S** data points at each density revealed that several conditions of co-culture resulted in significant downregulation of GAG accumulation in the cell layer from linearly intermediate values.

PRG4 Regulation

PRG4 secretion into the media during days 7-10 of co-culture was affected by percentage of **S** cells (p<0.001, **Figure A.2C**) and cell density (p<0.001). Secretion increased from 0.14 ± 0.02 pg/(cell•day) at 0% **S** cells to 5.48 ± 0.52 pg/(cell•day) at 100% **S** cells, and overall levels were slightly higher at the intermediate densities. Linear interpolation between the 0% **S** data points and the 100% **S** data points at each density revealed the effect of co-culture. PRG4 expression under conditions of 50% **S** and 75% **S** at 120,000 cells/cm^2 were significantly greater than linearly intermediate values (p<0.05, p<0.01, respectively), indicating that an interaction between cell populations exists, resulting in upregulation of PRG4 secretion.

The percentage of cells expressing PRG4, as determined on day 10 by flow cytometry, was affected by percentage of **S** cells (p<0.001, **Figure A.2D**) and cell density (p<0.01), with an interaction effect (p<0.05). PRG4 expression increased with

increasing percentage of **S** cells, from 4 ± 1% positive at 0% **S** cells to 46 ± 4% positive at 100% **S** cells, and also increased with lower density. The **S** cell population isolated on day 1 had an average expression level of 50 ± 4%, while **M** cells were only 4 ± 2% PRG4-positive. Linear interpolation between the 0% **S** data points and the 100% **S** data points revealed a significant upregulation in expression at many of the co-culture conditions. Downregulation in PRG4 expression was observed in the 100% **S** condition at the highest density, decreasing ~13% from its initial day 1 expression level ($p<0.05$).

Immunocytochemistry analysis confirmed the upregulation observed in flow cytometry analysis (**Figure A.3**), with a correlation of $r^2 = 0.86$, $p<0.001$. PRG4 expression patterns in 25% **S**, 50% **S**, and 75% **S** co-culture conditions were high relative to 100% **S** conditions, while 0% **S** samples showed little or no PRG4 expression. Differences in the degree of cell-cell and cell-matrix proximity are also illustrated at the different seeding densities.

In the separate experiment to identify the source of PRG4-expressing cells in co-culture, immunocytochemistry analysis of PKH67 labeled **M** cells on day 10 showed that M cells retained the PKH67 label and maintained a PRG4-negative phenotype (**Figure A.4**). PKH67 was initially taken up by 96% of **M** cells, as assessed by flow cytometry immediately after labeling, and was retained by 91% of **M** cells after 10 days of culture (Table 1). In 25% **S** co-culture conditions, <2% of cells were double-labeled with both PKH67 and mAb 3-A-4/R-phycoerythrin for PRG4 (**Figure A.4B**). However, upregulated PRG4 expression was still observed, as levels were ~50% rather than 25% of the 100% **S** condition (**Table A.1**). The percentage of **M** cells (% PKH+) in co-culture decreased from 75% to ~50%, (i.e. the percentage of **S** cells increased from 25% to ~50%). Thus, both percentage of **S** cells and percentage

of cells expressing PRG4 increased proportionally in co-culture. PKH67 had no marked effects on proliferation, GAG synthesis, or PRG4 secretion of cells.
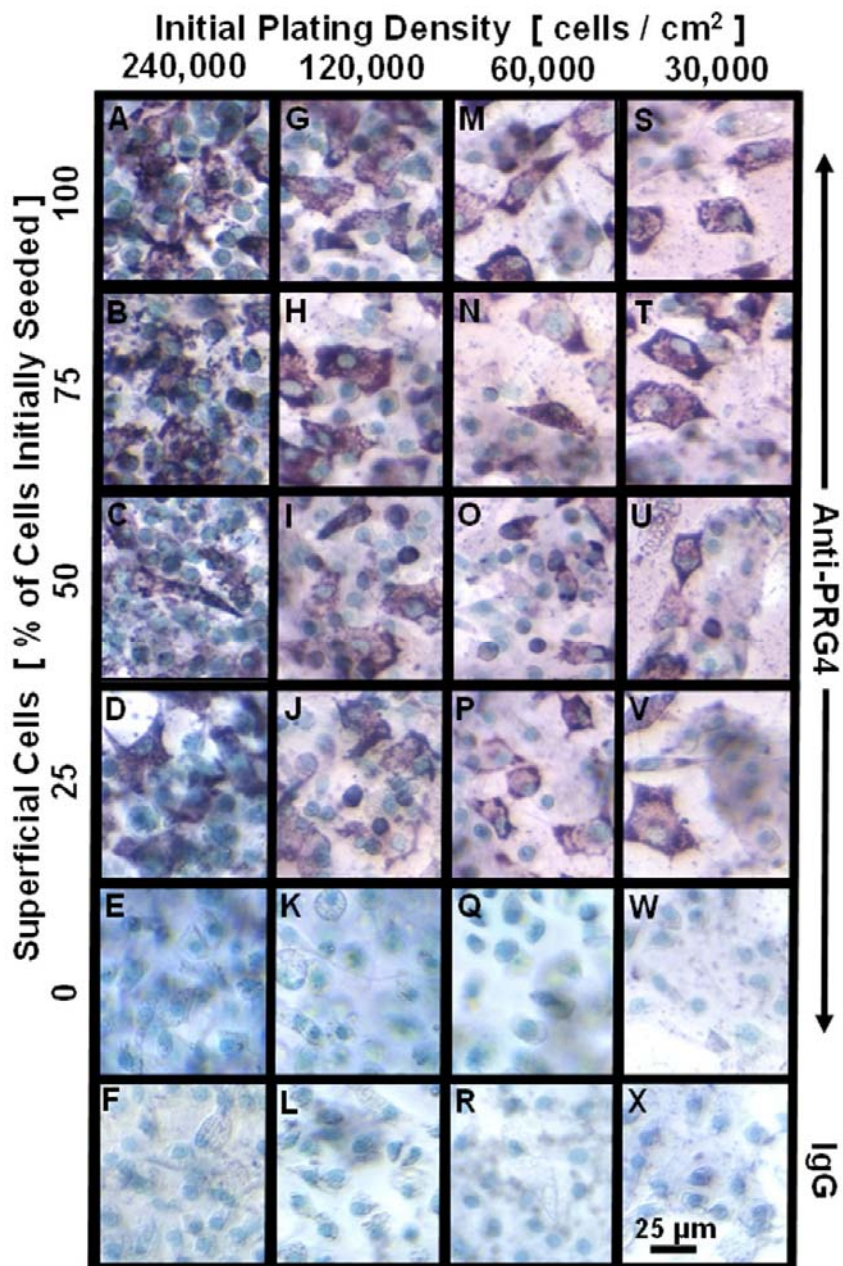
Figure A.3: The effect of co-culture on PRG4 expression, determined by immunolocalization with mAb 3-A-4 in cell layers on day 10. 240,000 cells/cm^2 (**A-F**), 120,000 cells/cm^2 (**G-L**), 60,000 cells/cm^2 (**M-R**), and 30,000 cells/cm^2 (**S-X**) densities show PRG4 expression in 25% **S** (**D,J,P,V**), 50% **S** (**C,I,O,U**), and 75% **S** (**B,H,N,T**) conditions that were high relative to 100% **S** (**A,G,M,S**). Conditions of 0% **S** (**E,K,Q,W**) are comparable to IgG isotype matched controls (**F,L,R,X**).
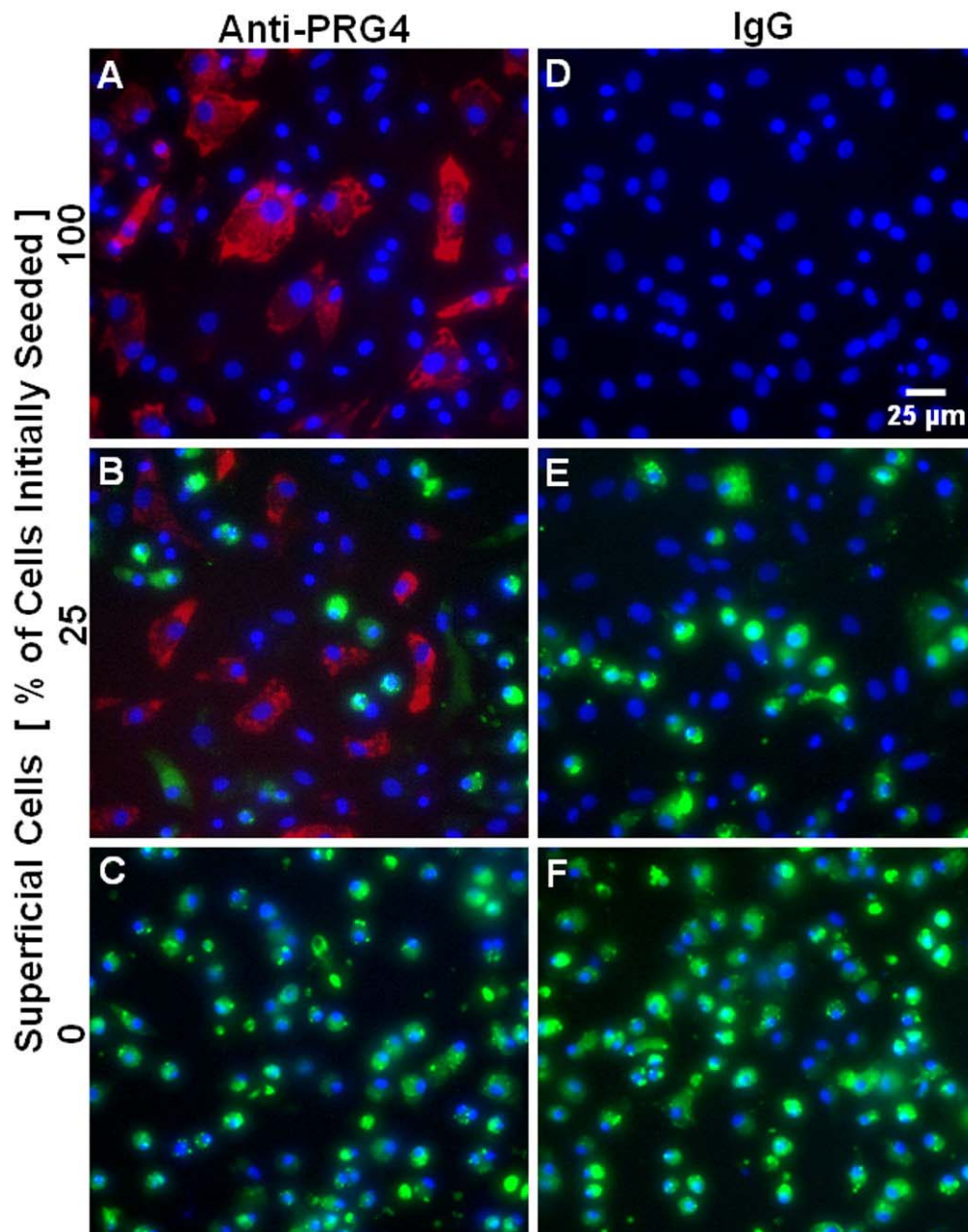
Figure A.4: Identification on day 10 of the source of PRG4-expressing cells. For **M** cells labeled with 4 µM PKH67, immunolocalization of PRG4 with mAb 3-A-4 (**A,B,C**) or isotype-matched IgG controls (**D,E,F**), and R-phycoerythrin-conjugated secondary antibody. PKH67 labeled cells appear green, PRG4-positive cells appear red, and cell nuclei appear blue with Hoescht 33258 counterstain.
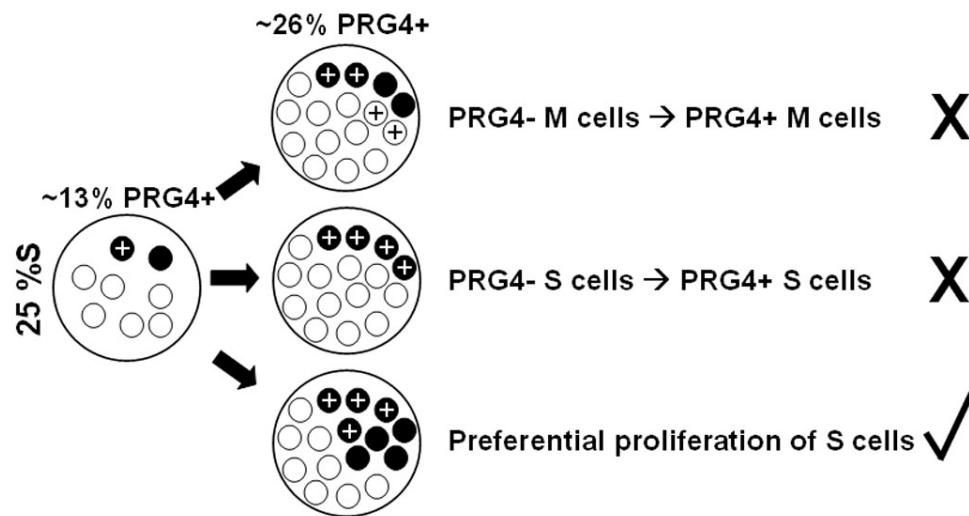
Figure A.5: The various cell fate responses that may account for the observed upregulation of PRG4 expression. It is likely that preferential proliferation of **S** cells is responsible, rather than a phenotype change of **M** or **S** cells. Black circles represent **S** cells, white circles represent **M** cells, and plus signs indicate PRG4 expression.

Table A.1: Percentage of cells expressing PRG4 and containing PKH67 cell tracker dye, as determined from fluorescent images of 100% **S**, 25% **S**, and 0% **S** culture conditions in which **M** cells were PKH67 labeled. Each value represents a percentage value from ~1,300-3,800 cells.

Group [% S seeded]	PKH [μM]	% PRG4+	% PKH+	% PRG4+ and PKH+
100	0	43	0	0
25	0	25	0	0
25	4	19	48	<2
0	0	4	0	0
0	4	<1	91	<1

A.5   Discussion

This study examined the regulatory effects of interaction between **S** and **M** chondrocytes on PRG4 phenotype. The concentration of hypothesized secreted regulators was modulated by adjusting the ratio of **S** to **M** cells initially seeded in monolayer, and by controlling cell density. Co-culture resulted in significant upregulation in PRG4 secretion and expression (**Figure A.2C,D**), with simultaneous downregulation in GAG accumulation (**Figure A.2B**). Thus, the data are consistent with the idea that chemical signals present in this co-culture system regulate chondrocytes.

Monolayer culture provides a model environment with several advantages and disadvantages for analyzing *in vitro* cell behavior. It allows soluble chemical signaling to be studied with minimal interference by gradients in external nutrients that are present in 3-D culture systems, but it does not eliminate the influence of insoluble chemical signals in the matrix that can bind soluble factors and affect the extent of signaling. The accumulation of an extracellular matrix, however, is not instantaneous in monolayer, and with short-term culture is not as extensive as in native tissue. The 2-D nature of monolayer culture can sometimes result in dedifferentiation of cells and the subsequent loss of cell phenotype, but native phenotypes of some cells can be maintained in this environment [29, 37]. Specifically, the PRG4 phenotypes of **S** and **M** chondrocyte subpopulations have proven to be stable in monolayer culture [32]. In this study, PRG4 expression in 100% **S** conditions was generally maintained at ~50% positive, while expression in 0% **S** conditions was maintained at ~0%. Thus, monolayer culture was useful for examining the effects of chemical signaling between **S** and **M** chondrocytes on cell phenotype.

The different cell subpopulations of cartilage can be distinguished by their PRG4 phenotype, but also by other parameters. For example, **M** cells preferentially secrete Cartilage Intermediate Layer Protein (CILP) [22] into the surrounding matrix. This study, however, focused on regulation of PRG4 phenotype due to its role in boundary lubrication of cartilage [17] and the frequency with which the **S** layer of cartilage that produces this protein is damaged with aging and osteoarthritis [2]. The spectrum of proteoglycans synthesized in this study could also be studied further. An additional focus of this study was on the interaction of **S** and **M** cells, but interactions between **S** and **D** or **M** and **D** cells could be a subject of future investigations, especially in systems with mature articular cartilage in which these zones are evident as classically defined. Further, both chemical [31] and mechanical stimuli [30] of cartilage explants can affect the PRG4 phenotype of cells in the **S** and upper **M** zone, but not **D** zone, and it is possible that this is facilitated by cellular interactions.

In the present study, various cell fate responses may have accounted for the observed regulation in chondrocyte phenotype (**Figure A.5**). The upregulation in PRG4 expression that occurred in co-culture may be a result of either a PRG4 phenotype switch or preferential proliferation of PRG4-expressing cells. For example, in 25% **S** conditions, initial PRG4 expression levels were ~13% and increased to ~26% by day 10 of co-culture. This upregulation in PRG4 expression occurred simultaneously with significant downregulation of GAG synthesis.

As cells of the **M** layer are more specialized in secreting GAG components of the extracellular matrix than **S** cells, there existed the possibility that **M** cells could be induced to switch from a PRG4-negative phenotype to a PRG4-positive phenotype. However, **M** cells labeled with a cell tracking dye to monitor PRG4 expression and co-cultured with **S** cells did not show increased PRG4 expression by day 10 (**Figure**

A.4), suggesting that this was unlikely. These results are not likely attributable to a lack of PKH67 labeling by **M** cells. In the 0% **S** condition, only 9% of **M** cells were not labeled, which translates into 7% of total cells in the 25% **S**: 75% **M** co-culture. Upregulation due to PRG4 expressing **M** cells with lack of PKH67 labeling would require all of these unlabeled **M** cells to express PRG4; however, this would also suggest that a much higher percentage of **M** cells with the PKH67 label would also express PRG4, rather than the 2% that was observed. The cell tracking experiment also revealed that after 10 days of co-culture, the percentage of **S** cells increased 2-fold along with the 2-fold increase in overall PRG4 expression of the co-culture (**Table A.1**). Thus, the PRG4 expression in the **S** cell population was maintained at its ~50% initial day 1 level, which suggests that the induction of the PRG4 phenotype on **S** cells with no initial expression is also unlikely.

Preferential proliferation of **S** cells in co-culture likely accounts for both the observed upregulation in PRG4 secretion and expression, and also the observed downregulation in GAG accumulation, as individual cultures of **S** cells accumulate significantly less GAG in the cell layer than **M** cells (**Figure A.2B**). The potential for **S** cells to proliferate rapidly under the appropriate microenvironmental cues would support studies in which the **S** zone of articular cartilage has been postulated to be the source of progenitor cells that provide transit amplifying progeny for appositional growth of cartilage [6, 13].

The PRG4 expression data by both flow cytometry and immunocytochemistry can be compared to the secretion data to obtain secretion rates for the PRG4 expressing cells. The trends in expression and secretion data (**Figure A.2C,D**) suggest that there may be different secretion rates for cells at different densities, and subsequently there may be variations in staining intensity of the cells. Variations in

staining intensity were not evident in the immunocytochemistry data, but were detected in the more sensitive flow cytometry analysis by small horizontal shifts in the mean fluorescence intensity of the PRG4-positive histograms.

Soluble chemical interactions between cells are important throughout the development of articular cartilage. For example, parathyroid hormone-related protein (PTHrP) controls the rate at which growth plate chondrocytes differentiate [36], while FGF signaling is involved in regulation of chondrocyte proliferation [26]. In the co-culture system of this experiment, it is possible that **M** cells are secreting a soluble chemical responsible for the selective proliferation of **S** cells. Further, the highest amounts of upregulation in PRG4 expression, or the highest amounts of preferential **S** cell proliferation, were observed in the 25% **S** co-culture conditions, in which the highest concentration of **M** cells and their secreted soluble chemicals were present.

No PRG4 phenotype change occurred in **S** or **M** cells in co-culture. Thus, it remains to be determined if autocrine or paracrine chemical signals are responsible for maintenance of the PRG4 phenotype. The PRG4 phenotype of chondrocytes in cartilage explants, in terms of PRG4 secretion and number of immuno-positive cells, is positively regulated and maintained by addition of TGF-β1, and negatively regulated by IL-1 [31]. Autocrine production of such chemicals by **S** cells may be responsible for the observed maintenance of PRG4 expression in 100% **S** conditions; alternatively, soluble factors present in the serum may have maintained the phenotype. Different cell surface receptor profiles [8] for chemical signals in chondrocytes from **S** and **M** zones could explain why one subpopulation would selectively respond to such a regulatory signal, and another would not.

Mechanical stimuli, which were absent in this study but exist in native cartilage tissue, can greatly affect the extent of chemical signaling by inducing the

release of matrix-bound soluble signals [35], augmenting convective transport of soluble signals, or altering cell-matrix interactions. It has been observed that cartilage tissue explants exposed to dynamic shear upregulate their PRG4 secretion and expression [30]. This upregulation may occur by affecting the secretion or transport of paracrine PRG4 regulators or regulatory signals present in the synovial fluid environment of joints.

Modulation of chondrocyte PRG4 secretion and expression may govern the successful fabrication of tissue-engineered cartilaginous constructs with appropriate zonal functions. The source of cells that express PRG4 for fabrication of such constructs may be limited and difficult to isolate, while passaging chondrocytes to obtain sufficient cell numbers results in decreased PRG4 mRNA [3]. This study revealed that the number of PRG4 expressing **S** cells can be increased in monolayer co-culture with **M** cells and the PRG4 secretion rate may be modulated by seeding density, both of which may have useful applications in cartilage tissue engineering.

A.6   Acknowledgments

A.7 References

1. Aydelotte MB, Greenhill RR, Kuettner KE: Differences between sub-populations of cultured bovine articular chondrocytes. II. Proteoglycan metabolism. *Connect Tissue Res* 18:223-34, 1988.

2. Buckwalter JA, Mankin HJ: Articular cartilage. Part II: degeneration and osteoarthrosis, repair, regeneration, and transplantation. *J Bone Joint Surg Am* 79-A:612-32, 1997.

3. Darling EM, Athanasiou KA: Growth factor impact on articular cartilage subpopulations. *Cell Tissue Res*:1-11, 2005.

4. DeLise AM, Fischer L, Tuan RS: Cellular interactions and signaling in cartilage development. *Osteoarthritis Cartilage* 8:309-34, 2000.

5. DiMicco MA, Sah RL: Dependence of cartilage matrix composition on biosynthesis, diffusion, and reaction. *Transport in Porous Media* 50:57-73, 2003.

6. Dowthwaite GP, Bishop JC, Redman SN, Khan IM, Rooney P, Evans DJ, Haughton L, Bayram Z, Boyer S, Thompson B, Wolfe MS, Archer CW: The surface of articular cartilage contains a progenitor cell population. *J Cell Sci* 117:889-997, 2004.

7. Farndale RW, Sayers CA, Barrett AJ: A direct spectrophotometric microassay for sulfated glycosaminoglycans in cartilage cultures. *Connect Tissue Res* 9:247-8, 1982.

8. Fukumura K, Matsunaga S, Yamamoto T, Nagamine T, Ishidou Y, Sakou T: Immunolocalization of transforming growth factor-beta s and type I and type II receptors in rat articular cartilage. *Anticancer Res* 18:4189-93, 1998.

9. Garcia AM, Frank EH, Trippel SB, Grodzinsky AJ: IGF-1 transport in cartilage: effects of binding and intratissue fluid flow. *Trans Orthop Res Soc* 22:410, 1997.

10. Gillis A, Gray M, Burstein D: Relaxivity and diffusion of gadolinium agents in cartilage. *Magn Reson Med* 48:1068-71, 2002.

11. Grodzinsky AJ, Levenston ME, Jin M, Frank EH: Cartilage tissue remodeling in response to mechanical forces. *Annu Rev Biomed Eng* 2:691-713, 2000.

12. Guilak F, Sah RL, Setton LA: Physical regulation of cartilage metabolism. In: *Basic Orthopaedic Biomechanics,* ed. by VC Mow, Hayes WC, Raven Press, New York, 1997, 179-207.

13. Hayes AJ, MacPherson S, Morrison H, Dowthwaite G, Archer CW: The development of articular cartilage: evidence for an appositional growth mechanism. *Anat Embryol (Berl)* 203:469-79, 2001.

14. Hunziker EB, Quinn TM, Hauselmann HJ: Quantitative structural organization of normal adult human articular cartilage. *Osteoarthritis Cartilage* 10:564-72, 2002.

15. Ikegawa S, Sano M, Koshizuka Y, Nakamura Y: Isolation, characterization and mapping of the mouse and human PRG4 (proteoglycan 4) genes. *Cytogenet Cell Genet* 90:291-7, 2000.

16. Jadin KD, Wong BL, Bae WC, Li KW, Williamson AK, Schumacher BL, Price JH, Sah RL: Depth-varying density and organization of chondrocyte in immature and mature bovine articular cartilage assessed by 3-D imaging and analysis. *J Histochem Cytochem* 53:1109-19, 2005.

17. Jay GD: Lubricin and surfacing of articular joints. *Curr Opin Orthop* 15:355-9, 2004.

18. Kim YJ, Sah RLY, Doong JYH, Grodzinsky AJ: Fluorometric assay of DNA in cartilage explants using Hoechst 33258. *Anal Biochem* 174:168-76, 1988.

19. Klein TJ, Schumacher BL, Blewis ME, Schmidt TA, Voegtline MS, Thonar EJ-MA, Masuda K, Sah RL: Tailoring secretion of proteoglycan 4 (PRG4) in tissue-engineered cartilage. *Tissue Eng* (In Press), 2005.

20. Klein TJ, Schumacher BL, Schmidt TA, Li KW, Voegtline MS, Masuda K, Thonar EJ-MA, Sah RL: Tissue engineering of stratified articular cartilage from chondrocyte subpopulations. *Osteoarthritis Cartilage* 11:595-602, 2003.

21. Knudson W, Loeser RF: CD44 and integrin matrix receptors participate in cartilage homeostasis. *Cell Mol Life Sci* 59:36-44., 2002.

22. Lorenzo P, Bayliss MT, Heinegard D: A novel cartilage protein (CILP) present in the mid-zone of human articular cartilage increases with age. *J Biol Chem* 273:23463-8, 1998.

23. Maroudas A: Biophysical chemistry of cartilaginous tissues with special reference to solute and fluid transport. *Biorheology* 12:233-48, 1975.

24. Maroudas A, Katz EP, Wachtel EJ, Mizrahi J, Soudry M: Physico-chemical properties and functional behavior of normal and osteoarthritic human cartilage. In: *Articular Cartilage Biochemistry,* ed. by K Kuettner, Schleyerbach R, Hascall VC, Raven Press, New York, 1986.

25. McGowan KB, Kurtis MS, Lottman LM, Watson D, Sah RL: Biochemical quantification of DNA in human articular and septal cartilage using PicoGreen and Hoechst 33258. *Osteoarthritis Cartilage* 10:580-7, 2002.

26. Minina E, Kreschel C, Naski MC, Ornitz DM, Vortkamp A: Interaction of FGF, Ihh/Pthlh, and BMP signaling integrates chondrocyte proliferation and hypertrophic differentiation. *Dev Cell* 3:439-49, 2002.

27. Mok SS, Masuda K, Häuselmann HJ, Aydelotte MB, Thonar EJ: Aggrecan synthesized by mature bovine chondrocytes suspended in alginate. Identification of two distinct metabolic matrix pools. *J Biol Chem* 269:33021-7, 1994.

28. Morales TI, Roberts AB: Transforming growth factor-β regulates the metabolism of proteoglycans in bovine cartilage organ cultures. *J Biol Chem* 263:12828-31, 1988.

29. Nandkumar MA, Yamato M, Kushida A, Konno C, Hirose M, Kikuchi A, Okano T: Two-dimensional cell sheet manipulation of heterotypically co-cultured lung cells utilizing temperature-responsive culture dishes results in long-term maintenance of differentiated epithelial cell functions. *Biomaterials* 23:1121-30, 2002.

30. Nugent GE, Aneloski NA, Schmidt TA, Schumacher BL, Voegtline MS, Sah RL: Dynamic shear stimulates cartilage biosynthesis of proteoglycan 4 (PRG4). *Arthritis Rhuem* (Submitted), 2005.

31. Schmidt TA, Schumacher BL, Han EH, Klein TJ, Voegtline MS, Sah RL: Chemomechanical coupling in articular cartilage: IL-1α and TGF-ß1 regulate chondrocyte synthesis and secretion of proteoglycan 4. In: *Physical Regulation of Skeletal Repair,* ed. by RK Aaron, Bolander ME, American Academy of Orthopaedic Surgeons, Chicago, 2005, 151-61.

32. Schmidt TA, Schumacher BL, Klein TJ, Voegtline MS, Sah RL: Synthesis of proteoglycan 4 by chondrocyte subpopulations in cartilage explants, monolayer cultures, and resurfaced cartilage cultures. *Arthritis Rheum* 50:2849-57, 2004.

33. Schumacher BL, Block JA, Schmid TM, Aydelotte MB, Kuettner KE: A novel proteoglycan synthesized and secreted by chondrocytes of the superficial zone of articular cartilage. *Arch Biochem Biophys* 311:144-52, 1994.

34. Stockwell RA. Biology of Cartilage Cells. New York: Cambridge University Press; 1979.

35. Vincent T, Hermansson M, Bolton M, Wait R, Saklatvala J: Basic FGF mediates an immediate response of articular cartilage to injury. *Proc Natl Acad Sci USA* 99:8259-64, 2002.

36. Vortkamp A, Lee K, Lanske B, Segre GV, Kronenberg HM, Tabin CJ: Regulation of rate of cartilage differentiation by Indian hedgehog and PTH-related protein. *Science* 273:613-22, 1996.

37. Wiesmann HP, Nazer N, Klatt C, Szuwart T, Meyer U: Bone tissue engineering by primary osteoblast-like cells in a monolayer system and 3-dimensional collagen gel. *J Oral Maxillofac Surg* 61:1455-62, 2003.

38. Wong M, Siegrist M, Goodwin K: Cyclic tensile strain and cyclic hydrostatic pressure differentially regulate expression of hypertrophic markers in primary chondrocytes. *Bone* 33:685-93, 2003.